

PHOSPHOREGULATION OF THE CDC25 PHOSPHATASE AND ITS EFFECTS ON

Schizosaccharomyces pombe MITOTIC ENTRANCE AND EXIT

By

Lucy Xiangxi Lu

Dissertation

Submitted to the Faculty of the

Graduate School of Vanderbilt University

in partial fulfillment of the requirements for

the degree of

DOCTOR OF PHILOSOPHY


in


Cell and Developmental Biology


December, 2012

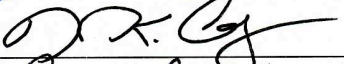
Nashville, Tennessee

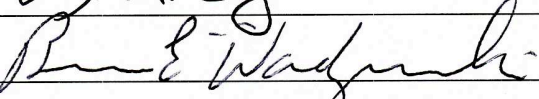
Approved by:



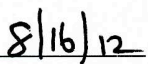


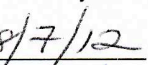


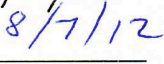


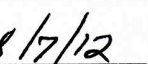


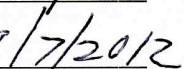
Date:











DEDICATED TO

my parents for traveling across the oceans so that I could have a better life.

&

To my grandparents who taught my family the importance of education and hardwork.

And during their lives, encouraged and loved me half way around the world.

ACKNOWLEDGEMENTS

I've been extremely lucky to have had positive and life changing experiences thanks to the encouragement, feedback, and company of so many wonderful individuals.

First of all, I would like to thank Dr. Kathy Gould, my infinitely patient mentor, who has been the example of a great leader, teacher, and scientist for me. It has been extremely rewarding to experience the growth in our relationship during my time in the lab. I started as a scared student and, under her guidance, have become a confident scientist. She has renewed my faith in a career in science. There is so much more I can to learn from her and I hope we continue our relationship throughout our careers.

During our time together, my committee members, Drs. William Tansey, Laurie Lee, David Cortez and Brian Wadzinski, have given me constructive feedback and encouragement that have been invaluable in my growth as a scientist. I am lucky to have had the support of such a talented group of scientists and mentors.

My graduate school experience would have been unthinkable without all the great people who I've interacted with daily in lab. A heart felt gratitude towards Anna Feoktistova who not only taught me how to design experiments and execute scientific techniques, but also have been a friend who stood up for me and truly cared about my wellbeing. Liping Ren who I've depended many times on for technical expertise and advice, and who's light heartness with all the students have made the lab an enjoyable place to work in. I enjoyed growing as a student and learning the nuances of the scientific society together with all the senior graduate students, Matt, Alyssa, and Adam, who I look up to as great scientists. Thanks to Janel and Junsong for technical, scientific, and

life advice. And finally, a special thankyou to the present and past members of Bay of China and Christmas Bay/the yet Un-named/Tranquility Bay for all the halarities, sharing stories, visiting Nashville entertainment facilities, raising a sick fish, and making making bench work such a pleasure.

My undergraduate school experience had been important in shapping my decision to join the MSTP program at Vanderbilt. Thanks to the UVA Chem department- Drs. Harman, Richardson, Fraser are inspiring in their commitment to teaching and were key to developing my curiosity for science. I am indebted to Dr. Vesna Todorovic, who welcomed me into her lab. Her mentorship, generosity, and encouragment gave me the courage to choose a career in science.

Thanks to present and past MSTP leadership, especially Drs. Terry Dermody, Susan Wente, Jim Bills, and Larry Swift, who stood by me in a very difficult time in my graduate school career and have been my cheerleader from the beginning of my journey in Vanderbilt. I am grateful to know that this wonderful group of leaders have and will support me in my past, present, and future academic career.

Finally, my life would have been empty without my friends and family. Thanks to my childhood and college friends who have kept me company online and in person. And thanks to the many wonderful friends in Nashville. My growth as a scientist would have been so much more difficult without the fun, encouragement and support of everyone. Thanks to Derek for the company, laughs, cries, and unwavering belief in everything that I do. And finally, my past and future success are all thanks to my parents, who have stood by me through all my mistakes and acheivements. I love and am so proud of you both.

TABLE OF CONTENTS

	Page
DEDICATION	ii
ACKNOWLEDGEMENTS	iii
LIST OF FIGURES	vii
LIST OF TABLES	ix
Chapters	
I. INTRODUCTION	1
The Eukaryotic Cell Cycle	2
Cyclin Dependent Kinases and Cell Cycle Transitions	7
Cdk1 Regulation in Mitotic Entry	8
Mitotic Exit	11
Cdc25 Function and Regulation	12
Amplification of Cdc25 Activity	14
Regulation of Cdc25 During Cell Cycle Checkpoints	15
Cdc25 During Mitotic Exit	18
Bistability, Ultrasensitivity and Feedback Loops in Cell Cycle Progression	20
Evidence for Mitotic Entry as a Bistable Event	22
<i>Schizosaccharomyces pombe</i> as a Model System for Cell Cycle Studies	24
Summary	27
II. MATERIALS AND METHODS	29
Strains, Medias, and General Methods	29
Molecular Biology Techniques	33
Immunoprecipitations and Immunoblots	35
Tandem Affinity Purification of Cdc25-TAP	35
<i>In vivo</i> Ubiquitylation Assay	36
<i>In vitro</i> Cdk1 Kinase Assay	37
Cdc25 Activity Assay	38
Microscopy	40
2D Tryptic Peptide Mapping	41
Mass Spectra Sample Preparation	41
Mass Spectra Data Analysis	42
Mathematical Model of the Bistable Mitotic Switch with Cdc25 Multisite Phosphorylation by Cdk1	43

Variation of Cell Size Due to Variation in Parameter Values	52
III. CDK1 PHOSPHORYLATION OF CDC25 REGULATES CDC25 ACTIVITY	53
Introduction.....	53
Results.....	55
Characterization of Cdk1 and Clp1 Specific Phosphosites on Cdc25	55
Cdk1 Phosphorylation Does Not Affect Cdc25 Nuclear Localization	59
Cdk1 Phosphorylation Does Not Affect Cdc25 Accumulation	60
Dephosphorylation of Cdc25 by Clp1 Does Not affect Cdc25 Ubiquitylation	65
Cdk1 Phosphorylation Directly Activates Cdc25	67
Discussion	68
Phosphoregulation of Cdc25 Activity.....	68
Cdc25 Nuclear Localization	69
Regulation of Cdc25 Degradation at Mitotic Exit	70
IV. MULTISITE PHOSPHOREGULATION OF CDC25 ACTIVITY REFINES THE MITOTIC ENTRANCE AND EXIT SWITCHES	72
Introduction.....	72
Results.....	73
Abolishing Cdk1 Phosphosites on Cdc25 Delays Mitotic Entry	73
Multisite Phosphorylation of Cdc25 by Cdk1 Allows for Ultrasensitivity ...	77
Mechanism of Cdc25 Activation by Cdk1.....	79
Cdc25 Phosphorylation by Ckd1 is Distributive or Semi-Processive	81
Mathematical Model of Cdc25 Activation and Mitotic Entrance.....	84
Cytokinesis Timing is Controlled by Clp1 Dephosphorylation of Cdc25	87
Discussion	90
Mitotic Switch Disruption Manifests as Increased Size Variation	90
Mechanism of Cdc25 Phosphorylation by Cdk1	90
Role of Cdc25 Multisite Phosphoregulation in Eukaryotes.....	91
The Cdc14 Phosphatase Plays Important Roles in the Mitotic Exit Switch ..	92
V. CONCLUSIONS AND FUTURE DIRECTIONS.....	94
Chapter Highlights	94
Future Directions	98
Wee1-Cdk1 Negative Feedback in the Mitotic Entrance Switch	98
Other Kinases that Affect Mitosis Through Cdc25	98
Functional Characterization of the Cdc25 N-terminus	100
Multisite Phosphorylation and Dephosphorylation in the Cell Cycle and Beyond	101
Conclusion	104
BIBLIOGRAPHY	105

LIST OF FIGURES

Figure	Page
1-1. The eukaryotic cell cycle with associated Cyclin Dependent Kinases.....	4
1-2. The meiosis cycle	6
1-3. Mitosis is controlled by the activation of Cyclin Dependent Kinase 1	10
1-4. Cdc25 isoforms share consensus in the catalytic domain.....	13
1-5. Cdc25 is a heavily regulated molecule	17
1-6. Cdc25 phosphoregulation by Cdk1 and Clp1 during mitosis.....	19
1-7. Bistability requires one or more feedback loops and at least one component of the feedback loop(s) with ultrasensitive characteristics	21
1-8. Cdk1 activity exhibits bistability	23
1-9. The <i>S. pombe</i> cell cycle	26
2-1. Schematic of the Cdc25 activity assay	39
2-2. Two parameter bifurcation diagram of the model for the MPF activation threshold	49
3-1. Characterization of Cdc25 phosphomutant	57
3-2. Cdk1 phosphoregulation does not regulate Cdc25 localization	60
3-3. Cdk1 phosphorylation does not regulate Cdc25 accumulation	63
3-4. Cdk1 phosphorylation does not regulate Cdc25 ubiquitylation	66
3-5. Cdk1 phosphorylation regulates Cdc25 activity at mitotic entrance	67
4-1. Disruption of Cdk1 phosphorylation on Cdc25 delays mitotic entrance.....	75
4-2. Multiple phosphorylation sites allow for ultrasensitive phosphorylation of Cdc25 by Cdk1	78
4-3. Removal of Cdk1 phosphosites on Cdc25.....	80

4-4	Activation of Cdc25 by Cdk1 multisite phosphorylation.....	83
4-5	Mathematical model of Cdc25 activation.....	86
4-6	Clp1 dephosphorylation of Cdc25 is vital for proper mitotic exit.....	89
5-1	Cdc25 is involved in two feedback loops that significantly contribute to mitotic bistability.....	97

LIST OF TABLES

Table	Page
2-1. Strains used in this study	30
2-2. Oligonucleotides used for mutagenesis	34
2-3. Parameter values for the model	50
2-4. Parameter changes for cell cycle mutants.....	51
3-1. List of confirmed Cdc25 (S/T)P phosphopeptides	58
4-1. The identity of each Cdc25 phosphomutant with mean length and SEM	82

CHAPTER I

INTRODUCTION

Modern science is now perfecting life saving technologies in *de novo* organ synthesis, stem cell therapies, and cancer treatment. Common to all these therapies is the fundamental understanding of the normal and pathological cell cycle and how cellular events are coordinated between and within cells. While the cell theory itself, that all organisms are made of one or more cells and that a new cell can only arise from division of the mother cell, was proposed close to two centuries ago by Schleiden and Schwann (reviewed in (Aszmann 2000)), it was no more than 40 years ago that we started to explore the basic tenants of chromosome segregation, cytoskeletal re-organization, and cell cycle protein regulation.

The past four decades has seen an explosion of discovery and understanding of key cell cycle regulators and their interactions. The modern age of biochemistry has also been facilitated by computational biology, which has taken the considerable knowledge amassed by cell cycle scientists and made tenable models that simulate multiple protein characteristics, protein interactions, cellular events, and cell-cell communications, allowing scientists to test and refine their lab based hypothesis in an integrative manner. Thus, classical biochemistry and computational biology constantly refine and challenge one another, resulting in innovative understandings for the normal and pathological cell cycle, ultimately, allowing for insight into the manipulation of the cell for the benefit of human understanding and health.

This thesis will describe biochemical, genetic and computational studies which have contributed to the understanding of the module of protein interactions centered on the mitotic entry protein Cdc25.

The Eukaryotic Cell Cycle

The cell cycle is a precisely regulated series of events that allow a cell to replicate its DNA, equally segregate the DNA, and divide into two daughter cells (reviewed in (Morgan 2007)). Eukaryotic cell cycle times range from 24 hours in rapidly dividing human cells to around 3 hours in *Schizosaccharomyces pombe* and less than 2 hours for *Saccharomyces cerevisiae*. Despite temporal differences, all normal cell cycles share two discrete phases: S phase and mitosis (M). During S phase, the entire genome is replicated, sister chromatids are linked, and the centrosome is replicated (but remains linked until mitosis). In mitosis sister chromatids are aligned (prometaphase) and pulled towards separate poles of the cell (anaphase). Mammalian cells go through open mitosis in which the nuclear envelope dissolves during mitosis and reforms after chromosome separation. In contrast, some fungi, such as the fission yeast *S. pombe* and budding yeast *S. cerevisiae*, go through closed mitosis where the nuclear envelope remains intact during mitosis. After mitosis, cells usually initiate cytokinesis, resulting in the production of two daughter cells. In most cells, the S phase and M phases are separated by two gap phases (G1 and G2) where new ribosomes, cytoplasmic components, membranes, mitochondria, ER and most cellular proteins are produced.

The cell cycle can vary for different cell types and for specialized events. For example *Drosophila melanogaster* embryos undergo 13 rapid cycles of S and M phases

without cytokinesis, forming a syncytium of nuclei before cell membrane invaginates into the syncytium to form individual cells (reviewed in (Mazumdar and Mazumdar 2002)). Endomitosis happens in mammalian megakaryocyte blood cells where multiple rounds of S phase without M phase or cytokinesis, resulting in increased ploidy (up to 64N compared to 2N of typical diploid cells) and increased cell volume. Build up of cell volume and DNA allows the megakaryocyte to rapidly synthesize protein and cytoplasm to shed in the form of platelets (reviewed in (Jackson 1990)).

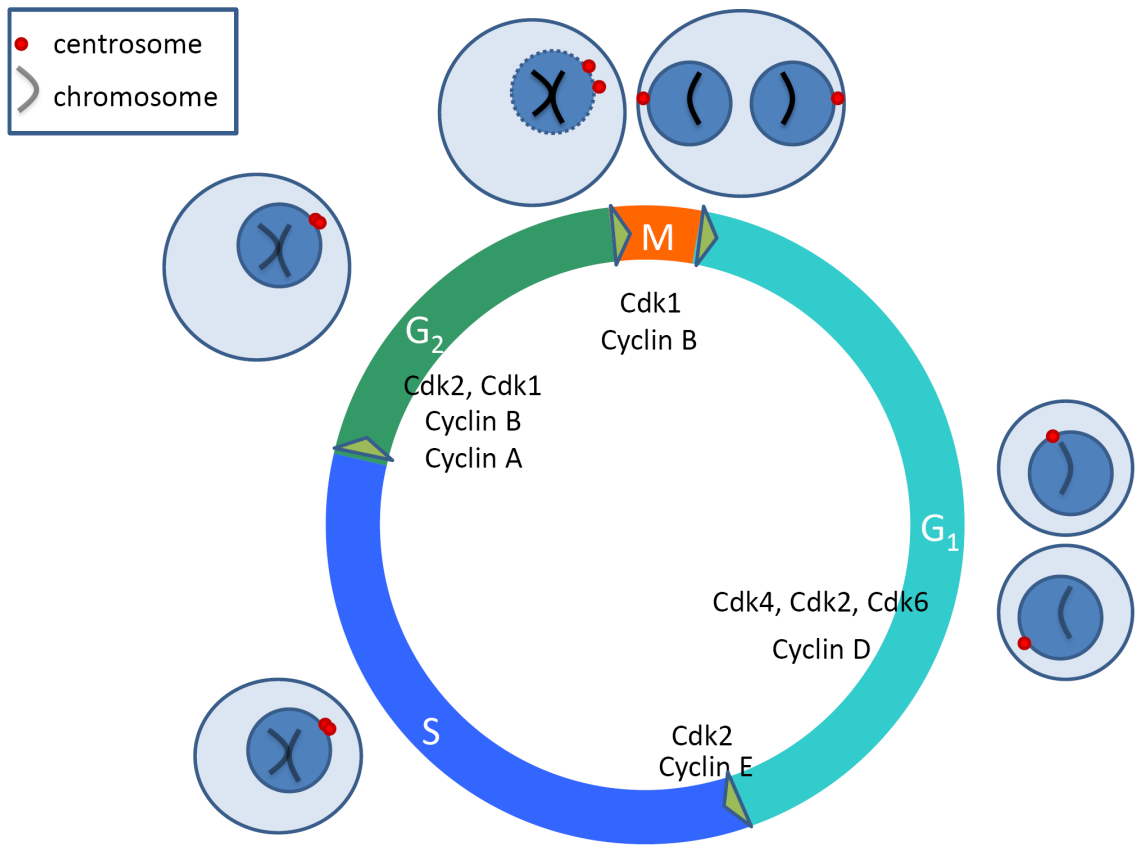


Figure 1-1. The eukaryotic cell cycle with associated Cyclin Dependent Kinases.

Interphase is composed of 2 gap phases (G₁ and G₂) in which the cell expands in volume, cytoplasmic and protein contents and a Synthesis (S) phase, where the cell doubles in DNA content and duplicates its centrosome. Mitosis (M) starts, in mammalian cells, with nuclear envelope breakdown and chromosome condensation. Mitosis ends after the cell separates its DNA. During cytokinesis, the cell divides into two daughter cells with identical copies of DNA. Each phase of the cell cycle and transitions between phases are driven by Cyclin Dependent Kinases (Cdks) that associate with their specific Cyclin partners to phosphorylate key substrates.

Another specialized cell cycle is meiosis, composed of meiosis I and II. During sexual reproduction, two haploid ($1N$) parent cells, from two individual organisms, combine their DNA to form a diploid ($2N$) cell. The new cell then goes through S phase to duplicate its DNA and link sister chromatids. In meiosis I, pairs of sister chromatids combine and exchange DNA through homologous recombination, then the two sister chromatids are segregated and cytokinesis occurs to result in two daughter cells. In meiosis II, the two daughter cells separate their sister chromatids and go through cytokinesis again, resulting in four haploid cells that are genetically distinct from their parents (reviewed in (Morgan 2007)).

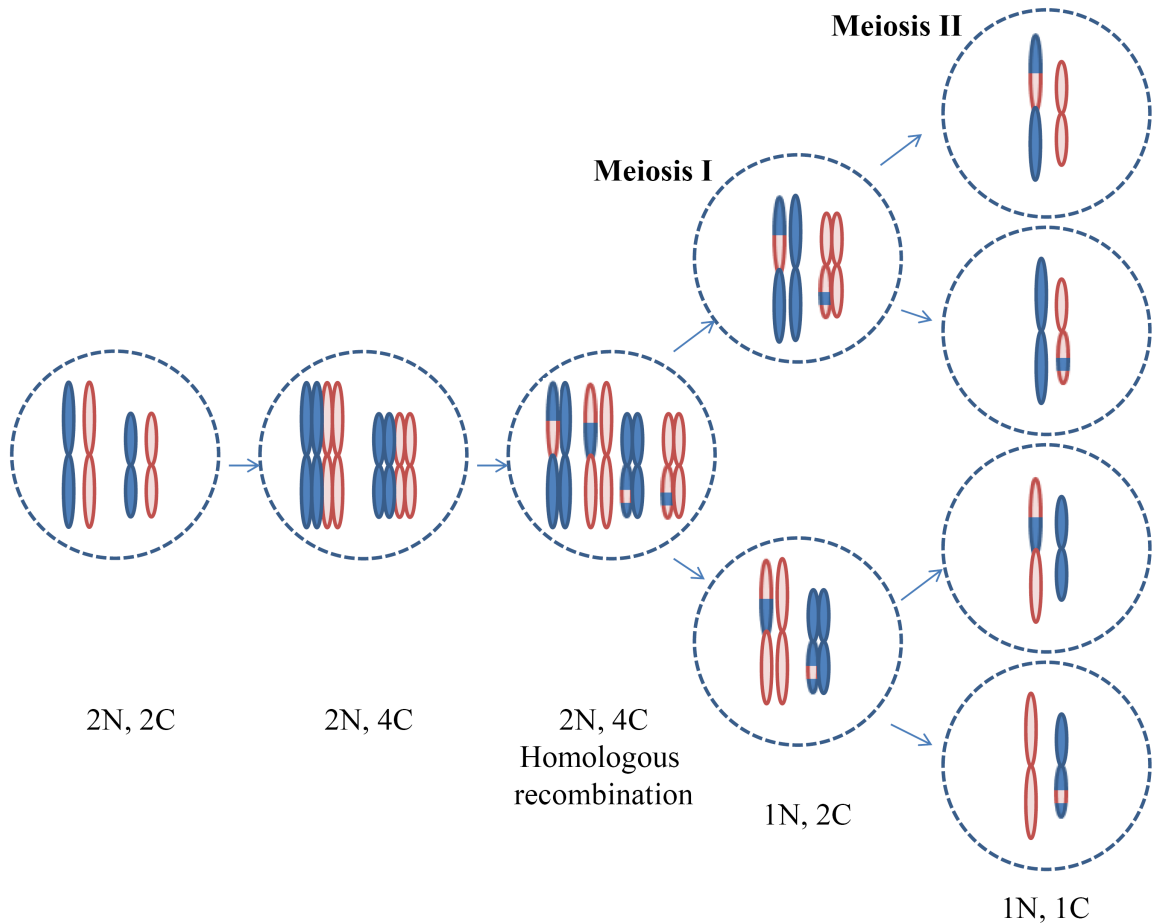


Figure 1-2. The meiosis cycle.

Meiosis I and II are used during sexual reproduction to allow for exchange of parental genetic material and result in random segregation of the newly exchanged genetic materials into 4 separate cells. Two haploid ($1N$) parent cells fuse to create a diploid cell with two genetically distinct sets of chromosomes, shown here in blue or red ($2N, 2C$). Cells then replicate their DNA ($2N, 4C$) and exchange genetic material through homologous recombination. During Meiosis I, cells divide each set of sister chromatids, resulting in 2 haploid daughters with sister chromatids still attached ($1N, 2C$). In meiosis II, the sister chromatids are segregated, resulting in 4 haploid daughter cells with one of each set of chromosomes ($1N, 1C$).

Cyclin Dependent Kinases and Cell Cycle Transitions

The Cyclin Dependent Kinases (Cdks) are a family of serine/threonine kinases that are essential for cell cycle transitions. Throughout the cell cycle, Cdks oscillate in activity and associate with regulatory Cyclins to temporally and biochemically coordinate events that drive cell cycle progression (reviewed in (Satyanarayana and Kaldis 2009); (Gopinathan, Ratnacaram et al. 2011)). The Cdk-driven cell cycle is monitored by checkpoints that detect errors, modulate Cdk activity and initiate error-correcting algorithms.

There are three main regulatory transitions during the cell cycle: G1/S (Start), G2/M (DNA damage checkpoint), and metaphase-anaphase (spindle assembly checkpoint). Before Start, the cell senses environmental conditions in G1 including nutrition and growth factor levels, and internal cell conditions such as senescence signals and DNA damage levels. When conditions are not correct for cell division, G1/S Cdk-Cyclins (Cdk4/6-CyclinD and Cdk2-CyclinE) are inhibited through degradation of Cyclins, inhibition of Cdk and DNA replication, and inactivation of Cdk activators. When conditions are suitable for proliferation, cells activate Cdk-Cyclins to initiate DNA transcription and other S phase events. At the G2/M transition, cells ensure that DNA replication is complete and there is no DNA damage before allowing Cdk1-CyclinB to drive mitotic entry. The cell inhibits Cdk1-CyclinB by activating Cdk1 inhibitors, inhibiting activators and sequestering Cdk1 activators (such as CyclinB and Cdc25) away from the nucleus, where most key mitotic events occur. Finally during the metaphase-anaphase checkpoint, the cell ensures that chromosomes have attached to the mitotic spindle and are aligned at the metaphase plate before the cell initiates late mitotic events

such as sister chromatid separation and Cdk1 inactivation through degradation of CyclinB and other Cdk1 activators (Reviewed in (Lukas, Lukas et al. 2004)).

Cdk1 Regulation in Mitotic Entry

In vertebrates, Cdk1 associates with CyclinA and CyclinB1 to control mitotic entry and mitotic events. In comparison, fission yeast triggers mitosis with a single CyclinB (Cdc13), and budding yeast contain six B-type Cyclins that function together, most likely in a semi-redundant manner, to stimulate mitotic events (reviewed in (Morgan 1997)). Despite differences in Cyclin-Cdk1 pairing, control of Cdk1 activity during mitotic initiation is common to all eukaryotes. During G2, Cdk1 is inhibited following phosphorylation of Thr 14 and Tyr 15 by the Wee1 and Myt1 kinases. In mammalian cells, Wee1 only phosphorylates Tyr 15, and Myt1 phosphorylates both Thr 14 and Tyr 15 (McGowan and Russell 1993; Mueller, Coleman et al. 1995). In fission yeast, Wee1 phosphorylation at Tyr 15 is primarily responsible for Cdk1 inhibition (Gould and Nurse 1989). When Wee1 is inactivated, cells are reduced to half the size of wild type cells due to lack of Cdk1 inhibition (Russell and Nurse 1987). In addition, the Mik1 kinase acts cooperatively with Wee1 in *S. pombe* to phosphorylate Tyr 15. Deletion of both Mik1 and Wee1 drives cells to mitotic catastrophe – with cells unable to stop mitosis upon DNA or environmental damage (Lundgren, Walworth et al. 1991).

Cdc25 phosphatases activate Cdk1 by removing Wee1 and Myt1 inhibitory phosphorylations. There is also evidence that, in mammalian cells, Cdc25 facilitates the initial mitotic Cdk-Cyclin complex formation (Timofeev, Cizmecioglu et al. 2010). Vertebrates have three Cdc25 isoforms (Cdc25 A, B, and C) that play various different

and redundant roles for Cdk1 activation during mitosis. Fission yeast has only one Cdc25 that facilitates several cell cycle transitions but is essential for mitotic entry (reviewed in (Karlsson-Rosenthal and Millar 2006)). Inactivation of Cdc25 in fission yeast results in cell cycle arrest and subsequent cell death (Russell and Nurse 1986).

Cdk1 also negatively regulates Myt1 and Wee1, and positively regulates Cdc25 to facilitate rapid Cdk1 activation for mitotic entry. In mammalian cells, Cdk1 phosphorylation initiates a cascade that ultimately inactivates Myt1 (Nakajima, Toyoshima-Morimoto et al. 2003). Cdk1 phosphorylates Wee1, and this phosphorylation is correlated with Wee1 degradation and inactivation in *Xenopus laevis* egg extracts and human cells (Michael and Newport 1998; Watanabe, Arai et al. 2004; Smith, Simanski et al. 2007). In mammalian cells, Cdk1 phosphorylates and further activates Cdc25C, stabilizes Cdc25A, and facilitates nuclear translocation of Cdc25B (Hoffmann, Clarke et al. 1993; Baldin, Pelpel et al. 2002; Mailand, Podtelejnikov et al. 2002). And finally, at the time my work began, it was known that in fission yeast, Cdc25 phosphorylation by Cdk1 at mitotic entry was associated with increases in Cdc25 levels, nuclear localization and activity (Wolfe and Gould 2004).

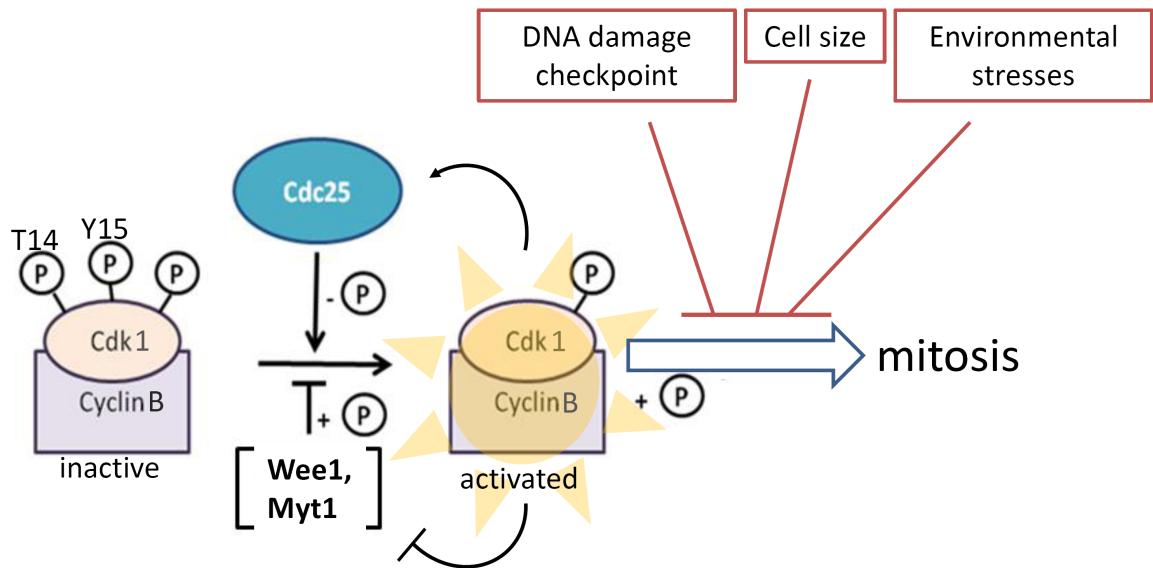


Figure 1-3. Mitosis is controlled by the activation of Cyclin Dependent Kinase 1.

At mitotic entrance, Cdk1 is associated with CyclinB. It is phosphorylated and inactivated by Wee1 and Myt1 kinases via phosphorylation at T14 and Y15. Cdc25 phosphatase removes the inhibitory phosphorylations and activates Cdk1. Cdk1 is then able to phosphorylate a number of substrates to initiate and maintain mitosis. Among its substrates, Cdk1 phosphorylates Cdc25 and Wee1, further activating Cdc25 and inactivating Wee1. Factors like damage from the environment, DNA damage, and small cell volume prevent Cdk1 activation through control of Cdc25 and Wee1 stability, activity and localization to pause the cell in G2 until the cell is ready for mitosis.

Mitotic Exit

Late mitotic and mitotic exit events are initiated after the metaphase-anaphase transition. After sister chromatids separate, the cell starts to reverse Cdk1 phosphorylations, which turns off early mitotic events, allows for progression of late mitotic events (such as full DNA segregation and cytokinesis) and reduces Cdk1 activity to allow for proper transition into a new cell cycle.

Two prominent components in promoting late mitotic events are the anaphase-promoting complex or cyclosome (APC/C) E3 ubiquitin ligase, which facilitates degradation of mitotic proteins, and phosphatases that remove phosphorylation from Cdk1 substrates. During early mitosis, Cdk1 phosphorylates and activates the APC/C ubiquitin ligase. Activated APC/C associates with co-factors Cdc20, and later Cdh1, to ubiquitylate mitotic proteins for proteasomal degradation. Most prominently, APC/C ubiquitylates and targets CyclinB for proteolysis, the persistence of which results in cell cycle arrest in anaphase (reviewed in (McLean, Chaix et al. 2011)).

The Cdc14 phosphatase specifically targets Cdk1 substrates during mitotic exit. In *S. cerevisiae*, Cdc14 dephosphorylates Cdh1 to allow for APC/C association, to facilitate total CyclinB protein ubiquitylation and degradation. In addition Cdc14 dephosphorylates Sic1p, a Cdk1 inhibitor that is targeted for degradation by Cdk1 phosphorylation (reviewed in (Stegmeier and Amon 2004)). Clp1, the Cdc14 phosphatase homologue in *S. pombe*, dephosphorylates and activates itself during mitosis (Wolfe, McDonald et al. 2006). Clp1 also dephosphorylates Cdc15 to allow for contractile actomyosin ring formation, a key component for contraction and abscission during cytokinesis (Guertin, Chang et al. 2000; Trautmann, Wolfe et al. 2001; Clifford, Wolfe et al. 2008; Dischinger,

Krapp et al. 2008; Roberts-Galbraith, Ohi et al.). Clp1 and human Cdc14B also dephosphorylate Cdc25 to directly dampen the Cdk1-Cdc25 co-activation loop. At the time this thesis began, in *S. pombe*, Cdc25 dephosphorylation was associated with Cdc25 degradation and inactivation (Wolfe and Gould 2004).

Cdc25 Function and Regulation

As stated previously, mammalian cells have three Cdc25 isotypes (Cdc25A, Cdc25B, and Cdc25C). All three isotypes control Cdk activity during cell cycle transitions in a mechanism similar to the single Cdc25 homologue in *S. pombe*. Cdc25A activates Cdk2-CyclinA/E and Cdk1-CyclinB and is thus involved in S phase progression and mitotic entry (Hoffmann, Draetta et al. 1994; Blomberg and Hoffmann 1999; Sexl, Diehl et al. 1999; Mailand, Podtelejnikov et al. 2002). Cdc25B and Cdc25C are mostly involved in activating Cdk1-CyclinB and function during mitotic entry and mitotic progression. In addition to different roles in the cell cycle, the three isoforms also play different developmental roles. *CDC25A*^{-/-} animals are embryonic lethal, implicating vital roles for Cdc25A in embryogenesis (Ray, Terao et al. 2007). *CDC25B*^{-/-} and *CDC25C*^{-/-} mice survive through adulthood; however, *CDC25B*^{-/-} female mice are sterile and have defects in meiotic resumption in oocytes (Lincoln, Wickramasinghe et al. 2002).

The mammalian and yeast Cdc25 proteins share conserved C-terminal catalytic domains which contain a CX₅R motif common to all dual specificity phosphatases (Fig. 1-4), (reviewed in (Karlsson-Rosenthal and Millar 2006; Trinkle-Mulcahy and Lamond 2006)). The N-terminal regulatory domains vary in sequence between yeast and human homologs, and even within the three human paralogs. In general, the regulatory domains

contain sites for phosphorylation, ubiquitylation, and interaction with regulators of nucleoplasmic transport.

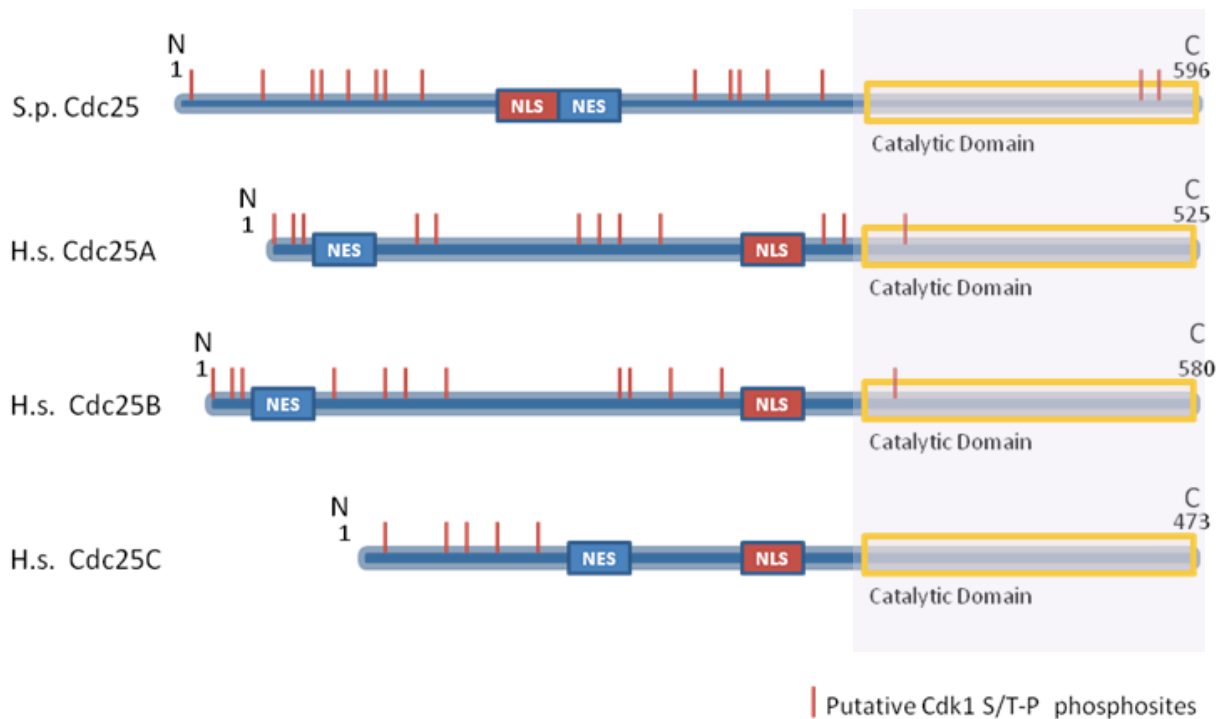


Figure 1-4. Cdc25 isoforms share consensus in the catalytic domain.

While human and *S. pombe* Cdc25 isoforms share high sequence identity in their catalytic domains, their N-terminal regulatory domains vary in size and sequence. Despite the differences in N-terminal sequences, all isoforms contain protein localization domains (NLS and NES) and phosphorylation sites for regulatory kinases.

Amplification of Cdc25 Activity

Cdc25 activity is controlled through transcriptional, translational, and post-translational methods. Transcriptional maintenance of Cdc25 varies in different organisms. In fission yeast, Cdc25 mRNA accumulates through the cell cycle starting in early interphase and peaking at the G2/M transition (Moreno, Nurse et al.). In humans, Cdc25A mRNA level peaks before Cdc25B level, which is maximal around the mitotic transition (Jinno, Suto et al. 1994). While mRNA expression of Cdc25 differs, all organisms use post-translational modifications that alter protein stability, localization, and catalytic activity ultimately regulating total Cdc25 activity.

Amplification of Cdc25 activity is mainly facilitated by the Cdks and Polo-like-kinases. In mammalian cells, Cdc25A is involved in both S phase and mitotic progression and is phosphorylated by Cdk2/CyclinE or Cdk1/CyclinB in a cell cycle-specific manner. Phosphorylation of Cdc25A by Cdk2 directly activates Cdc25A at the S phase transition (Hoffmann, Clarke et al. 1993). At the G2/M transition Cdk1 phosphorylation stabilizes Cdc25A (Mailand, Podtelejnikov et al. 2002). Cdk1 phosphorylates and activates Cdc25B and Cdc25C at mitotic entry. Cdc25C is involved in the co-activation feedback with Cdk1 to drive rapid mitotic entry while Cdc25A and Cdc25B act earlier in G2 and are involved in the initial Cdk1-CyclinB complex formation, and initial Cdk1 activation at the centrosome (Hoffmann, Clarke et al. 1993; Lindqvist, Källström et al. 2005; Timofeev, Cizmecioglu et al. 2010). In *S. pombe*, at the time this thesis began, Cdk1 hyperphosphorylation of Cdc25 was associated with increased Cdc25 concentration, nuclear accumulation and activation, although it was not clear if Cdk1 phosphoregulation

specifically modulated one or all three mechanisms of Cdc25 control (Kovelman and Russell 1996; Esteban, Blanco et al. 2004; Wolfe and Gould 2004).

The Polo-like-kinases (Plks) also phosphorylate and positively regulate Cdc25. Plks play multiple roles and interact with multiple substrates during the G2/M transition, mitotic progression, and cytokinesis (reviewed in (Archambault and Glover 2009)). The *Xenopus* Polo-like-kinase activates Cdc25 directly via phosphorylation (Kumagai and Dunphy 1996; Qian, Erikson et al. 2001). In humans, Plk1 and Plk3 phosphorylate Cdc25C and facilitate Cdc25 nuclear translocation at prophase to facilitate proper Cdc25-Cdk1 spatial interaction (Toyoshima-Morimoto, Taniguchi et al. 2002; Bahassi et al., Hennigan et al. 2004). Plk1 also phosphorylates Cdc25B at the centrosome during late G2 and is thought to facilitate Cdc25 and Cdk1 activation at the centrosome, considered to be one of the first events during mitotic entry (Lobjois, Jullien et al. 2009).

Regulation of Cdc25 During Cell Cycle Checkpoints

Cdc25 isoforms contain nuclear import and export signals that can be regulated through DNA damage and environmental stress responses. DNA damage checkpoint inhibits Cdc25 to delay mitosis until DNA is repaired. In mammalian cells, phosphorylation by the Chk1 and Chk2 kinases on Cdc25B and Cdc25C causes nuclear exclusion by promoting association with the nuclear exportin Crm1 and binding to 14-3-3 proteins to sequester Cdc25 in the cytoplasm (Graves, Lovly et al. 2001). Cdc25A phosphorylation by the Chk kinases induces degradation by ubiquitin-mediated processes (Mailand, Falck et al. 2000; Falck, Mailand et al. 2001). In *S. pombe*, Cdc25 phosphorylation by the Chk kinases both inactivates Cdc25 and facilitates 14-3-3 binding in the cytoplasm (Furnari, Blasina et al. 1999).

Cells also respond to environmental stresses, such as UV light damage, osmotic pressure changes and cytoskeletal disruptions, by inhibiting Cdc25. The p38 Mitogen Activated Protein Kinase (MAPK) cascade responds to these environmental stresses and through the effector kinase MAPK-Associated Protein Kinase 2 (MAPKAPK-2), phosphorylates Cdc25B and Cdc25C, to facilitate 14-3-3 binding leading to nuclear exclusion and delayed mitotic onset (Manke, Nguyen et al. 2005). In addition, p38 activity ultimately induces Cdc25A and Cdc25B degradation during S phase and M phase entry, respectively, in response to environmental stresses (such as Osmotic and UV, respectively) (Khaled, Bulavin et al. 2005; Uchida, Yoshioka et al. 2009; Uchida, Watanabe et al. 2011). Similar to mammalian cells, in *S. pombe*, the p38 kinase Sty1 responds to environmental stresses to activate downstream Srk1 (a MAPKAPK-2 related protein) to directly phosphorylate Cdc25 on the same sites as the Chk kinases to facilitate Cdc25 nuclear exclusion and inactivation (Lopez-Aviles, Grande et al. 2005).

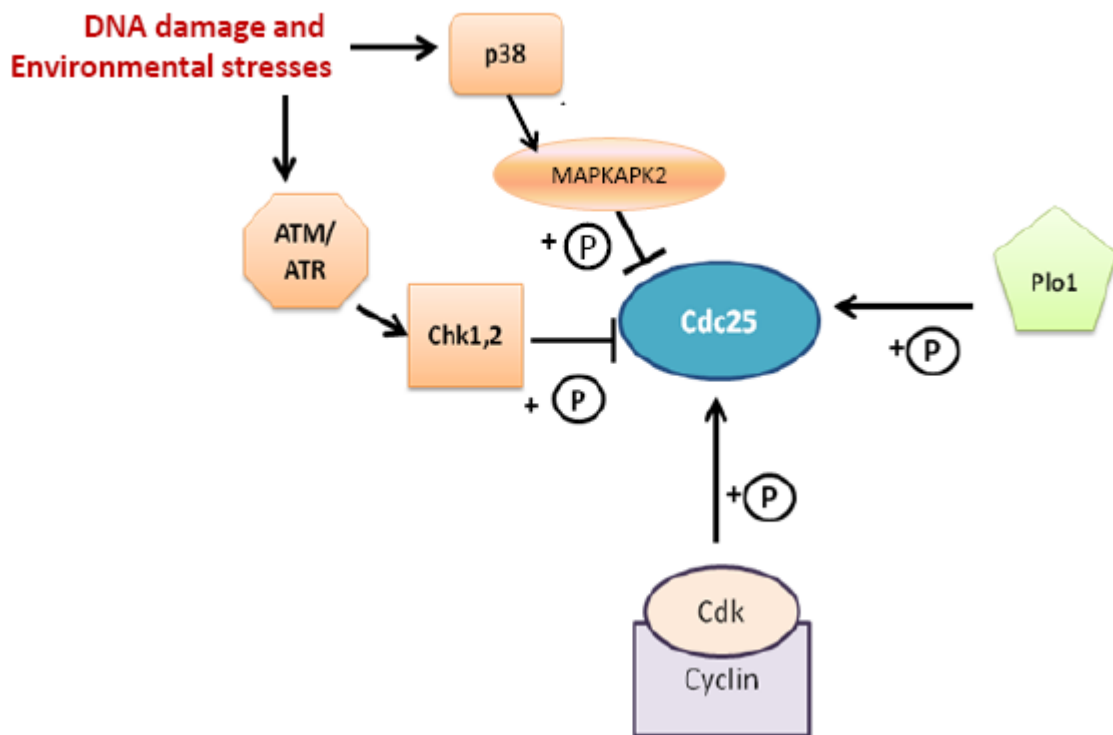


Figure 1-5. Cdc25 is a heavily regulated molecule.

DNA damage and environmental stresses activate downstream pathways that phosphorylate Cdc25 and inhibit mitotic entrance by facilitating Cdc25 degradation and preventing Cdc25 activation and nuclear translocation. Conversely, Polo-like kinase and Cdk phosphorylation of Cdc25 is correlated with increased Cdc25 activity and nuclear localization.

Cdc25 During Mitotic Exit

Starting in anaphase, Cdc25 becomes progressively dephosphorylated by the Cdc14 phosphatases and undergoes ubiquitin-mediated degradation (Donzelli, Squatrito et al. 2002; Wolfe and Gould 2004; Tumurbaatar, Cizmecioglu et al. 2011). Cdc25 dephosphorylation and inactivation quenches the Cdk1-Cdc25 positive feedback loop, and mitotic exit follows the reversal of Cdk1 kinase events. In *S. pombe*, *clp1* deleted cells are shorter than wild type cells. This is partly due to the mutant's inability to dephosphorylate and inactivate Cdc25, allowing for increased Cdk1 activity, which drives premature mitotic entry (Wolfe and Gould 2004).

How Cdc14 dephosphorylation of Cdc25 confers inactivation or degradation of Cdc25 is unclear. In humans, Cdc25A and Cdc25B are degraded by the ubiquitin-proteasome system and are ubiquitylated by both Skp1-Cul1-F Box (SCF) and anaphase promoting complex/cyclosome (APC/C) E3 ubiquitin ligases (Donzelli, Squatrito et al. 2002; Busino, Donzelli et al. 2003; Busino, Chiesa et al. 2004; Kieffer, Lorenzo et al. 2007). However, the proteins that signal for Cdc25 ubiquitylation and degradation are unknown. In *S. pombe*, there is evidence that Clp1 and APC/C are involved in Cdc25 destabilization at the end of mitosis (Wolfe and Gould 2004). In an *mts3-1* mediated metaphase arrest facilitated by the inactivation of a temperature sensitive proteasomal component, cells without Clp1 or APC/C have decreased Cdc25 ubiquitylation (Wolfe and Gould). The *S. pombe* Pub1 E3 ligase also may play a role in Cdc25 ubiquitylation. Pub1 has been shown to work with Clp1 to regulate the long-term destabilization of Cdc25 (Nefsky and Beach 1996; Esteban, Blanco et al. 2004; Esteban, Sacristán et al. 2008).

In addition to Cdc25 ubiquitylation and degradation, Clp1 also may play a role in Cdc25 localization. At the start of this thesis, it was shown that *clp1Δ* cells had increased Cdc25 nuclear localization during late anaphase (Wolfe and Gould 2004). Until the work described herein, it was not known if abnormal localization was due to increased Cdc25 abundance or disrupted Cdc25 nuclear export.

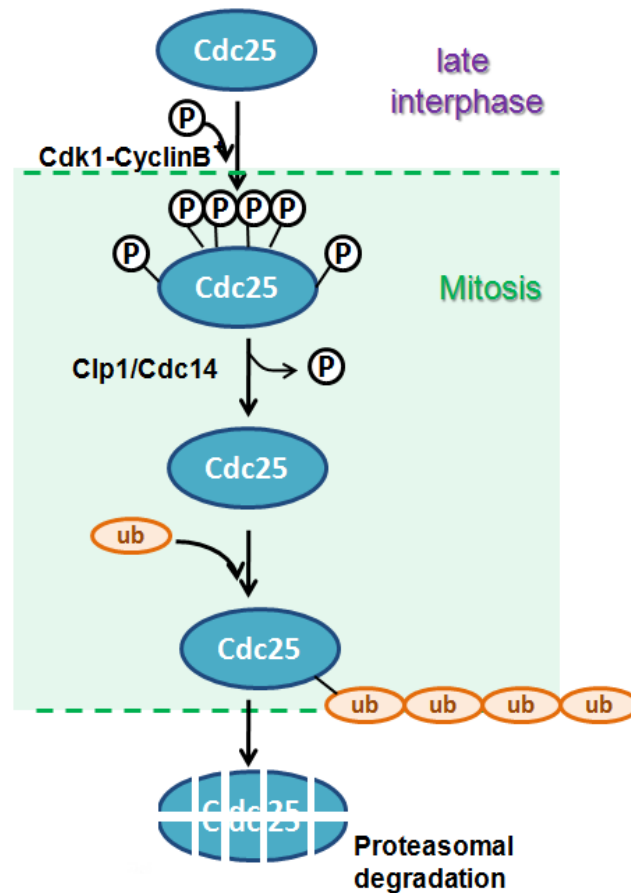


Figure 1-6. Cdc25 phosphoregulation by Cdk1 and Clp1 during mitosis.

At mitotic entrance, Cdc25 phosphorylation by Cdk1 is correlated with activation, nuclear localization and accumulation of Cdc25. After metaphase, Clp1 dephosphorylates Cdk1 sites on Cdc25. Clp1 dephosphorylation is followed by Cdc25 degradation and a decrease in activity.

Bistability, Ultrasensitivity and Feedback Loops in Cell Cycle Progression

The stepwise nature of the cell cycle requires the cell to “remember” previous cell cycle events, rapidly execute decisions when requirements for future events are satisfied, and stay in a new cell cycle state once a transition has occurred. This form of feed-forward mechanism has been proposed to be driven by feedback loops, in which an initially low disturbance in the system initiates a low amplitude signal that builds upon itself in an exponential manner until the system reaches a new equilibrium (Pomerening 2009).

Two types of feedback loops exist: positive or negative feedback. In the positive feedback loop, element A enhances the output of element B, and element B in turn enhances the output of element A. In the negative feedback loop, element A decreases the output of element B while element B also reduces element A’s output (Fig 1-7) (Pomerening 2009).

In biological systems, combinations of both positive and negative feedback loops work together to create bistable steady states. A bistable system contains two low energy stable states separated by a high energy transition state (reviewed in (Ferrell and Xiong 2001)). Generally, in the cell cycle, when the system has transitioned into one state it is nearly impossible for it to switch back to its previous state due to the high energy barrier between the two phases (for example, the transitions between G1 to S phases, G2 to mitosis phases, and mitosis back to G1) (Fig. 1-8).

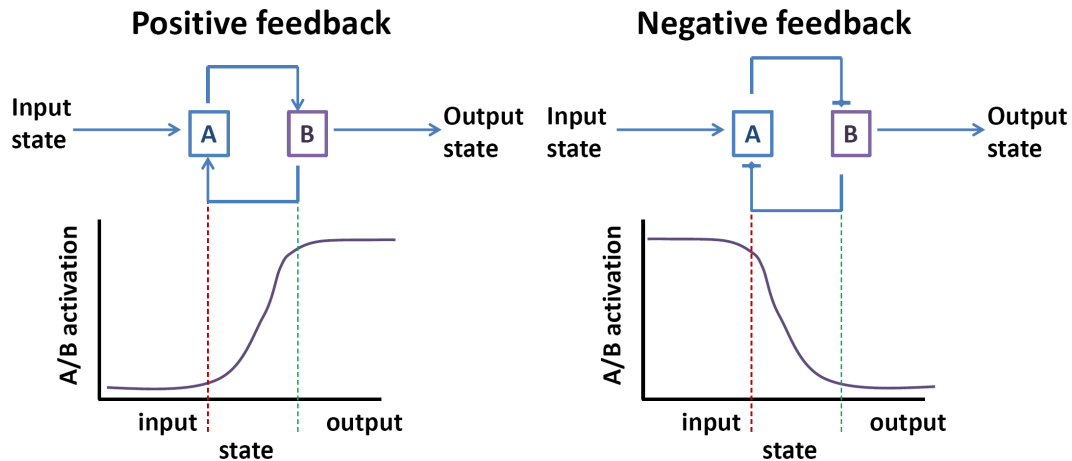


Figure 1-7. Bistability requires one or more feedback loops and at least one component of the feedback loop(s) with ultrasensitive characteristics.

Two types of feedback exist. In the positive feedback loop two elements co-activate one another while in the negative feedback loop, the two elements inactivate one another (top). For a system to be bistable, the system must contain one or more feedback loops. In addition, an element of the feedback loop (in this case A or B activities) must be ultrasensitive in nature, having sigmoid response curves (bottom).

For a system to be bistable, a component (or multiple components) of the contributing feedback loops must also exhibit ultrasensitivity (Fig 1-7). That is, the output response is low in the presence of “noise levels” of signal perturbations but once there is enough amplitude in the signal, the output response rapidly and exponentially increases until full response is reached, creating a sigmoidal (s-shaped) dose-response curve. The classic example of an ultrasensitive system is the hemoglobin molecule, a tetramer with four oxygen binding sites, used to store and deliver oxygen to human tissues. Binding is cooperative in hemoglobin. As one site binds O_2 , it increases the binding affinity of each remaining binding site. Thus, much more energy is needed for the initial O_2 binding event, but once a binding site “catches” an O_2 molecule, each subsequent binding event becomes easier and faster until hemoglobin is completely

saturated (reviewed in (Ferrell 2009)). Ultrasensitivity is useful in biological systems because it creates a sharp transition between “on” and “off” states. Thus, bistability allows the cell cycle to rapidly start DNA replication in S phase, stop protein and organelle synthesis during the switch into mitosis, and restart protein synthesis while prohibiting mitotic events during G1.

Evidence for Mitotic Entry as a Bistable Event

Pioneering work in cell cycle modeling predicted that a bistable trigger facilitates the switch-like transition between interphase and mitosis (Tyson 1991; Novak and Tyson 1993; Novak and Tyson 1993; Thron 1996). The model argues that bistability ensures that there are two stable steady states for the cell cycle, interphase or mitosis, and predicts a Cdk1 activity threshold for mitotic entry, and a lower Cdk1 activity threshold for mitotic exit, thus giving rise to hysteresis in the system.

Recent studies in *Xenopus laevis* and human cell extracts validated that the mitotic transition is driven by at least two major feedback loops: the Cdk1-Wee1 double negative feedback loop, in which Cdk1 and Wee1 inactivate one another by phosphorylation, and the Cdk1-Cdc25 positive feedback loop, where Cdk1 phosphorylates and activates Cdc25, while Cdc25 dephosphorylates and further activates Cdk1 (Pomerening, Sontag et al. 2003; Pomerening, Kim et al. 2005; Kim and Ferrell 2007; Deibler and Kirschner 2010; Trunnell, Poon et al. 2011).

In *Xenopus* egg extracts, ultrasensitivity in Wee1 inactivation is attributed to competition between essential and non-essential Cdk1 phosphosites on Wee1 and between Wee1 and other Cdk1 substrates (Kim and Ferrell 2007). More recently it was

also shown in *Xenopus* egg extracts that Cdk1 multisite phosphorylation of Cdc25 contributes to the highly ultrasensitive activation of Cdc25 and Cdk1 (Trunnell, Poon et al. 2011). These *ex vivo* results corroborate mathematical data showing important contributions of Wee1 and Cdc25 multisite phosphorylation to the bistability of mitotic entry (Yang, MacLellan et al. 2004; Domingo-Sananes and Novak 2010). While *ex vivo* and mathematical models suggest that both Cdk1-Wee1 and Cdk1-Cdc25 feedback loops contribute to the robustness of the mitotic entry switch, the existence of the feedback loop has not been explored in cycling cells, nor has the perturbations of the feedback loops *in vivo* been explored.

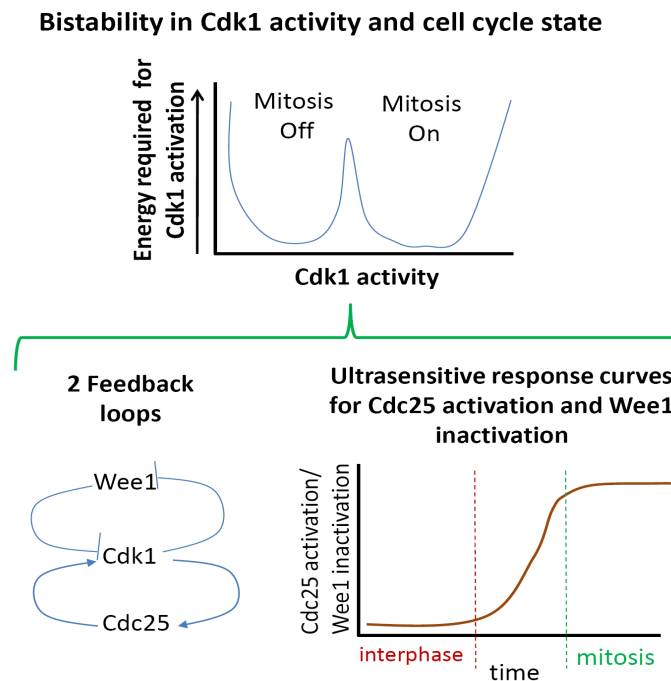


Figure 1-8. Cdk1 activity exhibits bistability.

The bistability of Cdk1 activity is contributed by two feedback loops: the Wee1-Cdk1 negative feedback loop, and the Cdk1-Cdc25 positive feedback loop. Of importance to Cdk1 bistability, in *Xenopus* cell lysates, both these feedback loops show ultrasensitivity in Cdc25 activation or Wee1 inactivation.

***Schizosaccharomyces pombe* as a Model Organism for Cell Cycle Studies**

S. pombe was originally isolated by Paul Lindner in 1783 from the East African beer called pombe in Swahili (Lindner 1893). By the 1950s, Mitchison and Leupold were separately using *S. pombe*. While Leupold took advantage of the propensity for *S. pombe* to grow as a haploid organism to study genetic events such as recombination, mutation and mating; Mitchison realized that the size of *S. pombe* was a good indication of cell cycle progression and related cell cycle changes to environmental and nutritional cues (reviewed in (Nurse 2004)).

Paul Nurse united the two fields of *S. pombe* studies in the mid 1970s. Using genetics to understand cell cycle components, Nurse published the landmark Nature paper in 1978 finding a link between accumulation of mRNA levels with cell cycle progression (Fraser and Nurse 1978). Around the same time that fission yeast was starting to be used for biochemical and genetic explorations of the cell cycle, studies in *Xenopus* and sea urchin egg extracts had found that a factor called MPF (mitosis promoting factor) is necessary for mitotic entrance. In addition, genetic studies in *S. cerevisiae* and *S. pombe* had isolated a number of cell cycle mutants that suggested a complex signal network drives cell cycle progression. In the following decade, the Nurse lab went on, using genetics, to isolate for the first time, cell cycle regulators such as *cdk1* (which was originally called *cdc2* in *S. pombe*), *wee1* (along with other *wee* mutants that were small or “wee”) and *cdc25* (*cell division cycle 25* mutant), along with many other *cdc*-deficient mutants. Expression of *cdc2* protein product confirmed that Cdc2 is the kinase component of MPF and the master regulator of mitosis when associated with CyclinB (Cdc13 in *S. pombe*) (reviewed in (Murray and Hunt 1993). Later, these genes,

and subsequent gene products were also found to play important roles in humans and other metazoans. Thus, *S. pombe* played an important role in the early identification of key cell cycle regulators.

The fission yeast, *S. pombe*, is an excellent system to explore eukaryotic cell cycle control due to its genetic and biochemical tractability as well as its easily observable growth and division patterns (Fig. 1-9). A characteristic that is important for this study into mitotic entry and mitotic events, is that *S. pombe* elongates lengthwise during interphase and halts its growth during mitosis and cytokinesis, thus, a measurement of cell length at septation is an effective assay to estimate length at mitotic entrance and in turn, time to mitosis

Furthermore to facilitate biochemical and genetic studies, *S. pombe* has a fully sequenced genome that can be manipulated experimentally. Fission yeast prefers to grow as a haploid, easily uptakes mutagenic plasmids via electroporation or other established transformation methods, and rapidly recombines its DNA with plasmid DNA. In addition, many established biological, genetic and biochemical techniques are available for *S. pombe* to dissect molecular mechanisms. Finally, *S. pombe* contains proteins that are conserved throughout eukaryotes, allowing for global understanding of the molecular mechanisms that control the cell cycle.

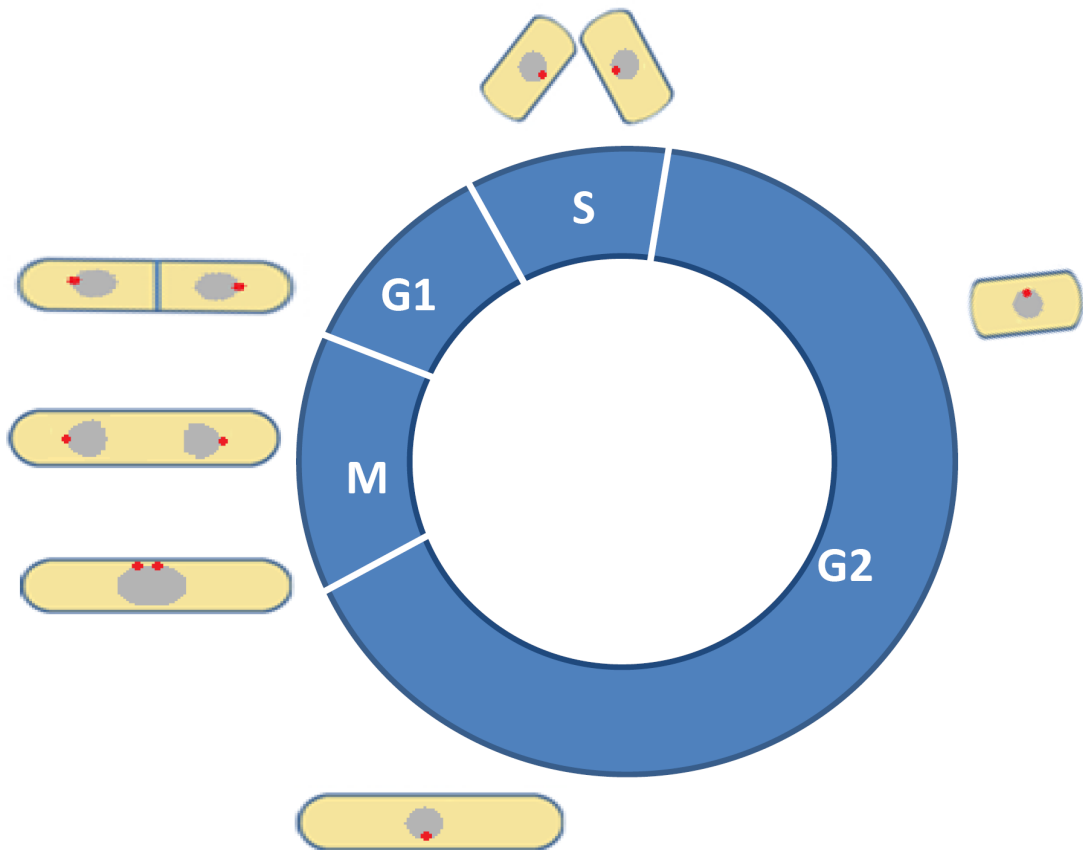


Figure 1-9. The *S. pombe* cell cycle.

S. pombe progresses through all normal phases of the eukaryotic cell cycle, making it a good model organism to study cell cycle control. In addition, *S. pombe* grows by tip elongation and divides by medial fission. Cells stop elongating after mitotic entry and remain the same length until cytokinesis, making septation length a sensitive assay to dissect disturbances in mitotic entrance and exit control.

Summary

In this thesis, I describe my studies on the role of Cdk1 phosphorylation on Cdc25 and how this in turn affects the timing of mitotic entry and mitotic events. In Chapter II, I describe the techniques used in this study. In Chapter III, I ask if Cdk1 phosphorylation controls Cdc25, nuclear localization, stabilization or activation. I found that Cdk1 phosphorylation directly activates Cdc25 but does not affect Cdc25 localization, stabilization during the cell cycle, or ubiquitylation and degradation at mitotic exit. In Chapter IV, I examine the mechanism of Cdk1 phosphorylation on Cdc25, showing that Cdc25 phosphorylation by Cdk1 is ultrasensitive, distributive, and disordered. In addition, I use *S. pombe* as an undisrupted cell system to show that removing Cdc25 phosphorylation by Cdk1 removes a cell's ability to precisely time mitosis, and maintaining Cdc25 on Cdk1 phosphosites during late mitosis prevents cells from precisely regulating the timing of the mitotic exit switch. Finally, I show collaborative mathematical modeling data, developed by Dr. Maria Rosa Domingo-Sananes and Dr. Bela Novak from Oxford University, that incorporates the mechanism of Cdc25 phosphorylation by Cdk1. From this model we are able to mathematically verify my experimental data on the effects of disrupting the Cdc25-Cdk1 positive feedback on mitotic timing. In Chapter V, I summarize our data and describe ongoing studies that will further examine Cdc25 phosphoregulation, mitotic switch timing, and the mechanisms of Cdc25 activation.

In all, this work underscores the usefulness of *S. pombe*, as an organism to study feedback in biological switches within undisrupted cells. In addition, I examined a previously undiscovered mechanism of Cdc25 phosphorylation and activation. Finally, I

show, for the first time, that Cdc25 is not only involved in mitotic entry but also functions in regulating late mitotic events to prepare the cell for mitotic exit.

CHAPTER II

MATERIALS AND METHODS

Strains, Media, and General Methods

Yeast strains used in this study (Table 2-1) were grown in Yeast Extract (YE) or Edinburgh minimal medium with appropriate supplements. *nda3-KM311* cells were grown at 32°C and arrested at 18°C for 6.5 hours. For block and release experiments, after arresting in 18°C, cells were released back into 32°C and collected at intervals. For hydroxyurea (HU) synchronized cells, cells were grown in 12 mM HU for 3.5 hours at 32°C. *mts3-1* or *mts3-1 lid1-6* cells were grown at 25°C and arrested for 4 hours at 36°C.

Strains were constructed using tetrad dissection or random spore analysis. To replace *cdc25* mutants at the endogenous *cdc25* locus, *cdc25+ / cdc25 Δ ^{ura4+}* diploids were transformed with the *cdc25* mutant gene in a pIRT2 vector. Haploid cells were selected for incorporation of the vector. Then, haploid cells that integrated mutant *cdc25* were recovered based on resistance to 5-fluorouracil (5-FOA). *cdc25⁺* and *cdc25* mutant genes were tagged at the 3' end of the ORF at their endogenous loci with V5::kan^R, linker-GFP::kan^R, or linker-HBH::kan^R cassettes as previously described (Bähler, Wu et al. 1998). Yeast transformations were carried out using the lithium acetate method (Keeney and Boeke 1994). Integrants of *cdc25* mutants and kan^R cassettes were screened by whole-cell PCR to ensure proper genomic placements. The GFP tags were also visualized with fluorescence microscopy to ensure expression.

All statistics were calculated with and graphs made using the Graphpad Prism software (GraphPad Software, CA) or using Microsoft Excel (Microsoft, WA).

Table 2-1: Strains used in this study

Strain	Genotype	Reference
KGY42	<i>h⁻ cdc25-22 ura4-D18 leu1-32</i>	Lab stock
KGY246	<i>h⁻ ade6-M210 leu1-32 ura4-D18</i>	Lab stock
KGY3612	<i>h⁻ nda3-KM311 ura4-D18 leu1-32</i>	Lab stock
KGY7836	<i>h⁻ cdc25-HBH::kan^R ura4-D18 ade6-M21X leu1-32</i>	Lab stock
KGY8415	<i>h⁻ sid4-HBH::kan^R ura4-D18 ade6-M210 leu1-32</i>	Lab stock
KGY9476	<i>h⁻ nda3-KM311 ura4-D18 leu1-32</i>	Lab stock
KGY9678	<i>h⁻ mts3-1 cdc25-HBH::kan^R ura4-D18 ade6-M21X leu1-32</i>	Lab stock
KGY9880	<i>h⁻ mts3-1 lid1-6 cdc25-HBH::kan^R ura4-D18 ade6-M21X leu1-32</i>	Lab stock
KGY9985	<i>h⁻ mts3-1 lid1-6 clp1::ura4⁺ cdc25-HBH::kan^R ura4-D18 ade6-M21X leu1-32</i>	Lab stock
KGY10264	<i>h⁺ sid4-RFP::kan^R cdc25-linkerGFP::kan^R ade6-M210 leu1-32 ura4-D18</i>	This study
KGY10280	<i>h⁺ sid4-RFP::kan^R cdc25-13A-linkerGFP::kan^R leu1-32 ura4-D18 ade6-216</i>	This study
KGY10326	<i>h⁺ cdc25-13A-V5::kan^R ura4-D18 ade6-216 leu1-32</i>	This study
KGY10327	<i>h⁺ cdc25-V5::kan^R</i>	This study
KGY10328	<i>h⁻ nda3-KM311 cdc25-V5::kan^R</i>	This study
KGY10329	<i>h⁻ nda3-KM311 cdc25-13A-V5::kan^R</i>	This study

Strain	Genotype	Reference
KGY10715	<i>h⁺ cdc25-S143A ura4-D18 ade6-M210 leu1-32</i>	This study
KGY11010	<i>h⁻ nda3-KM311 clp1::ura4⁺ cdc25-13A-V5::kan^R ade6-216 ura4-D18</i>	This study
KGY11683	<i>h⁹⁰ wee1::ura4⁺ cdc25-13A-V5::kan^R leu1-32 ura4-D18</i>	This study
KGY11686	<i>h⁺ cdc2-33 cdc25-13A-V5::kan^R ade6-216 leu1-32</i>	This study
KGY11687	<i>h⁹⁰ cdc2-33 cdc25-V5::kan^R</i>	This study
KGY11695	<i>h⁺ cdc25-5A-1 ade6-216 leu1-32</i>	This study
KGY11796	<i>h⁹⁰ cdc25-3A-1 (66A,143A,332A) ura4-D18 leu1-32 ade6-216</i>	This study
KGY11844	<i>h⁻ cdc13-117 cdc25-V5::kan^R</i>	This study
KGY11845	<i>h⁻ cdc13-117 cdc25-13A-V5::kan^R ura4-D18</i>	This study
KGY11846	<i>h⁻ cdr2::ura4⁺ cdc25-V5::kan^R ura4-D18</i>	This study
KGY11847	<i>h⁻ cdr2::ura4⁺ cdc25-13A-V5::kan^R leu1-32 ura4-D18</i>	This study
KGY11848	<i>h⁻ cdc2-L7 cdc25-V5::kan^R</i>	This study
KGY11849	<i>h⁺ cdc2-L7 cdc25-13A-V5::kan^R leu1-32</i>	This study
KGY11946	<i>h⁺ cdc25-11A ura4-D18 leu1-32 ade6-216</i>	This study
KGY11947	<i>h⁹⁰ cdc25-7A ade6-216 leu1-32</i>	This study
KGY11948	<i>h⁻ clp1::ura4⁺ cdc25-13A-V5::kan^R ura4-D18</i>	This study
KGY11949	<i>h⁺ cdc25-9A ura4-D18 leu1-32 ade6-M210</i>	This study
KGY11955	<i>h⁺ cdc25-3A-2 (104A,332A,351A) ura4-D18 leu1-32</i>	This study
KGY12200	<i>h⁻ cdr1::ura4⁺ cdc25-V5::kan^R ura4-D18 ade6-216 leu1-32</i>	This study

Strain	Genotype	Reference
KGY12201	<i>h⁻ clp1::ura4⁺ cdc25-V5::kan^R ura4-D18 ade6-216 leu1-32</i>	This study
KGY12202	<i>h⁻ wee1::ura4⁺ cdc25-V5::kan^R ura4-D18 leu1-32</i>	This study
KGY12023	<i>h⁺ clp1::ura4⁺ sid4-RFP::kan^R cdc25-13A-linkerGFP::kan^R ura4-D18 ade6-M210 leu1-32</i>	This study
KGY12022	<i>h⁺ cdr1::ura4⁺ cdc25-13A-V5::kan^R ura4-D18 ade6-216 leu1-32</i>	This study
KGY12072	<i>h⁻ clp1::ura4⁺ sid4-RFP::kan^R cdc25-linkerGFP::kan^R ura4-D18</i>	This study
KGY12615	<i>h⁺ cdc25-5A-2 ura4-D18 leu1-32 ade6-216</i>	This study

Molecular Biology Techniques

Plasmid constructions were performed with standard molecular biology techniques. DNA oligonucleotides (Table 2-2) were purchased from Integrated DNA Technologies, Inc. (Iowa). Site-directed mutagenesis was carried out using oligonucleotides in Quikchange Site-Directed or Lightning Multisite-Directed Mutagenesis Kits (Agilent, CA) according to the manufacturer's suggestions. DNA sequencing by GenHunter Corp. (Nashville, TN) was used to verify mutations in plasmids and following whole-cell PCR of mutations integrated at the *cdc25* locus.

Table 2-2. Oligonucleotides used for mutagenesis.

oligonucleotide name	oligonucleotide sequence
<i>cdc25-S3A</i>	5'-AACTAAAATGGATGCTCCGCTTTCTTCAC-3'
<i>cdc25-S3A GC</i>	5'-GTGAAGAAAGCGGAGCATCCATTTTAGTT-3'
<i>cdc25-S66A</i>	5'-TTGTTTCGACAGCTGCTCCTGCATCTTCCTT-3'
<i>cdc25-S66A GC</i>	5'-AAGGAAGATGCAGGAGCAGCTGTCTGAACAA-3'
<i>cdc25-S84T89A</i>	5'-GCATATCGATGAAGCCCCTGCCTTACCGGCGCCTCGTCGTACGCT-3'
<i>cdc25-S84T89A GC</i>	5'-AGCGTACGACGAGGCGCCGGTAAGGCAGGGGCTTCATCGATATGC-3'
<i>cdc25-S84A</i>	5'-TGCATATCGATGAAGCTCCTGCCTTACCGACTCC-3'
<i>cdc25-S84A GC</i>	5'-GGAGTCGGTAAGGCAGGAGCTTCATCGATATGCA-3'
<i>cdc25-T89A</i>	5'-GCGTACGCCGCGGAGCCGGTAAGGCAGGGGCTTCATCG-3'
<i>cdc25-T89A GC</i>	5'-CGATGAAAGCCCTGCCTTACCGGCTCCGCGCGTACGC-3'
<i>cdc25-T104S113S118A</i>	5'-CTTTCTTGTACTGTAGAAGCCCCTCTCGCTAACAAGACTATTGTTG CACCTCTCCCCGAGGCACCTCGAATGACGC-3'
<i>cdc25-T104S113S118A GC</i>	5'-GCGTCATTCGAGGGTGCCTCGGGGAGAGGTGCAACAATAGTCTTG TTAGCGAGAGGGGCTTCTACAGTACAAGAAAG-3'
<i>cdc25-T104A</i>	5'-TCTACTGTAGAAGCTCCTCTCGCTAAC-3'
<i>cdc25-T104A GC</i>	5'-GTTAGCGAGAGGAGCTTCTACAGTAGA-3'
<i>cdc25-S113S118A</i>	5'-AAGACTATTGTTGCTCCTCTCCCGGAGGCTCCCTCGAATGACG-3'
<i>cdc25-S113S118A GC</i>	5'-CGTCATTCGAGGGAGCCTCCGGGAGAGGAGCAACAATAGTCTT-3'
<i>cdc25-S143A</i>	5'-GTATTCCATTACCCAAGATGCCCTCGAGTTTCCAGCACTATTGC-3'
<i>cdc25-S143A GC</i>	5'-GCAATAGTGCTGGAAACTCGAGGGGCATCTTGGGTAATGGAATAC-3'
<i>cdc25-S308A</i>	5'-CAAGCTGCACCCATTAACCTATTGATATGTTACC-3'
<i>cdc25-S308A GC</i>	5'-GGTAACATATCAATAGGTTTAATGGGTGCAGCTTG-3'
<i>cdc25-S332S334A</i>	5'-CCTAGCTTGAAAGTTAGGGGCGCCTGCTCCGATGGCATTTCGC-3'
<i>cdc25-S332S334A GC</i>	5'-CCTAGCTTGAAAGTTAGGGGCGCCTGCTCCGATGGCATTTCGC-3'
<i>cdc25-S332A</i>	5'-TTGAAAGTTAGGGCCCCTTCTCCGATGA-3'
<i>cdc25-S332A GC</i>	5'-TCATCGGAGAAGGGGCCCTAACTTTCAA-3'
<i>cdc25-S351A</i>	5'-GATGAGCAAGATGCTCCAGTGCTTCGT-3'
<i>cdc25-S351A GC</i>	5'-ACGAAGCACTGGAGCATCTTGCTCATC-3'
<i>cdc25-T379A</i>	5'-GCCAAGATCTTGTGTGCGTGGCGCCAAAACAATCGACC-3'
<i>cdc25-T379A GC</i>	5'-GGTCGATTGTTTTGGCGCCACGCACACAAGATCTTGGC-3'

Immunoprecipitations and Immunoblots

Whole cell lysates were prepared in supplemented (1 mM PMSF, 1 mM benzamidine) NP-40 buffer (6 mM Na₂HPO₄, 4 mM NaH₂PO₄-H₂O, 1% NP-40, 300 mM NaCl, 2 mM EDTA, 50 mM NaF, 4 µg/mL leupeptin, 0.1 mM Na₃VO₄) and cells were lysed using bead disruption. Cdc25-V5 lysates were immunoprecipitated with anti-V5 antibody (Invitrogen, CA) and then incubated with Protein G sepharose (1:1 beads to NP40 buffer)(GE life sciences, NJ), for 1 hour each. For λ phosphatase treatment, protein G beads were washed with 1x phosphatase buffer (50 mM HEPES, 100 mM NaCl, 2 mM DTT, 0.1 mM MgCl₂, 0.1 mM EGTA). Beads were then incubated with λ phosphatase (NEB, MA) in phosphatase buffer for 30 mins at 30°C. Immunocomplexes were mixed with SDS sample buffer and boiled before separation by 8% acrylamide SDS-PAGE and visualized by immunoblot using anti-Cdc25 (gift of Paul Russell). Cell lysates were probed with anti-Cdk1 (PSTAIRE) (Invitrogen, CA) as a loading control. For immunoblot analysis, membranes were treated with a fluorescently labeled secondary antibody and laser scanned using the Odyssey machine (LI-COR, NE).

Tandem Affinity Purification of Cdc25-TAP

Tandem affinity purification of Cdc25-TAP was performed as described (Tasto et al. 2001). Briefly, approximately 2.5×10^9 *nda3-KM311 cdc25-TAP* cells were collected from a culture incubated at 19°C for 6.5 hours to arrest cells in prometaphase. Cells were lysed for 8 minutes (30 seconds lysis, 30 seconds rest) on ice using bead disruption in supplemented NP40 buffer. Lysates were transferred to 3x 50 ml falcon tubes and spun at 3000 RPM for 10 minutes. Supernatant was removed to new tubes and 800 µL IgG sepharose bead slurry (1:1 beads to NP-40 buffer) (GE Life Sciences, NJ) per tube was

added and then incubated at 4°C on a rotating platform for 1 hour. IgG beads were allowed to pack by gravity in a 0.8x4 cm Poly-prep chromatography column (Biorad, CA) at 4°C. Beads were washed with 30 mL IPP150 buffer (10 mM Tris HCl pH 8.0, 300 mM NaCl, 0.1% NP-40) and then washed with 10 mL TEV cleavage buffer (IPP150 buffer with 0.5 mM EDTA). Beads were then incubated in a capped column with 500 units of TEV protease (recombinant protein from *E. coli*) in 1 mL TEV cleavage buffer for 1.5 hours at 18°C on a rotating platform. The flow through was drained to a new sealed column and the old column was washed with 1 mL TEV cleavage buffer and flow through was collected in the new column with previous flow through. 6 mL of CBB (10 mM Tris-HCl, pH 8.0, 300 mM NaCl, 1 mM Mg²⁺ Acetate, 1 mM imidazole, 2 mM CaCl₂, 10 mM β mercapto-ethanol) and 6 μL 1M CaCl₂ were added to the new column. 300 μL of calmodulin beads (1:1 beads to CBB) (Agilent, CA) was added and the solution was incubated at 4°C on a rotating platform for 1 hour. Beads were washed 2x by gravity in CBB with 0.1% NP-40, then 1x in CBB with 0.02% NP-40 at 4°C. Protein was eluted with CEB (10 mM Tris-HCl, pH 8.0, 300 mM NaCl, 0.02% NP-40, 1 mM Mg²⁺ acetate, 1 mM imidazole, 20 mM EGTA, 10 mM β-mercapto-ethanol). Flow through was collected and protein pellet was collected through trichloroacetic acid precipitation (25% TCA).

In vivo Ubiquitylation Assay

Cdc25-HBH and Sid4-HBH proteins were purified using a previously developed fully denatured two-step purification method at room temperature (Johnson and Gould 2011). Cells were lysed using bead disruption in pH 8.8 buffer 1 (4 mM imidazole, 0.5% NP40, 300 mM NaCl, 50 mM NaPO₄, and 8 M urea). Lysates were incubated with Ni²⁺-

NTA agarose beads (Qiagen, CA) for 3 hours at room temperature. Beads were washed 4x in pH 6.3 buffer 3 (20 mM imidazole, 0.5% NP40, 300 mM NaCl, 50 mM NaPO₄, and 8 M urea). Protein was then eluted in pH 4.3 buffer 4 (0.5% NP40, 200 mM NaCl, 50 mM NaPO₄, 8 M urea, 10 mM EDTA, 2% SDS and 100 mM Tris HCl). The elution was adjusted to pH 8 and incubated overnight with streptavidin ultra-link resin (Pierce, IL) at room temperature. Streptavidin beads were then washed 4x in pH 8 buffer 6 (200 mM NaCl, 2% SDS, 100 mM Tris HCl and 8 M urea) and then 1x pH 8 buffer 7 (200 mM NaCl, 100mM Tris HCl, and 8 M urea). Beads were mixed with SDS sample buffer and boiled before separation by 8% acrylamide SDS-PAGE and visualized by immunoblot using anti-streptavidin (Li-COR Odyssey, NE) or anti-ubiquitin (Roche, IN).

***In vitro* Cdk1 Kinase Assay**

Recombinant MBP fusion proteins were produced in and purified from *E. coli*. Recombinant Cdc2-Cdc13 (Cdk1-CyclinB in *S. pombe*) was purified from baculovirus infected insect cells (gift of Robert Fisher). *in vitro* Cdk1 kinase and Cdc25 phosphatase assays were performed as previously described (Kovelman and Russell 1996; Wolfe and Gould 2004). For *in vitro* Cdk1 kinase assays, 100 ng (1x Cdk1 levels) or varying levels (0.02x to 10x) of recombinant Cdc2-Cdc13 was used to phosphorylate 1 µg of MBP tagged proteins in kinase buffer (10 µM Tris HCl, pH7.4, 10 µM MgCl₂, 100 nM DTT) supplemented with 10 µM cold ATP and 5 µCi γ -³²P-ATP. Proteins were incubated for 30 minutes at 30°C and reactions were terminated by addition of 1:1 SDS sample buffer. Samples were boiled and separated by SDS-PAGE. Coomassie blue staining or western

blot was used to visualize proteins. Autoradiography was used for detection of phosphorylated proteins.

Cdc25 Activity Assay

Cdc25 activity assays were performed as previously described (Kovelman and Russell 1996; Wolfe and Gould 2004). Briefly, 5×10^8 cells from *nda3-KM311* prometaphase blocked samples were lysed in buffer A (300 mM NaCl, 5 mM disodium EDTA, 10 mM EGTA, 25 mM MOPS-NaOH, 60 mM β -glycerol phosphate, 1 mM Na_3VO_4 , 1 mM DTT, 1 mM PMSF). As loading control, 10 μl of each lysate was combined with SDS sample buffer, boiled, resolved by SDS-PAGE, and immunoblotted with anti-Cdk1 (PSTAIRE) to detect Cdk1. Anti-V5 antibody and protein G sepharose (GE Life Sciences, NJ) were used to immunoprecipitate Cdc25-V5 from the rest of the lysates. Immunocomplexes were washed with Buffer C (100 mM NaCl, 5 mM disodium EDTA, 10 mM EGTA, 25 mM MOPS-NaOH, 1 M DTT, 50 mM NaF, 0.1% NP40). Beads containing the mitotic forms of Cdc25-V5 were added to protein lysates of *cdc25-22* blocked cells (6×10^7) lysed in buffer B (100 mM NaCl, 5 mM disodium EDTA, 10 mM EGTA, 25 mM MOPS-NaOH, 60 mM DTT, 50 mM NaF, 1 mM PMSF) incubated for 15 mins at 30°C and pelleted. Supernatants were moved to a new tube and beads were washed with buffer D (100 mM NaCl, 15 mM MgCl_2 , 10 mM EGTA, 25 mM MOPS-NaOH, 60 mM β -glycerol phosphate, 1 mM Na_3VO_4 , 1 M DTT, 1 mM PMSF). Protein bound beads were spun down and wash buffer was added to previously collected supernatants. SDS sample buffer was added to beads, samples were boiled and separated by SDS-PAGE. Cdc25-V5 was visualized with anti-Cdc25 antibody. For histone H1

kinase assays, Cdk1-Cdc13 was immunoprecipitated from the remaining supernatants using affinity purified anti-Cdc13 antibody (GJG8) and incubated with 1 mg histone H1 with 10 μ M cold ATP and 5 μ Ci γ - 32 P ATP as previously described (Gould, Moreno et al. 1991). Histone H1 was visualized by Coomassie blue staining after boiling with SDS sample buffer and SDS-PAGE separation. The relative activity of Cdc25 was estimated using the equation:

$$\text{Specific activity} = \frac{(\text{CPM})/[\text{Histone H1}]}{([\text{Cdc25}]/[\text{Cdk1}])}$$

Where (CPM) is counts per minute for 32 P-labeled histone H1 measured with a scintillation counter. [histone H1] is the relative amount of histone H1 visualized by Coomassie blue staining and quantified with ImageJ software. Final (CPM)/[histone H1] was calculated for each experimental group after subtraction of CPM in the untagged control. [Cdc25] and [Cdk1] are the relative amounts of Cdc25 and Cdk1 as determined by quantitative immunoblotting on an Odyssey instrument. Protein levels were calculated using ImageJ software.

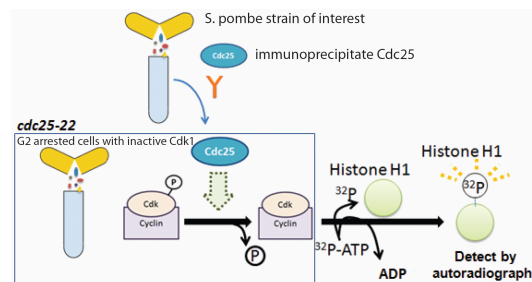


Figure 2-1. Schematic of the Cdc25 activity assay

Cdc25 is immunoprecipitated from a strain of interest then added to cell lysates from cells arrested in G2 with inactive Cdc2-Cdc13. Activated Cdc2-Cdc13 is then immunoprecipitated and its activation level is assayed by measuring its ability to phosphorylate histone H1, a native Cdk1 substrate.

Microscopy

For measuring cell lengths at septation, and fluorescence intensity measurements, cells were grown at 25°C or 32°C to midlog phase and live cell microscopy was performed using an Ultraview LCI spinning disk confocal microscope (PerkinElmer, Waltham, MA) with 0.6 μm spacing on Z-series optical sections, 60x NA, 1.4 Plan-Apochromat oil immersion object, 488 nm argon ion laser, and 594 nm helium neon laser or with the Olympus IX71 Personal Deltavision microscope (Applied Precision, Issaquah, WA) with 250 W Xenon LED transillumination, 60x NA, 1.56 oil immersion object and 2.25 μm optical axis integration. Images were processed using Metamorph7.1 (MDS Analytical Technologies, CA) or with softWoRx Explorer (Applied Precision) softwares.

Time lapse microscopy was done on the Personal Deltavision microscope (Applied Precision, Issaquah, WA) using the Onix Microfluidic Perfusion System (CellAsic, Hayward, CA) platform, at 30°C for 16 hours and analyzed using softWoRx software.

Tip to tip cell length in septating cells or nonseptating cells were measured by using either the SoftWoRx explorer or Metamorph7.1 software measure length functions. Total cellular Cdc25-GFP fluorescence was measured using ImageJ by equalizing background fluorescence between fields and selectively boxing two areas: (box1) an area including the cell and (box2) an area including both the cell and its surrounding background. Total fluorescence for the cell was obtained by subtracting total fluorescence of (box2) by (box1).

2D Tryptic Peptide Mapping

MBP-Cdc25 or MBP-Cdc25-S143A was purified and subjected to *in vitro* Cdk1 kinase assay as described (Gould, Moreno et al. 1991). ³²P-labeled proteins were mixed with SDS sample buffer and boiled before separation by 8% SDS-PAGE and were then transferred to PVDF membranes. Labeled proteins on PVDF membranes were pretreated with methanol for 30 seconds and incubated for 30 mins at 37°C in 50 mM ammonium bicarbonate and 0.1% Tween20. Membranes were washed in 1 ml of 50 mM ammonium bicarbonate and treated twice with 10 µg trypsin in 50 mM ammonium bicarbonate for 3h at 37°C to separate phosphopeptides from membrane. Phosphopeptides were lyophilized and separated on TLC plates in two dimensions (electrophoresis at pH 1.9 and then chromatography) as previously detailed (Boyle, van der Geer et al. 1991).

Mass Spectra Sample Preparation

Purified Cdc25 was TCA precipitated and resuspended in 8 M urea in 100 mM Tris-HCl, pH 8.5. Protein was reduced with 100 mM tris (2-Carboxyethyl) phosphine hydrochloride (Thermo Scientific, MA), and alkylated with 100 mM iodoacetamide (Sigma-Aldrich, MO). After diluting the sample to 2 M urea, the sample was digested overnight with 0.4 µg/µl trypsin or chymotrypsin at 37°C.

Peptides were loaded onto a diphasic MudPIT column on a pressure loader, separated on a 10 cm 3 µm C18 column using a 12-point MudPIT salt gradient (McDonald and Yates 2002) and analyzed with a LTQ mass spectrometer (Thermo Scientific). Agilent high performance liquid chromatography was used in line with FAMOS autosampler for 5 µl ammonium acetate injections. Each peptide elution was

separated using a 0 – 90% acetonitrile gradient. Peptide ions were acquired in positive mode with full precursor MS scan ranging from 400 to 2000 m/z, followed by fragmentation of ten most abundant precursors and their natural loss ions of either 98, 49, or 33 m/z, under collision induced dissociation (CID), isolation width of 2.0 for the parent ion and collision energy of 35V. The instrument acquired at least two spectra per eluting species under dynamic exclusion with repeat duration and exclusion duration of 1.5 times the chromatographic peak width at the base, and exclusion list of 150 ions.

Mass Spectra Data Analysis

MS2 spectra were extracted from Thermo RAW files and converted to DTA files using Scansifter v2.1.25 software (Ma, Dasari et al. 2009). Spectra with less than 20 peaks were excluded from our analysis. Cdc25 peptides were searched against the Sanger Institute (www.pombase.org) *S. pombe* protein database (May 2011). Database sequences along with contaminant sequences (keratin and IgG isotopes) were reversed and concatenated. Searches were performed with the Sequest algorithm (TurboSequest v.27 rev12) on a high performance computing cluster allowing for carbamidomethylation, oxidation of the methionine, phosphorylation of serine, threonine, and tyrosine, and acylation of the N-terminus. Peptide mass tolerance was set to 2.5 m/z. The DTAs were searched with trypsin and chymotrypsin as chosen endoproteases, allowing 10 modifications per peptide, and maximum of 2 missed cleavages. Cdc25 peptides were visualized and validated utilizing Scaffold 3 and Scaffold PTM software (Proteome Software, Inc. Portland, OR), with the following identification parameters: minimum of

90% probability for correct protein identification, minimum of 2 peptides per protein, and minimum 95% peptide match probability.

Mathematical Model of the Bistable Mitotic Switch with Cdc25 Multisite

Phosphorylation by Cdk1

I collaborated with Dr. Maria Rosa Domingo-Sananes and Dr. Bela Novak from Oxford University to modify a previous mathematical model of the mitotic switch (Domingo-Sananes and Novak 2010). We expanded on the mechanisms of Cdc25 phosphoregulation and activation by Cdk1, modeling that Cdc25 multisite phosphorylation is distributive, disordered and ultrasensitive in nature. In addition, we assumed that entry into mitosis takes place when the total concentration of Cdc25 reaches a threshold concentration since the previous model (and all other previous models of mitosis) have used Cdc13 (CyclinB) for the threshold and Cdc13 levels are not rate limiting in fission yeast (Bueno and Russell 1993). These changes allow the model described below to replicate the different lengths of the phosphorylation site mutants.

We assumed that both Cdc25 and Wee1 are phosphorylated at multiple sites by Cdk1, and that phosphorylation results in Cdc25 activation and Wee1 inactivation. The activities of Cdc25 and Wee1 will therefore depend on the concentrations of the different phosphoforms and their respective activities.

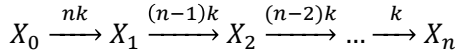
First, because the length of Cdc25 phosphomutants increases gradually as phosphorylation sites are mutated, we reasoned that the activity should increase gradually with each phosphorylation. The simplest assumption is that phosphorylation leads to a linear increase in activity.

Second, because the data indicate that it is the number of mutated sites that determines length at division and not the identity of these sites, we reasoned that the phosphorylation of Cdc25 follows a distributive and disordered phosphorylation mechanism. Finally, to achieve ultrasensitivity in the response of Cdc25 to MPF (Cdk1-Cdc13), we assumed that phosphorylation is cooperative in nature. That is, we assumed that the rate of each phosphorylation reaction increases linearly with the number of phosphorylations (the rate of dephosphorylation decreases with the number of phosphorylations). Assuming this mechanism leads to steady state equations for each phosphoform that closely resemble those for an ordered mechanism, as shown below.

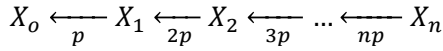
For simplicity, we assumed a similar scheme for Wee1 regulation by Cdk1 phosphorylation, although in this case, the activity decreases linearly with the number of phosphorylations. In our model, ultrasensitivity in the responses of Wee1 and Cdc25 to MPF results from the cooperative phosphorylation mechanism (Trunnell, Poon et al. 2011). In reality, there are probably other sources of ultrasensitivity such as phosphatase regulation (Novak, Kapuy et al. 2010) and substrate competition (Kim and Ferrell 2007). We could also have assumed more complicated changes in activity to closely fit the length of the phosphorylation site mutants, but this could lead to a much more complicated model and risks over-fitting the data.

To describe the model, we derived general equations for the multisite phosphorylation mechanism in order to calculate the concentration of each phosphoform. We consider a protein X with n possible phosphorylation sites, phosphorylated by a kinase k and dephosphorylated by a phosphatase p , and where X_i is the form with i phosphorylations (Kapuy, Barik et al. 2009). For a disordered mechanism, the rates of the

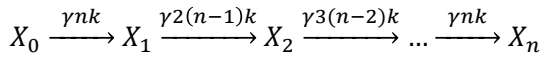
reactions change with the number of phosphorylations (Kapuy, Barik et al. 2009). For the phosphorylation reactions:



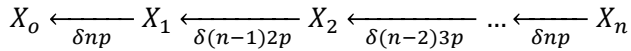
because the number of available sites decreases with each phosphorylation. Similarly, for the dephosphorylation reactions:



If we assume linear positive cooperativity, the phosphorylation rates increase by a factor γ after each phosphorylation site, so combined with the disordered mechanism, they become:



Similarly, the dephosphorylation rates decrease by a factor δ with each phosphorylation, and the rates of the dephosphorylation reactions are:



Written in this way, the factors γ and δ can be incorporated into the kinase and phosphatase activities, k and p . Assuming that all the phosphorylation and dephosphorylation reactions are in equilibrium, and that the sum of all the phosphoforms is X_T , the concentration of each phosphoform is described by an expression similar to that derived for ordered phosphorylation (Kapuy, Barik et al. 2009) because the factors for the disordered and the cooperative mechanisms cancel each other out:

$$X_i = X_T \frac{\left(\frac{k}{p}\right)^i}{\sum_{j=0}^n \left(\frac{k}{p}\right)^j} \tag{1}$$

We used this result to calculate the concentrations of each phosphoform of Cdc25 and Wee1. We assumed that Cdc25 has a total of n_c Cdk1 phosphorylation sites and that the sum of the concentrations of all the forms is $Cdc25_T$. To define the activity of Cdc25, we assumed that the completely unphosphorylated form has a minimum, background activity, k'_{25} , and the fully phosphorylated form has a maximal activity, k''_{25} . We assumed that the activity changes linearly, so that for each phosphoform of Cdc25, the activity is:

$$\phi_{25,i} = k'_{25} + \alpha i \quad (2)$$

where α is the slope of the activity increase, given by:

$$\alpha = \frac{k''_{25} - k'_{25}}{n_c} \quad (3)$$

And we can calculate the total Cdc25 activity, ϕ_{25} , as the sum of the products of the activity of each phosphoform and its concentration, for any value of the kinase to phosphatase ratio:

$$\begin{aligned} \phi_{25} &= \phi_{25,0}Cdc25_0 + \phi_{25,1}Cdc25_1 + \phi_{25,2}Cdc25_2 + \dots + \phi_{25,n_c}Cdc25_{n_c} \quad (4) \\ &= \sum_{i=0}^{n_c} \phi_{25,i}Cdc25_i \end{aligned}$$

Using the previous result for the concentration of the phosphoforms, the total Cdc25 activity is then:

$$\phi_{25} = Cdc25_T \left(k'_{25} + \alpha \frac{\sum_{i=0}^{n_c} i \left(\frac{k}{p}\right)^i}{\sum_{j=0}^{n_c} \left(\frac{k}{p}\right)^j} \right) \quad (5)$$

The summations on the fraction of the above equation can be simplified, since

$$\sum_{i=0}^n ix^i = \frac{x - (n+1)x^{(n+1)} + nx^{n+2}}{(1-x)^2} \quad (6)$$

and the sum of a geometric series:

$$\sum_{i=0}^n x^i = \frac{1 - x^{n+1}}{1 - x} \quad (7)$$

And finally, the equation for the activity of Cdc25 becomes:

$$\phi_{25} = Cdc25_T k_{25} \quad (8)$$

where

$$k_{25} = k'_{25} + \alpha \frac{\left(\frac{k}{p}\right) - (n_c + 1) \left(\frac{k}{p}\right)^{n_c+1} + n_c \left(\frac{k}{p}\right)^{n_c+2}}{\left(1 - \frac{k}{p}\right) \left(1 - \left(\frac{k}{p}\right)^{n_c+1}\right)} \quad (9)$$

which gives the response of Cdc25 to Cdk1 (Fig. 3-8A), since in this case:

$$\frac{k}{p} = \frac{V_{a25} MPF}{V_{i25}} \quad (10)$$

Where MPF is the concentration of active Cdk1-Cdc13 dimers, and V_{a25} a rate constant for phosphorylation of Cdc25 by MPF, and V_{i25} is the rate constant for Cdc25 dephosphorylation by a constant phosphatase activity, part of which corresponds to Clp1.

To model the effect of mutating the Cdk1 phosphorylation sites on Cdc25, we reduced the parameter describing the total number of phosphorylations, n_c . However, the parameter α remained the same, since the activity profile of the different phosphoforms does not change by reducing the number of sites.

For Wee1, we assumed that the completely dephosphorylated form has a maximal activity k''_{wee} , and the fully phosphorylated form has a minimum activity k'_{wee} . If Wee1 has n_w possible Cdk1 phosphorylation sites, and that the concentrations of all the phosphoforms sum to $Wee1_T$, we derive an equation for the Wee1 activity respect to MPF (Fig. 3-8C), ϕ_{wee} , similar to that for Cdc25:

$$\phi_{wee} = Wee1_T k_{wee} \quad (11)$$

where

$$k_{wee} = k_{wee}'' + \beta \frac{\left(\frac{V_{iwee}MPF}{V_{awee}}\right) - (n_w + 1)\left(\frac{V_{iwee}MPF}{V_{awee}}\right)^{n_w+1} + n_w\left(\frac{V_{iwee}MPF}{V_{awee}}\right)^{n_w+2}}{\left(1 - \left(\frac{V_{iwee}MPF}{V_{awee}}\right)\right)\left(1 - \left(\frac{V_{iwee}MPF}{V_{awee}}\right)^{n_w+1}\right)} \quad (12)$$

where V_{iwee} is a rate constant for Wee1 phosphorylation by MPF, and V_{awee} is the rate constant for Wee1 dephosphorylation by a constant phosphatase, and $\beta = (k'_{wee} - k''_{wee})/n_w$.

To complete the model, we write a differential equation for MPF, which is regulated by Wee1 and Cdc25:

$$\frac{dMPF}{dt} = k_{25}Cdc25_T(Cyc_T - MPF) - \phi_{wee}MPF \quad (13)$$

Where Cyc_T , the total amount of Cyclin, is the sum of the active and inactive Cdk1-Cdc13 dimers. Assuming that the system is in steady state, for any value of Cyc_T is possible to calculate $Cdc25_T$ respect to MPF :

$$Cdc25_T = \frac{\phi_{wee}MPF}{k_{25}(Cyc_T - MPF)} \quad (14)$$

To fit our model to the experimental data, we assumed that the length of cells at division is proportional to the Cdc25 threshold for MPF activation, that is, the saddle-node bifurcations shown in Figure 4-5A. Because Cdc13 does not seem to be rate-limiting for MPF activation, we assumed that when $Cdc25_T$ reaches the threshold, Cyclin levels are already very high, so a change in their values has little effect on cell size (see two-parameter bifurcation diagram, Fig. 2-2).

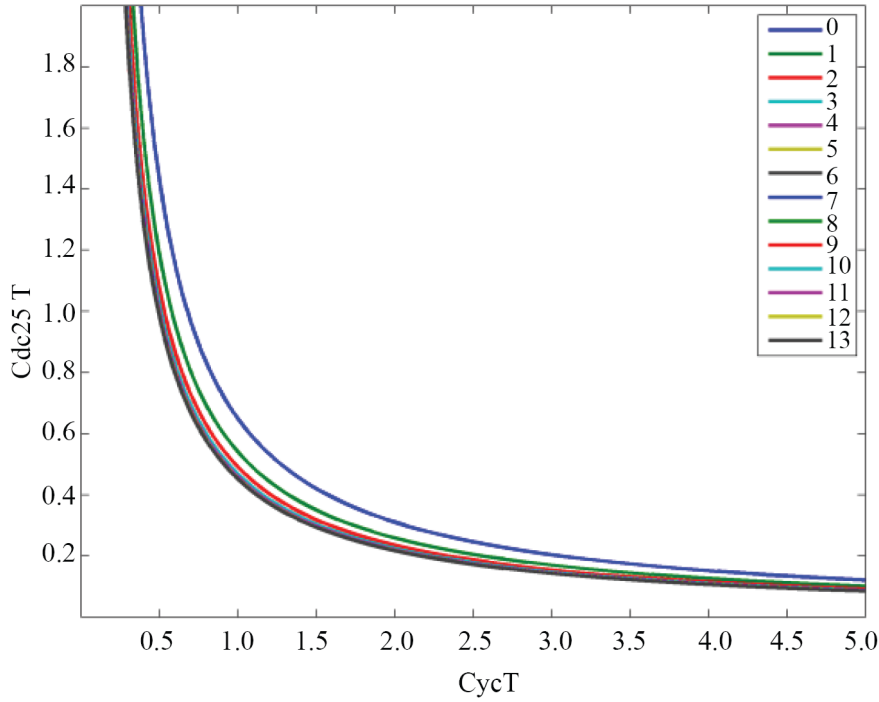


Figure 2-2. Two parameter bifurcation diagram of the model for the MPF activation threshold.

Observe that the Cyclin (Cdc13) level is not rate limiting in the lower right corner of the diagram and MPF activation depends on Cdc25 level only.

For each Cdc25 phosphomutant, we numerically determined the value of the $Cdc25_T$ threshold, θ , and calculate a scaling factor to fit these thresholds obtained from the model to the experimental data. Since we assumed that the cyclin threshold is proportional to length at division:

$$l = \eta\theta \tag{15}$$

where l is the length at division and η is the scaling factor. Therefore, for each mutant, the scaling factor is:

$$\eta = \frac{l}{\theta} \tag{16}$$

We used the average of the scaling factors for all the phosphomutants, η_a , to fit the model to the experimental data, both for all the phosphomutants, cell cycle mutants,

and for the variability analysis, so that the estimated length at division, for each mutant is:

$$l_e = \eta_a \theta \quad (17)$$

Table 2-3 shows the parameter values used for the model, and Table 2-4 describes the parameters changed to model the cell cycle mutants.

Table 2-3. Parameter values for the model

Parameter	Value
V_{a25}	1
V_{i25}	0.2
V_{awee}	0.2
V_{iwee}	2
n_c	13 (wild type)
n_w	11
k'_{25}	0.1
k''_{25}	1
α	0.0692
k'_{wee}	0.1
k''_{wee}	1
β	-0.0818
$Wee1_T$	1
Cyc_T	5

Table 2-4. Parameter changes for cell cycle mutants

Mutant	Parameter change	Comment
<i>clp1Δ</i>	$V_{i25} = 0.1$	Reduce phosphatase on Cdc25 to half of the wild type
<i>wee1Δ</i>	$Wee1_T = 0.6$	Reduce Wee1 levels. Some activity remains, which corresponds to Mik1.
<i>cdc13-117</i>	$V_{a25} = \xi V_{a25,wt}$ $V_{iwee} = \xi V_{iwee,wt}$ $\xi = 0.9$	Reduce MPF activity on Wee1 and Cdc25 by a factor ξ
<i>cdc2-L7</i>	$V_{a25} = \xi V_{a25,wt}$ $V_{iwee} = \xi V_{iwee,wt}$ $\xi = 0.95$	Reduce MPF activity on Wee1 and Cdc25 by a factor ξ
<i>cdc2-33</i>	$V_{a25} = \xi V_{a25,wt}$ $V_{iwee} = \xi V_{iwee,wt}$ $\xi = 0.95$	Reduce MPF activity on Wee1 and Cdc25 by a factor ξ
<i>cdr1Δ</i>	$V_{awe} = 0.25$	Increase phosphatase activity on Wee1
<i>cdr2Δ</i>	$V_{awe} = 0.3$	Increase phosphatase activity on Wee1

Variation of Cell Size Due to Variation in Parameter Values

To determine whether elimination of one of the two positive feedback loops in the mitotic switch could explain the increased variability in cell size observed in the *Cdc25-13A* mutant cells, we decided to look at the effects of noise in parameter values on cell length in our mathematical model. We generated 10,000 random parameter sets for the model of wild type and the same number for the model of the *cdc25-13A* mutant, which lacks the Cdc25-MPF positive feedback loop. To add noise to the model parameters, for each parameter, in each set, we sampled values from a normal distribution with mean equal to the parameter value in the deterministic model and a standard deviation of 2.5%. We did this for all parameters except for the number of phosphorylation sites on Wee1 and Cdc25, which are part of model architecture. Parameters α and β were recalculated appropriately using the randomly generated values of the minimal and maximal activity of Cdc25 and Wee1. For each random set we then calculated the $Cdc25_T$ threshold for MPF activation and the estimated length, using equation 17, thus obtaining a distribution of length values, shown in Figure 4-5B.

CHAPTER III

CDK1 PHOSPHORYLATION OF CDC25 REGULATES CDC25 ACTIVITY

Introduction

At mitotic entry, Cdc25 phosphorylation by Cdk1 is associated with increased Cdc25 concentration, nuclear localization, and activity. While all three mechanisms are thought to contribute to the Cdc25-Cdk1 positive feedback loop that drives rapid mitotic entry, no studies thus far has examined which mechanism of Cdc25 control is directly driven by Cdk1 phosphoregulation.

We previously found that, in *S. pombe*, *clp1Δ* cells had increased levels of Cdc25. As Clp1 specifically dephosphorylates Cdk1 sites, increased Cdc25 accumulation at mitotic entry in *clp1Δ* cells suggested that Cdk1 phosphorylation at mitotic entry could stabilize Cdc25 at mitotic entrance, allowing for rapid activation of Cdk1.

In addition to mitotic entry, we also observed Cdc25 levels at mitotic exit were higher in *clp1Δ* compared to *clp1⁺* cells. Retention of Cdk1 sites on Cdc25 in *clp1Δ* cells may prevent Cdc25 degradation at mitotic exit. To test ubiquitylation-mediated degradation of Cdc25, we over-expressed ubiquitin through a pREP1 vector in cells. Through an ubiquitin immunoprecipitation followed by immunoblotting for Cdc25-MYC we found that, compared to cells with *clp1⁺*, Cdc25 seemed to be decreased in ubiquitylation in *clp1Δ* cells arrested at metaphase. Through the same method, we also found that *lid1-6* cells, with inactivated APC/C ubiquitin ligase, had decreased Cdc25-MYC ubiquitylation during metaphase. Thus we concluded that Cdk1 phosphorylation may stabilize Cdc25 at mitotic entry and allow for Cdc25 accumulation while

dephosphorylation of Cdc25 by Clp1 is important for the APC/C-mediated ubiquitylation and degradation of Cdc25 during late mitosis (Wolfe and Gould 2004).

We also previously tested for Cdc25 localization in *clp1*⁺ and *clp1Δ* cells. Cdc25 is normally retained in the nucleus until late anaphase after which Cdc25 rapidly disappears from the nucleus. In *clp1Δ* cells, Cdc25 is retained in the nucleus until septation, when cells are already in S phase (Wolfe and Gould 2004). Thus, Cdk1 phosphorylation on Cdc25 may retain Cdc25 in the nucleus or prevent Cdc25 export from the nucleus during late mitosis.

In human cells, Cdk1 localizes to the nucleus at mitotic entry partly due to Polo-like kinase phosphorylation of CyclinB that forces nuclear localization of the Cdk1-CyclinB complex (Toyoshima-Morimoto, Taniguchi et al. 2001). In addition, Cdk1 phosphorylation of CyclinB also facilitates rapid nuclear accumulation in an auto-amplification loop (Santos, Wollman et al. 2012). If Cdk1 phosphorylation can drive nuclear localization of Cdc25, then the rapid phosphorylation of Cdc25 by Cdk1 at mitotic entry can serve as a rapid feed forward loop that allows efficient association of Cdc25 and Cdk1.

In this section, we explore the effects of Cdk1 phosphorylation and Clp1 dephosphorylation of Cdc25 on Cdc25 activity, localization, ubiquitylation and stability. We find that Cdk1 phosphorylation directly activates Cdc25 but does not affect Cdc25 abundance during mitotic entry; instead, Cdc25 accumulation is directly related to the size of the cell. In addition, Cdk1 phosphorylation of Cdc25 does not seem to affect Cdc25 nuclear localization at mitotic entrance. Finally, we find Clp1 dephosphorylation of Cdc25 does not facilitate Cdc25 ubiquitylation or degradation at mitotic exit.

Results

Characterization of Cdk1 and Clp1 Specific Phosphosites on Cdc25

To examine how Cdk1 phosphorylation affects Cdc25, we eliminated Cdk1 phosphosites on Cdc25 by mutating all 13 Ser and Thr in the minimal Cdk1 consensus sites (Ser/Thr-Pro) outside of the Cdc25 catalytic domain to non-phosphorylatable alanines (Cdc25-13A). *In vitro*, active recombinant Cdk1-CyclinB phosphorylated recombinant MBP-Cdc25 but not MBP-Cdc25-13A (Fig. 3-1A), indicating that all major *in vitro* Cdk1 sites were abolished in Cdc25-13A. Through tandem-affinity-purification of Cdc25 from prometaphase arrested cells, when Cdc25 is maximally phosphorylated (Kovelman and Russell 1996; Esteban, Blanco et al. 2004; Wolfe and Gould 2004), followed by LC-MS/MS, we identified phosphorylation on all but 2 of these Cdk1 consensus sites (Table 3-1).

We next looked at Cdc25-13A phosphostatus *in vivo*. Endogenously tagged Cdc25-13A-V5 or Cdc25-V5 phosphorylation was assessed by SDS-PAGE mobility in cells arrested in prometaphase. Most of the gel shift due to phosphorylation was eliminated in Cdc25-13A-V5, consistent with Cdk1 being the major kinase for Cdc25 in mitosis, though some remained, suggesting that another kinase(s) contributes to mitotic Cdc25 phosphorylation (Fig. 3-1B).

Clp1 reverses Cdk1-dependent phosphorylations on Cdc25 (Esteban, Blanco et al. 2004; Wolfe and Gould 2004). We therefore expected that the mobility shift of Cdc25-13A would not be affected by *clp1Δ*. Indeed, Cdc25-13A-V5 displayed the same SDS-PAGE mobility with or without Clp1 (Fig. 3-1C), indicating that Cdc25-13A is not a

Cdk1 substrate *in vivo* and that Clp1 is unable to affect the phosphorylation of Cdc25 due to another protein kinase(s).

Finally, *cdc25-13A* cells are significantly longer at septation compared to *cdc25⁺* cells, consistent with delayed mitotic entry and decreased Cdk1 activation due to removal of the Cdk1-Cdc25 positive feedback loop (Fig. 3-1D).

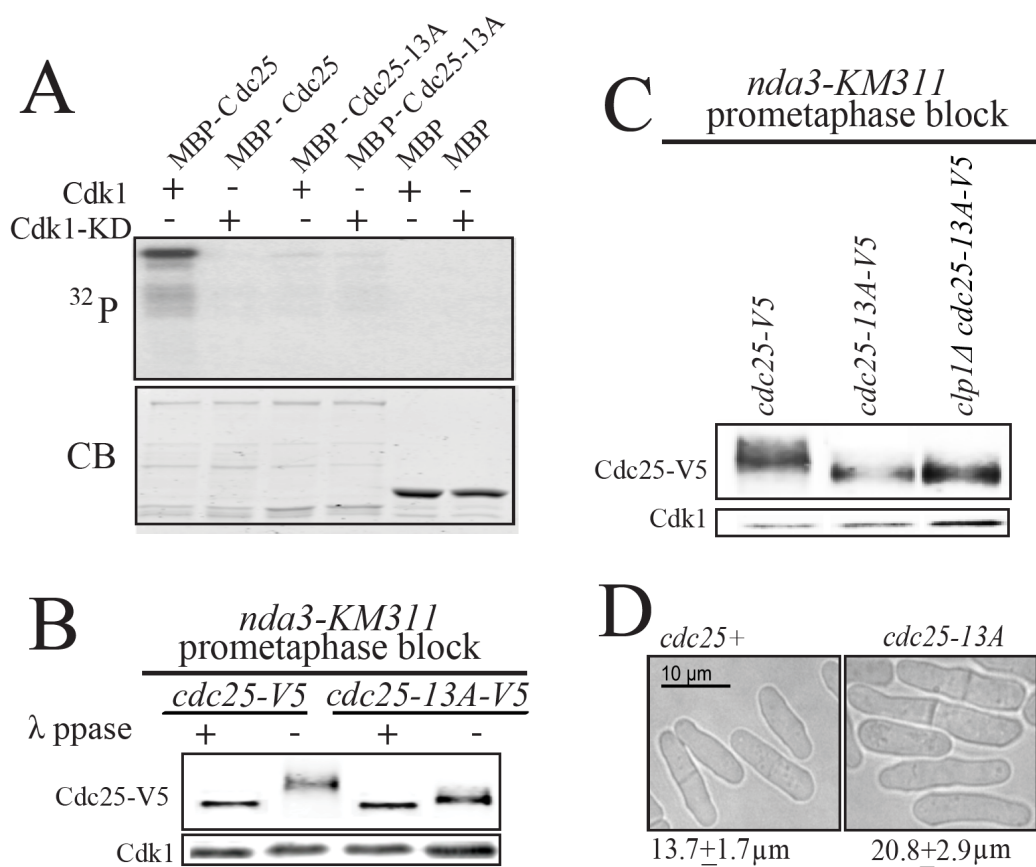


Figure 3-1. Characterization of Cdc25 phosphomutant.

(A) Recombinant MBP-Cdc25, MBP-Cdc25-13A, or MBP was incubated with active Cdk1-CyclinB (Cdk1) or kinase dead Cdk1-CyclinB (Cdk1-KD) in an *in vitro* kinase assay. Proteins were separated by SDS-PAGE and visualized by Coomassie blue (CB) (bottom panel) and autoradiography (top panel). (B and C) Cdc25-V5 was immunoprecipitated (IP) from the indicated strains arrested in prometaphase and IPs were treated or not with λ phosphatase before immunoblotting with anti-Cdc25 antibody (top panel). Cdk1 levels from lysates used for IPs are visualized with PSTAIRE antibody (bottom panel). (D) DIC images of *cdc25+* and *cdc25-13A* cells. Cell lengths at septation were measured and standard error of the mean (SEM) is presented.

Table 3-1. List of confirmed Cdc25 (S/T)P phosphopeptides

Phosphorylation site localization probability is derived from SEQUEST and Scaffold PTM algorithms, which consider the number of possible modification sites and intensity of site-specific ions. Delta mass (Daltons) describes the error around the parent ion of the peptide of interest.

phosphorylation site	peptide sequence	localization probability	delta mass (Da)
S66	GKTCSTAS <u>S</u> PASSL	100%	1.56
S84	MHIDES <u>S</u> PALPT <u>T</u> PR	100%	1.44
T89	MKIDES <u>S</u> PALPT <u>T</u> PR	100%	1.44
T104	SL <u>S</u> CTVET <u>T</u> PLANK	100%	1.58
S113	ANKTIV <u>S</u> PLPE <u>S</u> PSNDALTESY	100%	0.77
S118	ANKTIV <u>S</u> PLPE <u>S</u> PSNDALTESY	100%	0.77
S143	YSITQD <u>S</u> PR	100%	1.02
S332	VR <u>S</u> PS <u>P</u> MAFAMQEDAEYDEQDTPVLR	100%	1.29
S334	VR <u>S</u> PS <u>P</u> MAFAMQEDAEYDEQDTPVLR	100%	1.29
T351	SPSPMAFAMQEDAEYDEQD <u>T</u> PVLR	100%	0.612
T379	LGLFK <u>S</u> QDLVC <u>T</u> PK	100%	1.37

Cdk1 Phosphorylation Does Not Affect Cdc25 Nuclear Localization

The ultrasensitive feedback loop between Cdk1 and Cdc25 could be driven by increase of Cdc25 activity, nuclear localization or abundance at prometaphase; subsequent dephosphorylation of Cdk1 sites on Cdc25 by Clp1 is associated with decreased Cdc25 activity, decreased Cdc25 nuclear localization and Cdc25 degradation (Kovelman and Russell 1996; Esteban, Blanco et al. 2004; Wolfe and Gould 2004). We asked if Cdk1 phosphorylation specifically modulates Cdc25 nuclear localization by observing the localization of Cdc25-GFP or Cdc25-13A-GFP through the cell cycle. Both Cdc25-GFP and Cdc25-13A GFP nuclear localization was highest at mitotic entrance, around spindle pole body (SPB) (visualized with Sid4-RFP) separation. Both Cdc25-GFP and Cdc25-13A-GFP stayed in the nucleus until late mitosis, until the SPBs have separated completely. Cdc25 nuclear localization rapidly disappeared after late anaphase and nuclear localization is almost completely gone after cells septated (Fig. 3-2). From this we concluded that since Cdc25-13A seems to localize to and from the nucleus normally during the cell cycle, Cdk1 phosphorylation does not directly control Cdc25 nuclear localization.

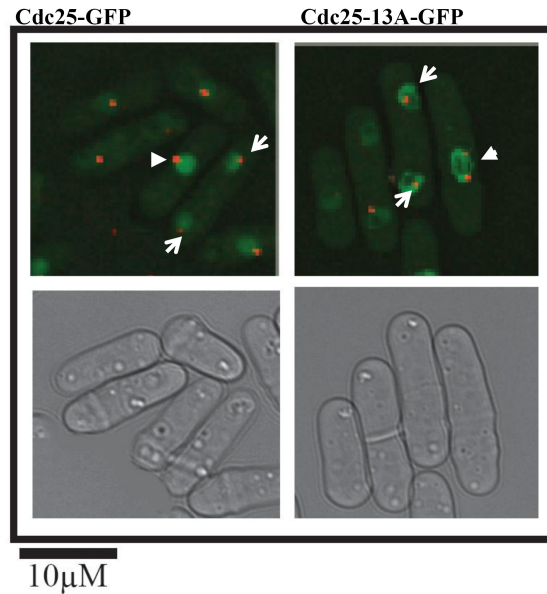


Figure 3-2. Cdk1 phosphorylation does not regulate Cdc25 localization. *cdc25-GFP sid4-RFP* or *cdc25-13A-GFP sid4-RFP* were grown in YE media at 25°C. Arrowheads indicate prometaphase cells. Arrows point to anaphase nuclei.

Cdk1 Phosphorylation Does Not Affect Cdc25 Accumulation

Next, we used cells with Sid4-RFP and Cdc25-GFP or Cdc25-13A-GFP to ask if Cdk1 phosphorylation affects Cdc25 abundance or stability during mitotic entrance. Cells in interphase were grouped according to cell lengths in 2 μm intervals, and mitotic cells, as judged by SPB separation, were separated into prometaphase and anaphase cells (Fig. 3-3A). During interphase, Cdc25-GFP and Cdc25-13A-GFP fluorescence increased as a function of cell length until mitosis. *cdc25-GFP* cells reached mitosis between 13.5 μm and 15.5 μm with Cdc25-GFP fluorescence at 49.2 ± 4.0 arbitrary units (AU). At the same length, *cdc25-13A-GFP* cells compared to *cdc25-GFP* had no significant difference in GFP fluorescence (47.0 ± 2.0 AU). However, *cdc25-13A* cells did not enter mitosis until they were significantly longer (with 89.4 ± 5.2 AU) (Fig. 3-3A). These results suggest that

Cdk1 phosphorylation does not play a role in maintaining Cdc25 abundance; instead, more Cdc25-13A-GFP than Cdc25-GFP is needed to induce mitotic entry.

To pursue this idea further, we blocked *cdc25-GFP* and *cdc25-13A-GFP* cells in S-phase using hydroxyurea (HU) and then monitored Cdc25 abundance and cell length as cells were released back into the cell cycle. During the HU-imposed S-phase arrest, *cdc25-GFP* and *cdc25-13A-GFP* cells were not significantly different in cell length or Cdc25 protein concentration, as assessed by GFP fluorescence (Fig. 3-3B). Because HU blocks cells in S phase by activating the DNA replication checkpoint and *cdc25-13A* cells arrested upon HU treatment (Fig. 3-3B and C) (Langerak and Russell 2011), we conclude that while Cdc25-13A cannot be phosphorylated by Cdk1, it remains responsive to checkpoint kinases that phosphorylate Cdc25 upon DNA damage. Following release from the HU block, *cdc25-13A-GFP* cells septated after *cdc25-GFP* cells (Fig. 3-3C). These results suggest that the delay in mitotic entry in *cdc25-13A* cells results from a change in Cdc25 specific activity.

We also measured Cdc25 abundance in late interphase cells compared to cells in mitosis. There was no significant change in GFP fluorescence levels between late interphase and mitotic *cdc25-GFP* or *cdc25-13A-GFP* cells (Fig. 3-3A), suggesting again that the increased Cdk1 activity at mitotic entry does not affect Cdc25 abundance. Interestingly, neither *cdc25-GFP* nor *cdc25-13A-GFP* cells had significant changes in GFP fluorescence levels between metaphase and mid anaphase (Fig. 3-3A), suggesting that Clp1 dephosphorylation of Cdc25 after metaphase also does not mediate Cdc25 degradation.

Finally, we examined the abundance and phosphostatus of Cdc25-13A relative to Cdc25 during mitotic progression by immunoblotting. Cells were arrested in prometaphase, released, and sampled at frequent intervals. While the phosphorylation level of Cdc25 and Cdc25-13A both decreased, Cdc25-13A was less phosphorylated initially and was dephosphorylated faster in both *clp1*⁺ and *clp1*Δ strains (Fig. 3-3D), suggesting that a kinase(s) and phosphatase(s) other than Cdk1 and Clp1 modulate Cdc25 phosphostatus during mitosis; it is possible that kinases/phosphatases responsible for regulating Cdc25 during checkpoint and stress responses (Langerak and Russell 2011) contribute to this residual phosphoregulation. Neither Cdc25 nor Cdc25-13A decreased in abundance as cells exited mitosis, confirming that Cdk1-mediated phosphorylation is not involved in protecting Cdc25 from degradation (Fig. 3-3D). Thus, although *clp1*Δ cells have elevated Cdc25 levels (Esteban, Blanco et al. 2004; Wolfe and Gould 2004), this must be an indirect effect of Clp1 on another cellular process.

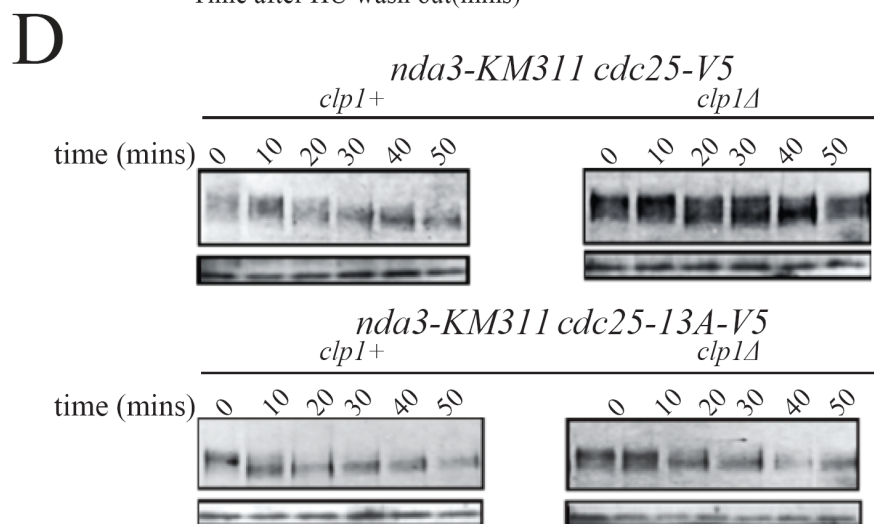
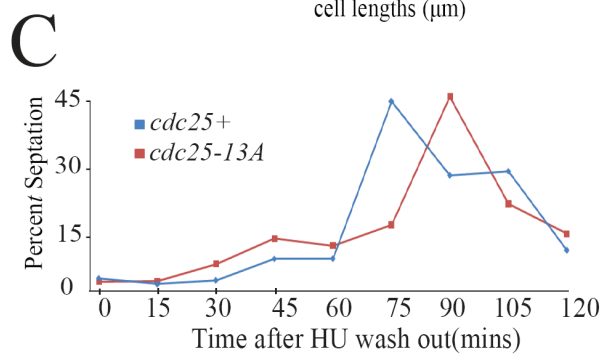
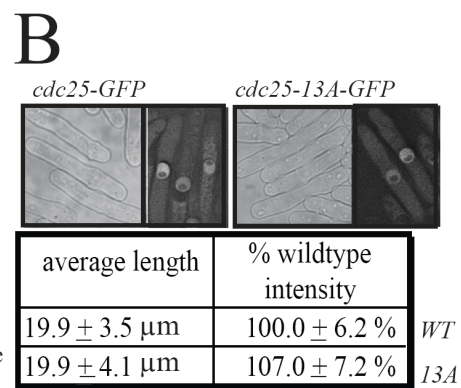
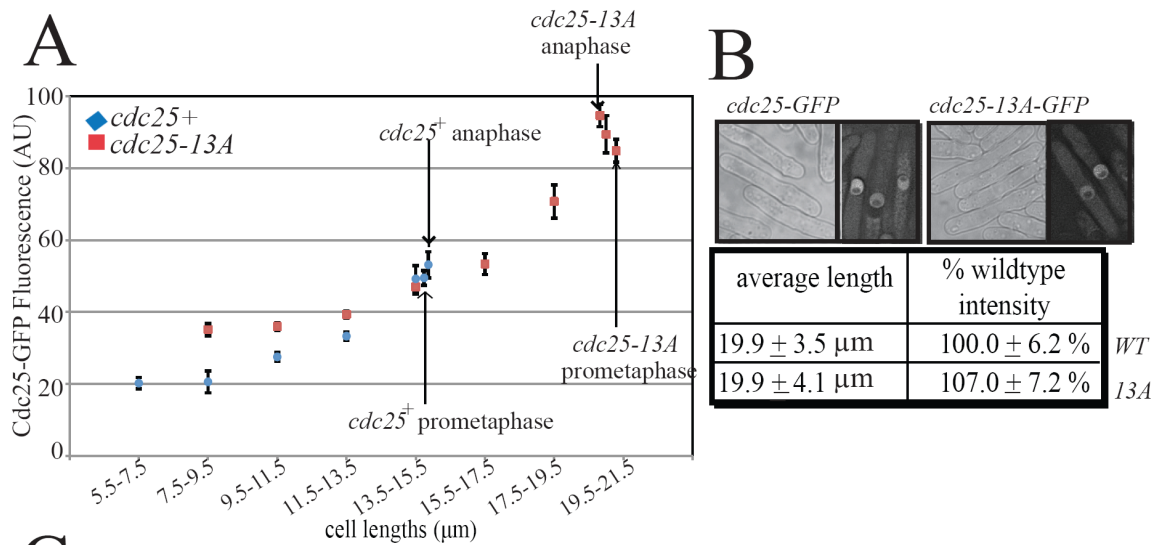


Figure 3-3. Cdk1 phosphorylation does not regulate Cdc25 accumulation.

(A) Cdc25-GFP or Cdc25-13A-GFP fluorescence was quantified in cells at various lengths (25-50 cells per group). Cells in different phases of mitosis, determined by Sid4-RFP-marked SPB(s) position, are indicated with arrows, interphase cells are unmarked, and average length and fluorescence intensity of these cell groups were measured separately. SEM is presented as error bars. (B) The indicated strains were blocked in S phase with HU and cells were visualized by DIC and fluorescence microscopy. Tip to tip lengths were measured. Cdc25-GFP or Cdc25-13A-GFP fluorescence was averaged and calculated as a percentage of average wildtype Cdc25-GFP intensity. SEM is presented. (C) Indicated strains were blocked in S phase using HU and cells were visualized by DIC. Cells were released by washing out HU and collected at the indicated times. Percent septation was calculated (100 cells per time point). (D) Cdc25-V5 was IP'ed with anti-V5 antibody from the indicated strains collected from a *nda3-KM311* block and release at the indicated times. Cdc25-V5 was visualized with anti-Cdc25 antibody (top panel). Cdk1 levels in lysates used for IPs are visualized with PSTAIRE antibody (bottom panel).

Dephosphorylation of Cdc25 by Clp1 Does Not Affect Cdc25 Ubiquitylation

We next asked if Cdk1 phosphorylation affects Cdc25 ubiquitylation during mitotic exit. In Wolfe and Gould 2004, we blotted for Cdc25-MYC after immunoprecipitating for His-ubiquitin over-expressed from a pREP1 vector. More Cdc25-MYC-His-ubiquitin conjugates were found in *clp1*⁺ cells compared to *clp1Δ* cells. More Cdc25-MYC-His-ubiquitin conjugates were also found in cells with APC/C compared to cells with a non-functional APC/C due to a temperature sensitive mutation to the Lid1 subunit (*lid1-6*).

Because an assay that detects overexpressed His-ubiquitin conjugates does not precisely examine endogenous protein ubiquitylation levels, we arrested cells in metaphase with a temperature sensitive mutation (*mts3-1*) in a proteasome component and performed an *in vivo* Cdc25 ubiquitylation assay by purifying endogenous Cdc25 tagged with HBH (Cdc25-HBH). Comparing cells with or without *clp1*⁺, we found that Cdc25 ubiquitylation status was not different between *clp1*⁺ and *clp1Δ* cells (Fig. 3-4A). Thus Cdk1 phosphorylation does not protect Cdc25 from ubiquitylation. In addition, in *mts3-1 lid1-6* cells blocked at metaphase with non-functional APC/C, Cdc25-HBH ubiquitylation levels were reduced compared to cells with functional APC/C (Fig. 3-4B). We conclude that during late mitosis, Cdc25 ubiquitylation may be mediated by the APC/C but increased Cdk1 phosphorylation, in *clp1Δ* cells, does not protect Cdc25 from ubiquitylation and degradation. The previous finding of decreased Cdc25-MYC-His-Ubiquitin in *clp1Δ* cells is probably an artificial finding due to the highly variable expression levels of His-ubiquitin from the pREP1 vector.

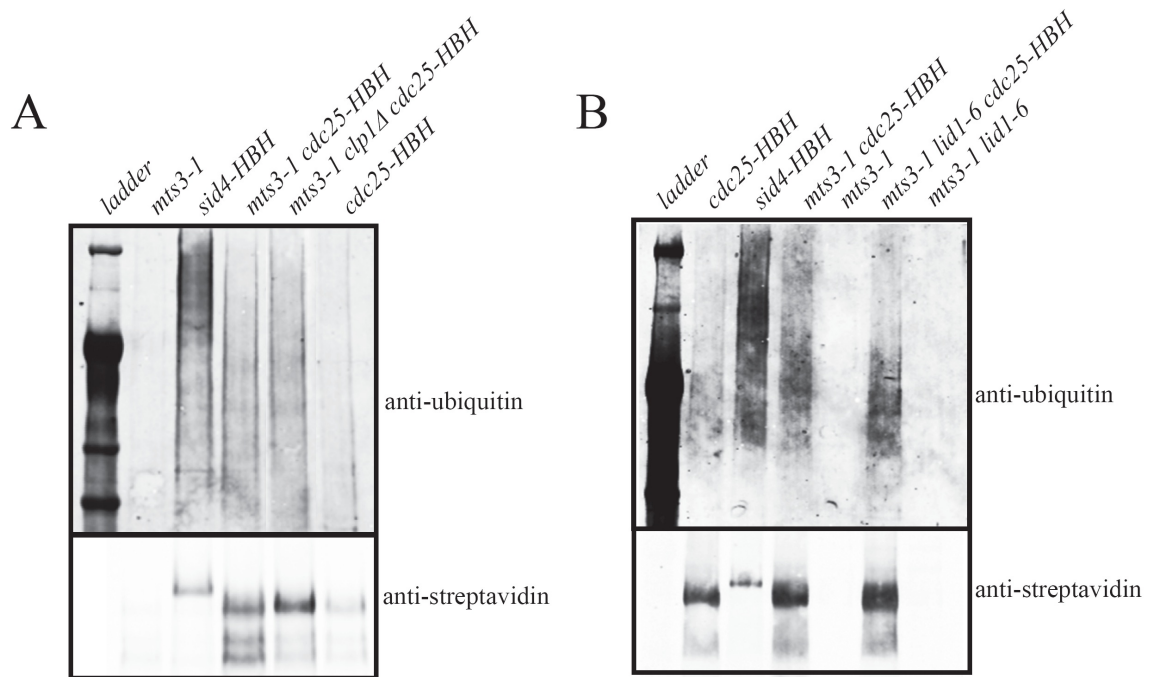


Figure 3-4. Cdk1 phosphorylation does not regulate Cdc25 ubiquitylation.

(*A* and *B*) Temperature sensitive strains (*mts3-1*, *lid1-6*) were incubated at 36°C for 4 hours. Cdc25-HBH or Sid4-HBH was immunoprecipitated from indicated strains with streptavidin beads. Cdc25-HBH or Sid4-HBH was detected using anti-streptavidin antibody (bottom panels) and ubiquitin conjugates were detected using anti-ubiquitin antibody (top panels).

Cdk1 Phosphorylation Directly Activates Cdc25

Finally, we examined if Cdk1 phosphorylation directly enhances Cdc25 activity using a previously described Cdc25 activity assay (Kovelman and Russell 1996; Wolfe and Gould 2004). Immunoprecipitated Cdc25 or Cdc25-13A from prometaphase-arrested cells was tested for its ability to stimulate inactive Cdk1-CyclinB in protein lysates derived from interphase cells. The level of Cdk1 activity was measured using the exogenous substrate, histone H1. Compared to Cdc25-13A, Cdc25 stimulated significantly higher histone H1 phosphorylation by Cdk1 (Figs. 3-5A and B). Thus, we conclude that Cdk1 phosphorylation does not affect Cdc25 abundance but directly activates Cdc25.

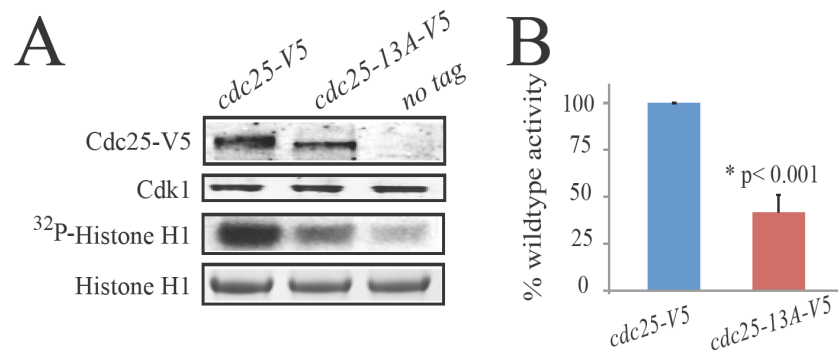


Figure 3-5. Cdk1 phosphorylation regulates Cdc25 activity at mitotic entrance.

(A) *nda3-KM311*, *nda3-KM311 cdc25-V5* and *nda3-KM311 cdc25-13A-V5* were blocked at prometaphase and protein lysates were prepared. Cdk1 levels in each lysate are visualized with PSTAIRE antibody (second panel from the top). The remaining lysates were subjected to IP with anti-V5 antibody and the IP'ed proteins were incubated in protein lysates from *cdc25-22* arrested cells. IP'ed Cdc25 was resolved by SDS-PAGE and detected by immunoblotting (top panel). Next, Cdk1-CyclinB was IP'ed from each lysate and incubated with histone H1 in an *in-vitro* kinase assay. Histone H1 was resolved by SDS-PAGE and visualized by Coomassie (CB) staining (bottom panel) or autoradiography (third panel). (B) The specific activities of Cdc25 and Cdc25-13A in 5 separate experiments performed as in (A) were averaged and the SEM is presented. P-value was determined using the Student's T-test.

Discussion

In this study, we explored how Cdk1 phosphorylation specifically amplifies Cdc25 activity to facilitate the rapid activation of Cdk1 to drive mitotic entry. While increased Cdc25 specific activity, accumulation, Cdc25 stability and Cdc25 nuclear localization were all associated with Cdk1 phosphorylation at mitotic entry, we find that only Cdc25 specific activity is directly affected by Cdk1 phosphorylation.

Phosphoregulation of Cdc25 Activity

Previous studies examining Cdk1 phosphoregulation of Cdc25 assumed that phosphorylation correlates with Cdc25 activation; however, a definitive link between these two events has never been shown within a single study (Yang, MacLellan et al. 2004; Domingo-Sananes and Novak 2010; Trunnell, Poon et al. 2011). To our knowledge this study is the first to comprehensively map Cdk1 specific phosphosites *in vitro* and *in vivo* and verify that these sites specifically contribute to Cdc25 activity.

While Cdk1 phosphorylation contributes importantly to Cdc25 activity, it is not the sole activator of Cdc25, as Cdc25-13A that cannot be phosphorylated by Cdk1 is still active enough to drive mitotic entry while cells cannot enter mitosis without Cdc25 activity. Several possibilities could explain this activity. Cdc25 could have residual levels of catalytic activity without need for further modifications. Other kinases, such as the Polo-like kinase, that has been shown to directly activate Cdc25 in *Xenopus* (Kumagai and Dunphy 1996), or Aurora kinase, which phosphorylates Cdc25B at the centrosome (Cazales, Schmitt et al. 2005), may play roles in activating the protein. Finally, Cdc25 may interact with Cdk1-CyclinB in a manner that facilitates the basal activation of Cdk1-CyclinB without requiring Cdc25 catalytic activity. Evidence for this latter possibility can be found in human cells, where knockdown of both Cdc25A and B significantly

decreases the association of CyclinB with Cdk1 and overexpression of Cdc25A or Cdc25B increases association of CyclinB with Y15 phosphorylated Cdk1 (Timofeev, Cizmecioglu et al. 2010), suggesting Cdc25A and Cdc25B may directly contribute to Cdk1 and CyclinB complex formation. Much more is left to learn of the mechanisms of direct Cdc25 activation, Cdc25 interaction with Cdk1-CyclinB, and proteins that may contribute to Cdc25 activation.

Cdc25 Nuclear Localization

While Cdk1 phosphorylation does not control Cdc25 nuclear localization in *S. pombe*, nuclear localization seems to be a mechanism of Cdc25 control shared between species to temporally and spatially unite Cdc25-Cdk1 in the nucleus where important mitotic events are regulated. While it is known that DNA damage checkpoint kinases phosphorylate and maintain Cdc25 in the cytoplasm via 14-3-3 protein binding (Lopez-Girona, Furnari et al. 1999), the mechanisms that control nuclear transport of Cdc25 at mitotic entrance is less understood. In *S. pombe* Cdc25 nuclear translocation, observed from Cdc25-GFP expressed from a pREP41 vector, was abrogated in cells that lack the importin β Sal3 (*sal3 Δ* cells) (Chua, Lingner et al. 2002); however, what factors control Cdc25-Sal3 binding, or how or if endogenous Cdc25 associates with Sal3 need to be further explored. Phosphorylation by Polo and Aurora kinases facilitate Cdc25 localization in human cells, yet how these phosphorylations drive Cdc25 localization to the nucleus or the centrosome, respectively, is not known (Toyoshima-Morimoto, Taniguchi et al. 2002; Cazales, Schmitt et al. 2005). In addition, it is possible that specific non-phosphorylation related events such as direct association of Cdc25 with nuclear proteins could drive rapid nuclear localization of Cdc25. It will be interesting to further

investigate what specific factors mediate nuclear localization in Cdc25 in *S. pombe* and more globally in all eukaryotic organisms.

Regulation of Cdc25 Degradation at Mitotic Exit

We show here that Cdc25 ubiquitylation levels are not increased in *clp1Δ* cells, as would be expected if Cdk1 phosphorylation protects against Cdc25 ubiquitylation and degradation signals. In addition, Cdc25 levels do not appear to decrease substantially during mitotic progression, suggesting that even though APC/C facilitates some Cdc25 ubiquitylation during anaphase, complete Cdc25 degradation or mitotic exit happens much later – during mitotic exit or early interphase. Cdc25-GFP and Cdc25-13A-GFP fluorescence levels do not go down between prometaphase and anaphase, and Cdc25 can be seen clearly in the nucleus even during late mitosis– when the SPBs have completely separated, at which point cells may have already completed most mitotic events. Maximal decrease of Cdc25-GFP fluorescence intensity happens between complete SPB separation and cytokinesis. Cdc25 degradation is an integral event for controlling cell cycle timing, as increased Cdc25 accumulation, in *clp1Δ* cells, forces premature mitotic entry (Wolfe and Gould 2004). Thus it will be important to further investigate when Cdc25 is specifically degraded and what factors mediate this degradation.

It is interesting to note that while mutations in the APC/C decrease Cdc25 ubiquitylation at metaphase, Cdc25 ubiquitylation is not completely abrogated, suggesting that other ubiquitin ligases play a role in Cdc25 ubiquitylation later in the cell cycle. Human Cdc25 isoforms are ubiquitylated by both the APC/C and the SCF ubiquitin ligases and these ubiquitylations are involved in Cdc25 degradation during late mitosis/early G1 and in interphase respectively (Donzelli, Squatrito et al. 2002).

Furthermore, Pub1, a HECT E3 ubiquitin ligase may play a role in Cdc25 degradation in *S. pombe*. Cdc25 levels are maintained slightly longer into mitosis in *pub1Δ* cells compared to *pub1*⁺ cells, although the specific ubiquitylation status of Cdc25 in *pub1Δ* cells has yet to be examined (Esteban, Sacristan et al. 2008). Much more will need to be learned of what specific E3 ubiquitin ligases interact with Cdc25 and what roles ubiquitylation plays on Cdc25 accumulation during mitosis and throughout the cell cycle.

CHAPTER IV

MULTISITE PHOSPHOREGULATION OF CDC25 ACTIVITY REFINES THE MITOTIC ENTRANCE AND EXIT SWITCHES

Introduction

As detailed in Chapter I, at mitotic entry, the Cdc25 family of phosphatases activate Cdk1-CyclinB complexes by removing inhibitory phosphorylations on Cdk1 catalyzed by Wee1 family kinases. Activated Cdk1-CyclinB phosphorylates its substrates and drives mitotic entry (Morgan 2007; Lindqvist, Rodriguez-Bravo et al. 2009).

Evidence from *in vitro* kinase studies along with *Xenopus* and human cell extracts (detailed in Chapter I) suggest that both requirements for bistability in Cdk1 activation during mitotic entry are satisfied: two feedback loops (the Cdk1-Cdc25 positive feedback loop and the Cdk1-Wee1 negative feedback loop) and ultrasensitivity in activation or inactivation of Cdc25 and Wee1. Despite these extensive *ex vivo* studies, no study to date has verified the ultrasensitivity of Cdk1 substrate phosphorylation and bistability of Cdk1 activation exist *in vivo*, within non-disrupted cycling cells. In addition, there has not been a study looking at the consequences of disrupting these feedback loops and thus disrupting the ultrasensitivity of Cdk1 activation *in vivo*.

In addition to mitotic entry, mitotic exit and the spindle assembly checkpoint may also be modulated by a bistable switch (Holt, Krutchinsky et al. 2008; Pomerening 2009; He, Kapuy et al. 2011). In *S. cerevisiae*, Cdc14 contributes to the abruptness of the metaphase-anaphase switch by interacting with Securin, a protein that protects sister

chromatid separation until anaphase onset, in an ultrasensitive positive feedback loop. Cdc14 dephosphorylates Securin to target it for ubiquitylation and degradation. Degradation of Securin activates Separase, which further activates Cdc14 (Holt, Krutchinsky et al. 2008). Our lab and others found that Clp1 dephosphorylates Cdc25 on Cdk1 phosphosites, and this correlates with Cdc25 inactivation and degradation (Esteban, Blanco et al. 2004; Wolfe and Gould 2004). Because Cdc25 activates Cdk1, the activity of which inhibits Clp1 activity (Wolfe, McDonald et al. 2006), the interaction between Clp1 and Cdc25 may form a feedback loop that contributes to the mitotic exit switch in *S. pombe*.

Here, we use *S. pombe* to further understand how Cdc25 phosphorylation by Cdk1 contributes to the mitotic entry and exit switches in cycling cells. Using this *in vivo* model, we find that the Cdk1-Cdc25 positive feedback loop is important for the precision of mitotic entry and maintenance of uniform cell length. We suggest a new mathematical model of mitotic entry based on our observations of the mechanisms of Cdc25 phosphorylation. Finally, we show that the interactions of Clp1, Cdk1 and Cdc25 create a double negative feedback loop that significantly contributes to the robustness of mitotic exit, specifically controlling the timing of cell division.

Results

Abolishing Cdk1 Phosphosites on Cdc25 Disrupts the Mitotic Switch

We used *cdc25*⁺ and *cdc25-13A* cells to ask if eliminating Cdk1 phosphosites on Cdc25 altered mitotic entry. *S. pombe* grows lengthwise during interphase and stops growing at mitotic entrance, so cell length at septation equates to cell length at mitotic

entrance (Fantes 1977). The increased septation length of *cdc25-13A* cells relative to wildtype indicated a mitotic entrance delay. In mitotic entrance mutants that are already longer than wildtype (*cdc2-L7*, *cdc13-117*, *cdc2-33*, *cdr1Δ*, and *cdr2Δ*), *cdc25-13A-V5* exacerbated their defects. In strains that enter mitosis prematurely (*clp1Δ* and *wee1Δ*), *cdc25-13A-V5* delayed their mitotic entry (Fig. 4-1A). Thus, direct Cdk1 phosphorylation of Cdc25 is important for promoting mitotic entry.

If the Cdk1-Cdc25 positive feedback loop affects the precision of mitotic entrance, then disrupting this loop would be expected to increase the variation of mitotic entry timing, and thus septation length within the population. Indeed, compared to *cdc25-V5* cells, *cdc25-13A-V5* strains exhibited a 2- to 6-fold increase in variation of cell length, as measured by standard deviation (Fig. 4-1A). To examine the regulation of mitotic timing on a single-cell level, we followed individual cells for 2-5 divisions by time-lapse microscopy and calculated the difference in septation lengths between mother and daughter cells. Compared to *cdc25⁺* cells, *cdc25-13A* cells in every genetic background had significantly more varied lengths between generations (Fig. 4-1B, representative examples in Fig. 4-1C). The increased spectrum of *cdc25-13A* cell lengths within a population and between generations shows that the precision of mitotic entrance is disrupted when Cdk1 cannot phosphorylate Cdc25.

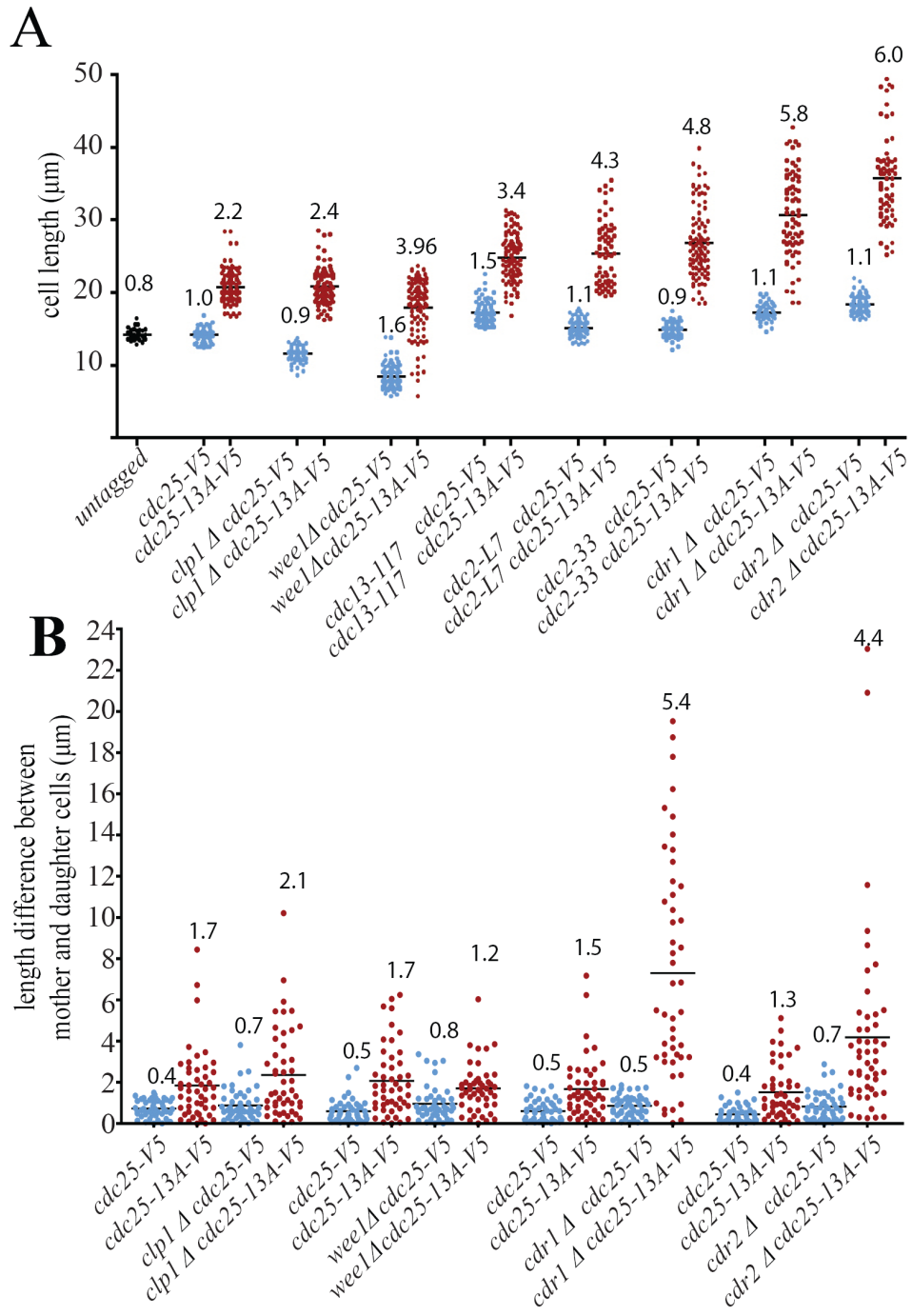


Figure 4-1 continued

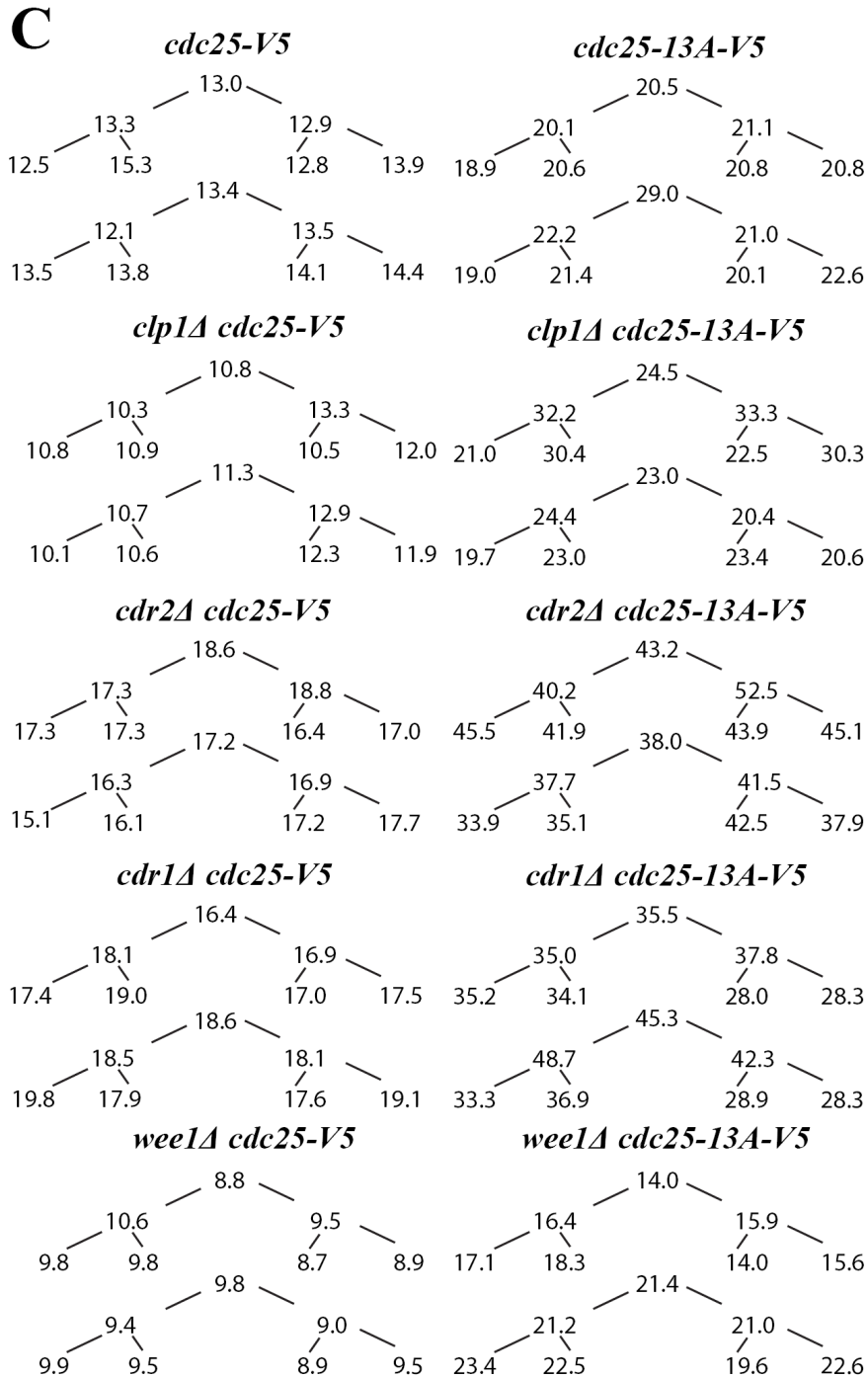


Figure 4-1. Disruption of Cdk1 phosphorylation on Cdc25 delays mitotic entrance.

(A) Scatter plot of the septation lengths of the indicated strains. >100 cells of each strain were measured. Mean lengths are indicated by the horizontal bars. (B) Scatter plot of length differences between mother and daughter cells of the indicated strains. For each strain n=50. (A&B) The standard deviation is displayed above each scatter plot. (C) Representative measurements for cell lengths for (B). For each indicated strain, 2 separate family trees showing cell lengths (μm) for 3 generations are shown.

Multisite Phosphorylation of Cdc25 by Cdk1 Allows for Ultrasensitivity.

Ultrasensitive phosphorylation of Cdc25 by Cdk1 allows Cdc25 to be rapidly activated and filters out “noise” activity at high and low Cdc25 phosphorylation and Cdk1 activity levels. In *Xenopus*, xCdc25C has been shown to be phosphorylated by Cdk1 in an ultrasensitive manner (Trunnell, Poon et al. 2011). To understand if Cdc25 is ultrasensitively phosphorylated by Cdk1 in *S. pombe*, we performed *in vitro* kinase assays where we varied Cdk1 concentrations and measured ^{32}P -ATP incorporation on MBP-Cdc25 or MBP-Cdc25-11A (protein with 11 of the 13 Cdk1 sites mutated to alanines). As Cdk1 levels increased, MBP-Cdc25 was rapidly phosphorylated in an ultrasensitive manner (sigmoid shaped graph); however, MBP-Cdc25-11A incorporated ^{32}P in a slower and more linear manner (Fig. 4-2). We conclude that the multiple Cdk1 sites on Cdc25 allow for ultrasensitive phosphorylation by Cdk1, and abolishing most of these sites significantly reduces ultrasensitive phosphorylation, and thus activation, of Cdc25.

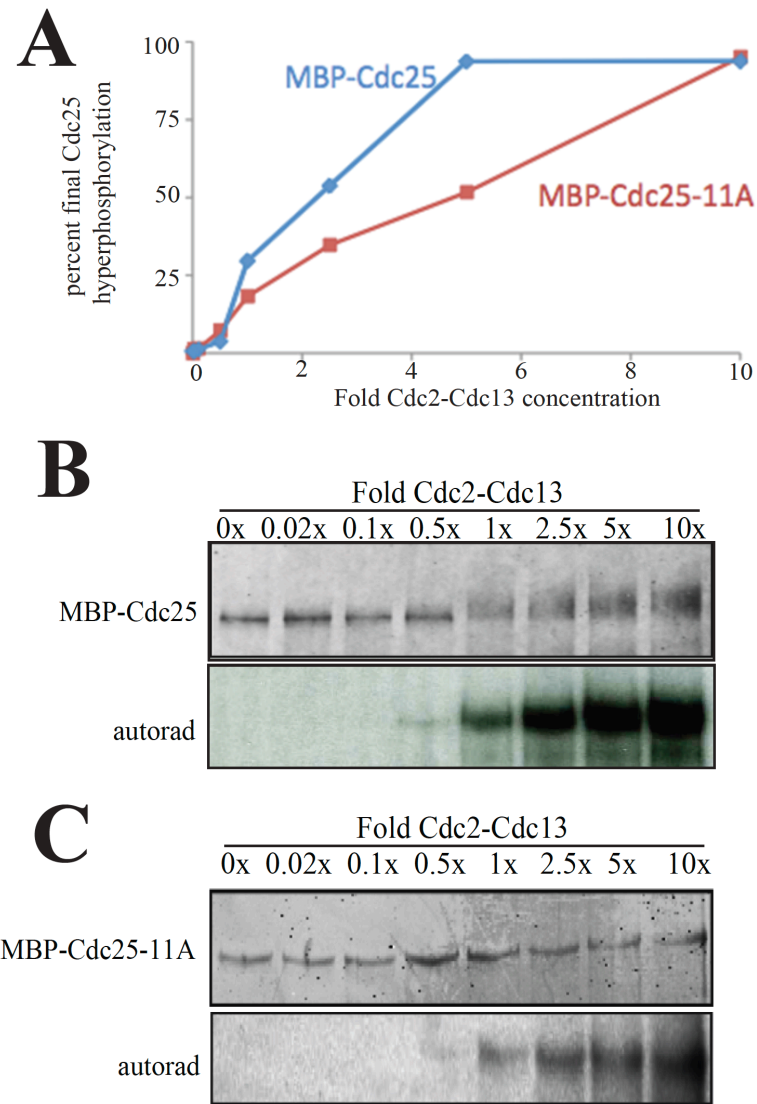


Figure 4-2. Multiple phosphorylation sites allow for ultrasensitive phosphorylation of Cdc25 by Cdk1.

Recombinant MBP-Cdc25 or MBP-Cdc25-11A was incubated *in vitro* with indicated levels of active Cdk1-CyclinB (Cdc2-Cdc13). (A) Cdc25 hyperphosphorylation was assessed by autoradiography, measured by scintillation counting and presented as a percentage of maximal Cdc25 phosphorylation at 10x Cdk1 levels. For each Cdk1 concentration, data from 3 independent experiments were averaged. (B and C) Proteins were separated by SDS-PAGE and Cdc25 was visualized by anti-Cdc25 antibody (top panel) or autoradiography (bottom panel).

Mechanisms of Cdc25 Activation by Cdk1

To examine if there are preferred Cdk1 sites on Cdc25 responsible for its activation, we performed an *in vitro* Cdk1 kinase assay followed by 2D tryptic peptide mapping and found one major and multiple other phosphopeptides derived from Cdc25 (Fig. 4-3 A). By LC-MS/MS analysis, Ser 143 (S143) was identified as a prominent phosphosite (Fig. 4-3 B and C). When S143 was mutated to non-phosphorylatable alanine to produce Cdc25-S143A, the major phosphopeptide was eliminated from the 2D map (Fig. 4-3 A). We replaced *cdc25*⁺ with *cdc25-S143A* to assess its importance *in vivo* and found that this mutation did not significantly change septation length ($14.6 \pm 0.1 \mu\text{m}$) compared to wildtype ($14.2 \pm 0.1 \mu\text{m}$) (Fig. 4-4A). In addition, the SDS-PAGE phospho-shift of Cdc25-S143A-V5 from an *nda3-km311* arrest was not significantly different from Cdc25-V5 (Fig. 4-4B). This indicated that while S143 is a favored phosphosite *in vitro*, it is not necessary for efficient Cdc25 activation *in vivo*. Next we mutated 5 sites (*cdc25-5A*) identified from *in vitro* Cdc25 phosphorylation, or variations of these sites in clusters of 3 mutations (*cdc25-3A-1*, *cdc25-3A-2*) to alanines and replaced endogenous *cdc25*⁺ with these mutants (Figs. 4-3C , 4-4A, Table 4-1). These mutations statistically increased cell septation lengths, but only by 0.9 to 1.3 μm , showing that loss of these sites is not sufficient to reduce Cdc25 activity to that of Cdc25-13A levels. Mutating 5 other *in vivo* Cdk1 sites on Cdc25 identified by MS (*cdc25-5A-2*) (Fig. 4-3C, 4-4A, Table 4-1), also did not increase cell length to a large extent ($15.5 \pm 0.2 \mu\text{m}$) (Fig. 4-4A). We conclude that Cdk1 does not seem to have preferred sites of phosphorylation for Cdc25 activation.

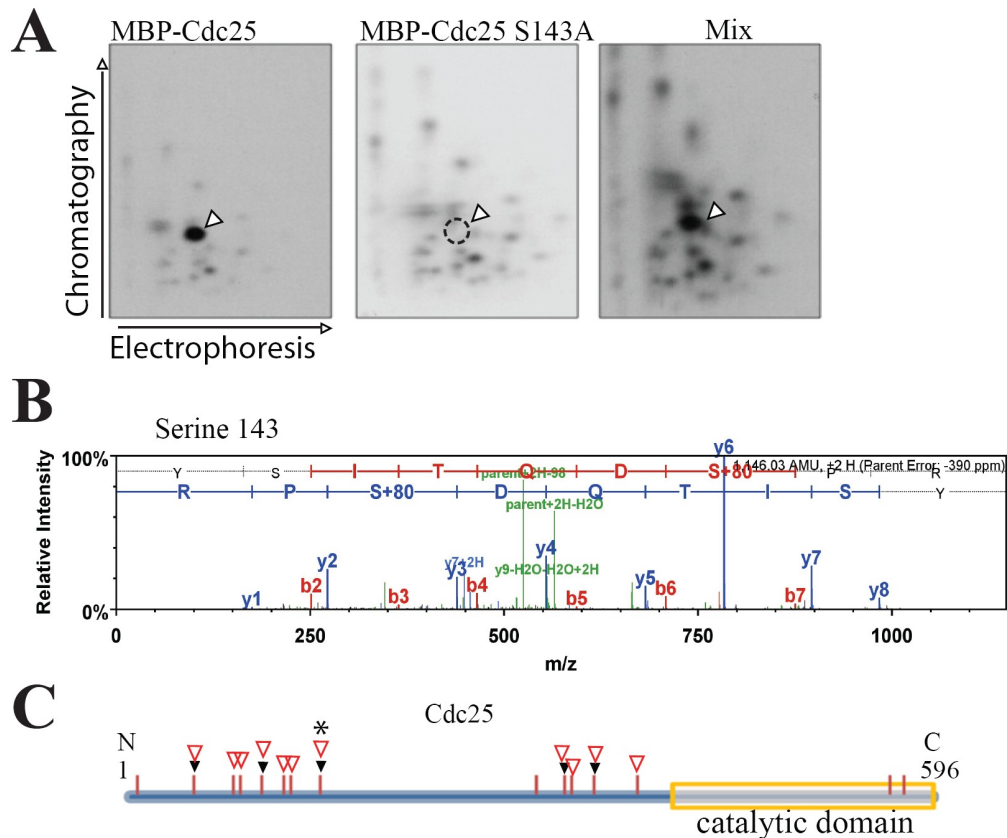


Figure 4-3. Removal of Cdk1 phosphosites on Cdc25.

(A) 2D tryptic peptide maps of MBP-Cdc25 or MBP-Cdc25 S143A, or a mix of the two proteins, after *in vitro* kinase assay with Cdk1. Open triangles indicate location of phosphorylated S143. Dotted line encircles S143 lost when mutated to Alanine. (B) Representative MS2 spectra of the S143-containing phosphopeptide. The peptide sequence ladder depicts identified Y and B ions (blue and red respectively) of the peptide. Green peaks describe m/z of parent ions prior to fragmentation. Black peaks describe unidentified ions. (C) Schematic of Cdc25 with phosphorylation sites identified by MS indicated. Black triangles indicate sites identified from *in vitro* phosphorylation reactions; open red triangles indicate sites identified on Cdc25 purified from prometaphase arrested cells. (*) indicates Ser143.

Cdk1 phosphorylation could activate Cdc25 by a stepwise mechanism, in which a specific number of phosphorylations are necessary for full Cdc25 activation or by a gradually cooperative mechanism in which Cdc25 is gradually activated as it becomes more highly phosphorylated. Furthermore, phosphorylation could occur in an ordered or a disordered manner (Kapuy, Barik et al. 2009; Domingo-Sananes and Novak 2010; Trunnell, Poon et al. 2011). To differentiate between these possibilities, we mutated more Cdk1 phosphosites on Cdc25, decreasing 2 available phosphosites in each subsequent phosphomutant (*cdc25-7A* to *cdc25-11A*) (Fig. 4-4A, Table 4-1) and immunoprecipitated endogenously V5 tagged Cdc25 mutants. The extent of Cdc25 SDS-PAGE phosphoshift decreased progressively as phosphosites were eliminated. However, the mutation of particular sites did not appear to preclude phosphorylation on other sites (Fig. 4-4B), suggesting phosphorylation is disordered although the order could be changed in the mutants. For these mutants, the change in cell length between subsequent phosphomutants was initially small, however, cell length increased significantly with additional mutations (Fig. 4-4A) suggesting gradual Cdc25 activation with increasing number of phosphorylations. We conclude that Cdk1 phosphorylates and activates Cdc25 in a disordered and gradual manner.

Cdc25 Phosphorylation by Cdk1 is Distributive or Semi-processive

Cdk1 phosphorylation of Cdc25 may also occur by a distributive mechanism, in which each phosphorylation on Cdc25 requires a separate Cdk1 binding and unbinding event, as modeled *in silico* (Domingo-Sananes and Novak 2010; Trunnell, Poon et al. 2011). Alternatively, Cdk1 can act as a priming kinase for subsequent processive phosphorylation by itself or other kinases (Isoda, Sako et al. ; Koivomagi, Valk et al.). Using an *in vitro* kinase assay in which the amount of Cdk1 was varied, we found that

intermediate levels of Cdk1 yielded partially phosphoshifted Cdc25, indicating the existence of partially phosphorylated Cdc25 isoforms (Fig. 4-4 C). Because processive phosphorylation would yield small amounts of fully shifted protein even at low Cdk1 concentrations, we conclude that Cdc25 phosphorylation by Cdk1 is distributive, or at least only semi-processive.

Table 4-1: The identity of each Cdc25 phosphomutant with mean length and SEM

S/TP sites	<i>cdc25+</i>	<i>S143A</i>	<i>3A-1</i>	<i>3A-2</i>	<i>5A-1</i>	<i>5A-2</i>	<i>7A</i>	<i>9A</i>	<i>11A-1</i>	<i>11A-2</i>	<i>11A-3</i>	<i>13A</i>
S3								X	X	X		X
S66			X		X		X	X	X	X	X	X
S84						X	X	X	X		X	X
T89									X	X	X	X
T104				X	X		X	X	X	X	X	X
S113						X			X	X	X	X
S118						X	X	X	X	X	X	X
S143		X	X		X		X	X	X	X	X	X
S308						X			X	X	X	X
S332			X	X	X		X	X				X
S334						X		X		X	X	X
T351				X	X		X	X	X	X	X	X
T379									X	X	X	X
mean length (µm)	14.2	14.6	15.1	15.4	15.6	15.5	15.9	17.0	19.1	19.3	19.3	20.1
SEM (µm)	0.1	0.1	0.1	0.2	0.2	0.2	0.1	0.1	0.1	0.1	0.1	0.1

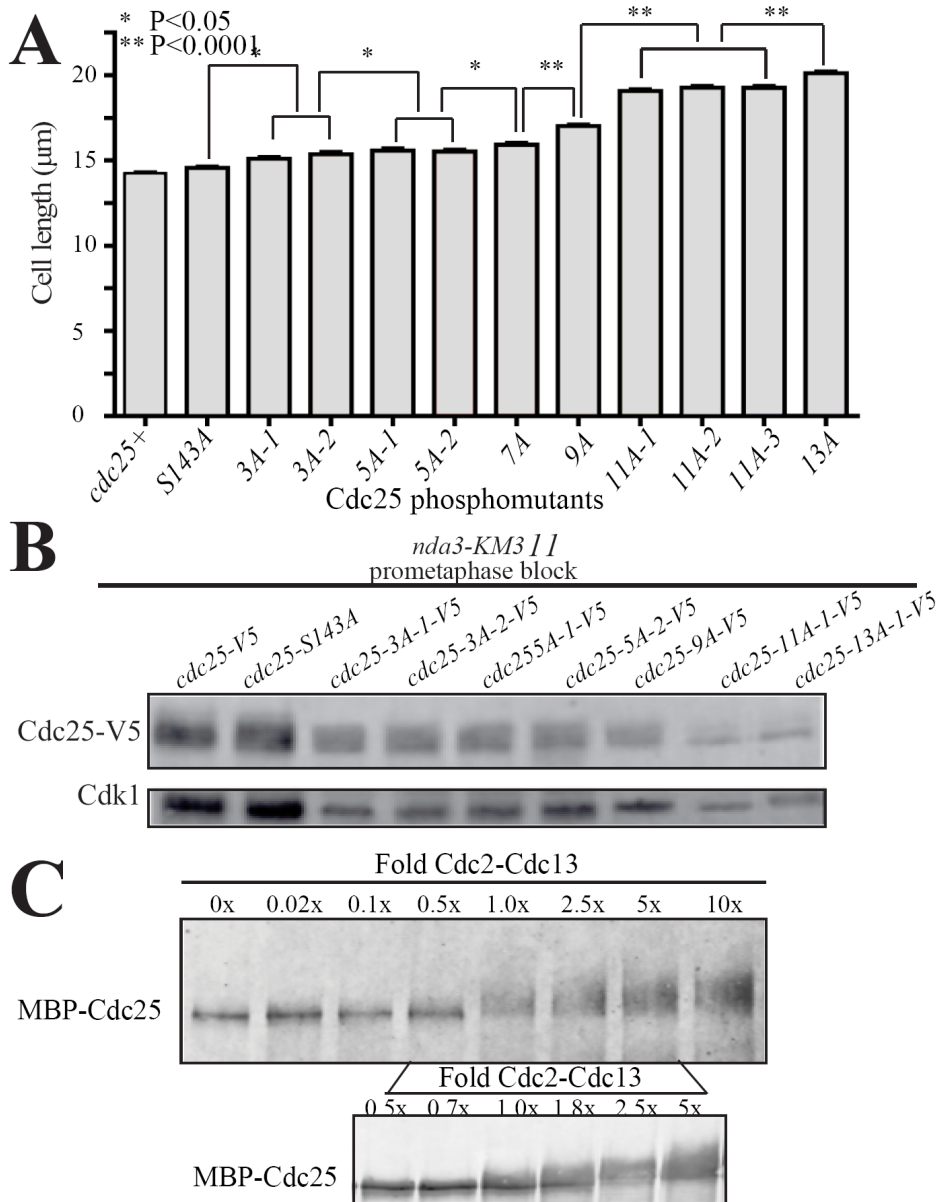


Figure 4-4. Activation of Cdc25 by Cdk1 multisite phosphorylation.

(A) Cell lengths at septation of the indicated *cdc25* phosphomutant alleles were determined and SEM is shown. (B) Cdc25-V5 was immunoprecipitated with anti-V5 antibody from indicated strains arrested in prometaphase and visualized with anti-*cdc25* antibody (top panel). Cdk1 levels from lysates used for IPs are visualized with PSTAIRE antibody (bottom panel). (C) Recombinant MBP-Cdc25 was incubated *in vitro* with indicated levels of active Cdk1-CyclinB (Cdc2-Cdc13). Proteins were separated by SDS-PAGE and Cdc25 was visualized by anti-Cdc25 antibody.

Mathematical Model of Cdc25 Activation and Mitotic Entrance

The contribution of Cdk1 multisite phosphorylation of Cdc25 to the bistability of the G2/M transition was previously modeled (Domingo-Sananes and Novak 2010). We modified this model by assuming that Cdk1 phosphorylates Cdc25 in a cooperative, disordered manner (see Chapter II). Furthermore, we assumed a linear increase in Cdc25 activity with increasing number of phosphorylations, which results in an ultrasensitive response of Cdc25 to active Cdk1-CyclinB (referred to as Mitosis Promoting Factor, MPF) (Fig. 4-5C). This leads to a bistable response of MPF to Cdc25 levels, shown by S-shaped curves for $cdc25^+$ in Fig. 4-5A. The S-shaped curve is composed of three branches: top and bottom branches correspond to interphase (bottom branch) and mitosis (top branch) stable steady states with a middle branch representing unstable steady states (dotted branch) (Fig. 4-5 A). During interphase, MPF activity rises slowly as Cdc25 concentration increases. When Cdc25 levels reach the end of the lower branch, the Cdk1-Cdc25-Wee1 feedback loops engage to fully activate Cdk1 and abruptly switch cells into mitosis (the top branch on the curve). Once in mitosis, MPF activity levels are high and the system stays in mitosis until Cdc25 level drops below a lower threshold than was required for mitotic entry, at which point the system transitions abruptly to interphase (Fig. 4-5A). Therefore, in this system there is a threshold level of Cdc25 required to reach mitosis. Because the Cdc25 level increases as the cell grows, we assume that this Cdc25 threshold for MPF activation is proportional to size at mitotic entry.

Using this model, we tested mathematically how decreasing available phosphosites on Cdc25 would be expected to alter mitotic entry. Figure 4-5A shows that as the number of potential phosphosites decreases, the Cdc25 threshold for MPF

activation increases, which implies that mitotic entry is delayed and cell size increases. This observation fits our experimental data showing increased cell lengths at septation in our Cdc25 phosphomutants (Fig. 4-3A and Fig. 4-5D, Table 3-1). The mathematical model also predicts a significant decrease in both Cdc25 activity and ultrasensitivity as the number of phosphorylation sites on Cdc25 is reduced (Figs. 4-5C).

To see if the variation in cell lengths of *cdc25-13A* at mitotic entrance (Fig. 4-1A) could be predicted by our model, we generated the size distribution for 10^4 cells at mitotic entrance for both *cdc25+* and *cdc25-13A* cells by randomly varying model parameters (See Chapter II). Indeed the modeled *cdc25-13A* average size is not only larger than wildtype cells, but importantly, the distribution of sizes in the mutant is much wider than wildtype (Fig. 4-5B). This could account for part of the experimental variation that we observed (Fig. 4-1A), and emphasizes the role of the Cdk1-Cdc25 positive feedback loop in controlling the precision of the mitotic switch.

Finally, we used our model to explore the contribution of disrupting Cdc25 phosphorylation (Cdc25 vs. Cdc25-13A) in mitotic entrance mutants (*cdc2-L7*, *cdc2-33*, *cdc13-117*, *clp1Δ*, *cdr1Δ*, *cdr2Δ*) (Fig. 4-5E). The strong consensus between experimental data and calculated lengths of mitotic entrance mutants (Figs. 4-5D and E) emphasize the contribution of Cdc25 multisite phosphorylation in the precision of mitotic entrance within the dynamic of multiple protein interactions.

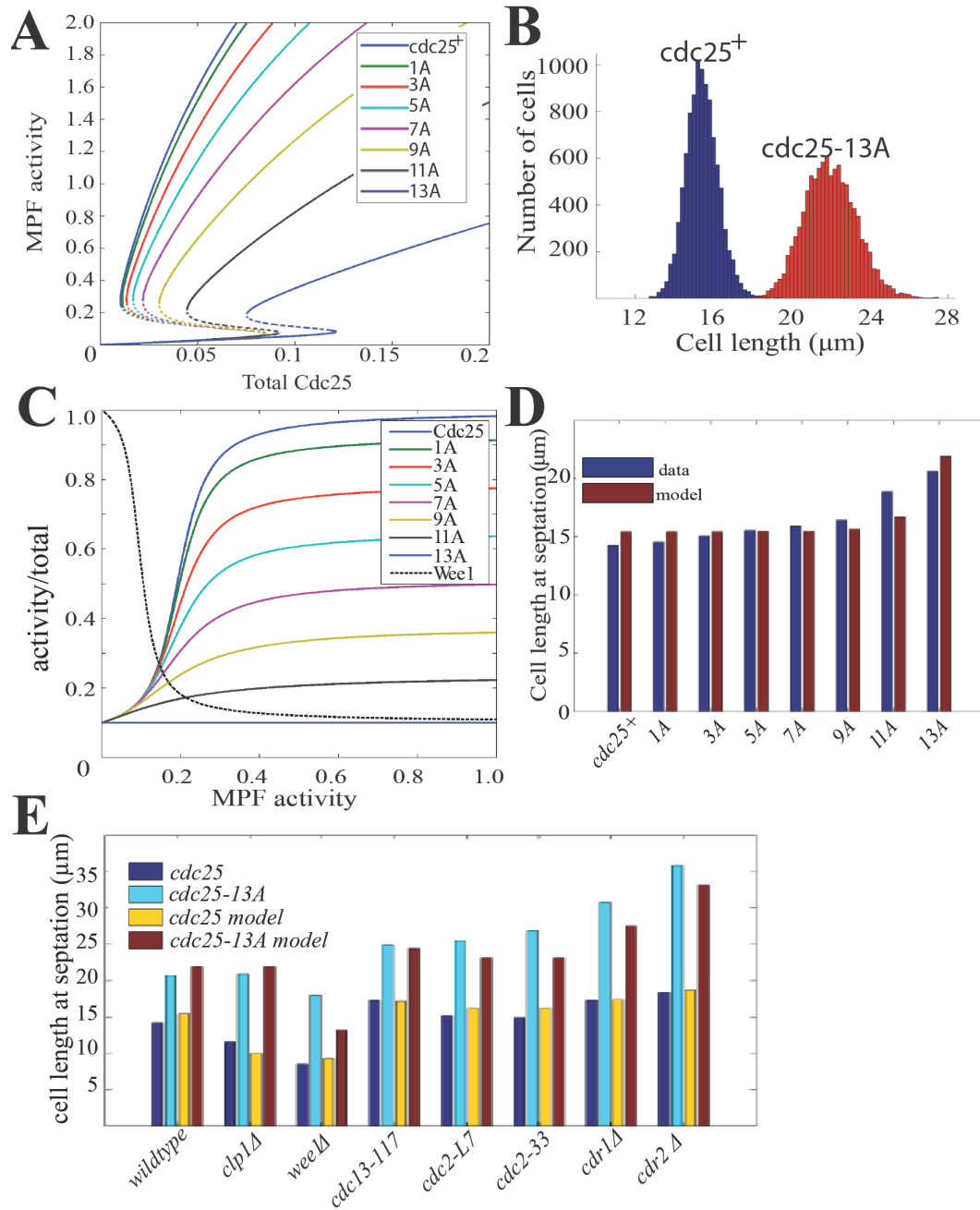


Figure 4-5: Mathematical model of Cdc25 activation.

(A) MPF activity as a function of total levels of Cdc25 for *cdc25⁺* and different *cdc25* phosphomutants. Dotted lines show unstable transition states. (B) Model predicts distribution of cell lengths for *wildtype* and *cdc25-13A* cells. For each cell type, 10^4 cells (parameter sets) were generated by randomly varying model parameters. (C) Cdc25 or Wee1 activity as a function of Mitosis Promoting Factor (MPF) activity. (D and E) Experimental and mathematically predicted values of cell lengths at septation for indicated strains.

Cytokinesis Timing is Controlled by Clp1 Dephosphorylation of Cdc25

We previously found that retention of Cdk1 phosphorylation on Cdc25 in *clp1Δ* cells delays Cdk1 inactivation (Wolfe and Gould 2004). To define which steps of mitotic exit were altered as a result, we monitored mitotic progression until septation in *clp1⁺ cdc25-GFP*, *clp1⁺ cdc25-13A-GFP*, *clp1Δ cdc25-GFP* and *clp1Δ cdc25-13A-GFP* cells, by measuring the distance between SPBs (marked by Sid4-RFP) as an indication of spindle length. *S. pombe* has three phases of spindle dynamics (Nabeshima, Nakagawa et al. 1998). In phase 1 a short 2-2.5 μm spindle is formed. In phase 2, spindle length is maintained while chromosomes align (metaphase and anaphase A). Phase 3 corresponds to anaphase B, wherein the spindle elongates. After phase 3, the mitotic spindle collapses and cells divide (Fig. 4-6A).

Because Clp1 dephosphorylates Cdc25 during anaphase (Esteban, Blanco et al. 2004; Wolfe and Gould 2004), we measured the time in and after phase 3 to assess the contribution of Cdc25 dephosphorylation. Phase 3 was significantly longer in *cdc25-13A-GFP* cells for both *clp1⁺* and *clp1Δ* strains (25.6±1.1 and 24.6±1.2 mins, respectively) compared to *cdc25-GFP* cells (22.0±1.3 and 21.4±2.2 mins, respectively) (Fig. 4-6B and C). This change reflects the longer cell length and time required for the spindle to fully elongate, as *clp1⁺ cdc25-13A-GFP* and *clp1Δ cdc25-13A-GFP* cells are on average longer at division (19.5±1.0 μm and 20.2±0.8 μm respectively) compared to *clp1⁺ cdc25-GFP* and *clp1Δ cdc25-GFP* cells (14.5±0.4 μm and 12.9±0.4 μm respectively). The time from mitotic spindle collapse at the end of phase 3 to septation in *clp1Δ cdc25-GFP* cells was at least 10 minutes longer compared to all other strains, which were not significantly different between one another (Fig. 4-6B), confirming that Clp1 dephosphorylation of

Cdc25 plays an important role in controlling the time to cell division. Eliminating Cdk1 phosphorylation in *cdc25-13A* cells restored normal timing of this cell cycle phase (Fig. 4-6B).

To understand if Clp1 and Cdc25 are involved in a double negative feedback loop that contributes to the abruptness of cytokinesis, we calculated the variation of total time from anaphase onset to cell septation (mitotic exit) in individual cells. If a feedback loop exists, then removing the ability of Clp1 to dephosphorylate Cdc25 in *clp1Δ* cells should reduce the synchrony of mitotic exit. Significantly, we found that *clp1Δ cdc25+* cells had a larger range in mitotic exit times compared to all other strains (Fig. 4-6D). Thus, our data indicate that Clp1 and Cdc25 are in an ultrasensitive double negative feedback loop that regulates the precise timing of cytokinesis and this may explain the low, but reproducible, rate of cytokinetic failure in *clp1Δ* cells (Trautmann et al., Cueille et al).

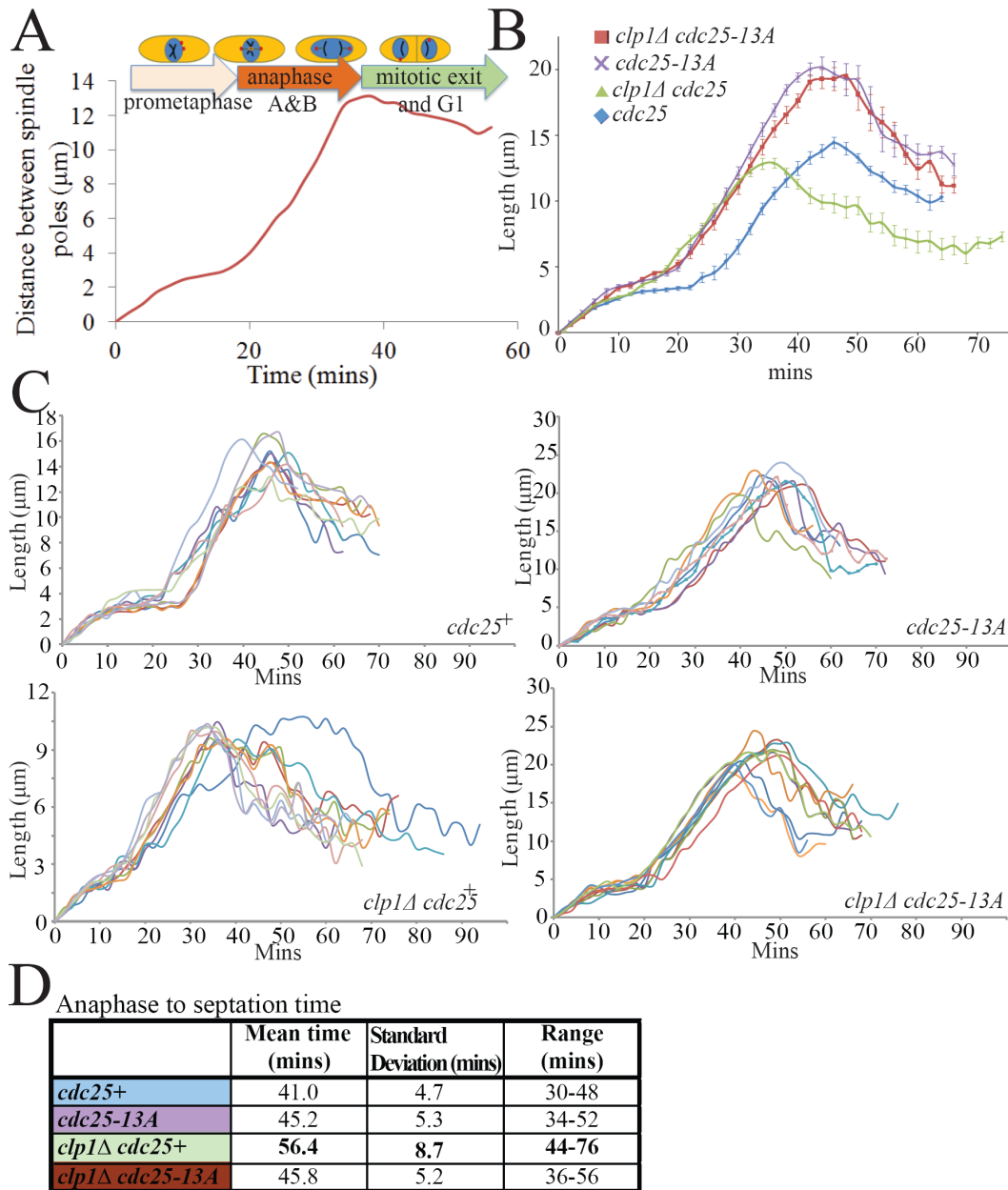


Figure 4-6. Clp1 dephosphorylation of Cdc25 is vital for proper mitotic exit.

(A) Schematic of mitotic events for a *wildtype* cell. Red spots represent spindle pole, blue circle represents nucleus, black lines represent chromosomes. Graph measures distance between spindle poles as a function of time until septation. (B) The distances between SPBs for 10 cells per strain was measured from the beginning of mitosis until the time of septation at 2 mins intervals and averaged. SEM is indicated for each time point. (C) line graphs of individual cells showing distance between spindle poles as a function of time for each of the indicated strains. (D) Mean, standard deviation and range of total time from anaphase to septation for each strain .

Discussion

In this study, we used *S. pombe* as an *in vivo* model to explore the interactions between Cdk1, Clp1, and Cdc25. *In vivo* systems provide volume constraint, compartmentalization of organelles, and precise activation of cell cycle checkpoints, variables that cannot be accounted for in cell extract systems used thus far to study bistability in mitotic control. We show, for the first time *in vivo*, that Cdk1 multisite disordered phosphorylation activates Cdc25 and is crucial for the precision of the mitotic entrance switch and as a result, the maintenance of constant cell length and size.

Mitotic Switch Disruption Manifests as Increased Size Variation

Division lengths and growth rates for undisturbed *S. pombe* cells are remarkably invariant (Sveiczer, Novak et al. 1996). However, *cdc25-13A* cells have increased division length variance, a mark of a disturbed mitotic switch. While size differences in a population could be due to subpopulations with distinct but stable mitotic switches, our single cell analysis showed that mitotic entry was less predictable in each *cdc25-13A* cell, irrespective of the mother's length at septation. Thus, we show for the first time *in vivo*, that when the Cdk1-Cdc25 positive feedback loop is removed, this manifests as decreased precision in mitotic timing. Whether reduced mitotic entry precision in *cdc25-13A* cells is due to a more stochastic mitotic switch or graded Cdk1 activity creating difficulty in executing a specific function (e.g. spindle pole separation) remains to be explored.

Mechanism of Cdc25 Phosphorylation by Cdk1

Our study shows that *in vivo*, Cdk1 phosphorylates Cdc25 in a disordered and distributive (or at least semi-processive) manner, confirming previous *in silico* models

postulating that only a distributive multisite phosphorylation mechanism can result in ultrasensitivity in protein phosphorylation (Domingo-Sananes and Novak 2010). While a preferred Cdk1 phosphorylation site on huWee1 is important for its degradation at mitosis (Watanabe, Arai et al. 2004), whether a specific Cdk1 site on Cdc25 is important for Cdc25 activation has never been systematically studied. The relative ease of genetic manipulation in *S. pombe* allowed us to thoroughly study the effect on mitotic entry of mutating subsets of Cdk1 sites on Cdc25. Our data provide no evidence of selective requirements for individual sites; rather we propose that all 13 Cdk1 phosphosites on Cdc25 contribute equally to mitotic entry by the ultrasensitive phosphorylation and subsequent activation of Cdc25.

Role of Cdc25 Multisite Phosphoregulation in Eukaryotes

Cdc25 activation by Cdk1 multisite phosphorylation, whether by stabilizing Cdc25 or by direct activation, is likely a conserved mechanism that contributes to the switch-like initiation of mitosis in eukaryotes. In all species, Cdc25 proteins have at least 6, and up to 13 possible Cdk1 phosphosites, according to the minimal Cdk1 consensus sequence (S/T-P), allowing for the possibility of ultrasensitive Cdc25 activation by multisite phosphorylation whether by stabilizing Cdc25 or by catalytic activation. Intriguingly, vertebrates, such as humans, with up to three Cdc25 isoforms may have evolved multiple isoforms to perhaps more precisely modulate the mitotic switch. In humans, all Cdc25 isoforms contribute to mitotic entrance, however, only Cdc25B localizes to the centrosome in a Cdk1 and Plk1 phosphorylation dependent manner during late interphase and early mitosis (Boutros and Ducommun 2008). In addition, Cdc25A and Cdc25B have 12 potential Cdk1 phosphosites while Cdc25C has only 6. These

differences may provide a means of fine-tuning the mitotic entry switch where localization may provide specificity in regulating different events while different numbers of available phosphosites may provide temporal control in ultrasensitive activation of different Cdc25 isoforms. Besides multisite phosphorylation, other mechanisms also may contribute to the ultrasensitive responses of Cdc25 and Wee1 to Cdk1, such as competition among Cdk1 substrates and protein phosphoisoforms for enzyme binding (Georgi, Stukenberg et al. 2002; Rape, Reddy et al. 2006; Kim and Ferrell 2007), and regulation of opposing enzymes such as Clp1 (Ferrell 2008).

The Cdc14 Phosphatase Plays Important Roles in the Mitotic Exit Switch

Our study also suggests the existence of a double-negative feedback loop between Clp1 and Cdc25 at the mitotic exit switch. Both *S. pombe* Clp1 and *S. cerevisiae* Cdc14 are mediators of the mitotic exit switch. While Cdc14 directly promotes APC activity, which initiates CyclinB degradation and separation of sister chromatids, allowing for the switch-like transition of metaphase to anaphase (Holt, Krutchinsky et al. 2008; Lopez-Aviles, Kapuy et al. 2009; He, Kapuy et al. 2011), Clp1 in *S. pombe* does not affect CyclinB (Cueille, Salimova et al. 2001). Instead, we have confirmed and extended our previous work (Wolfe and Gould 2004) showing that Clp1 dampens Cdk1 activity by dephosphorylating and inactivating Cdc25 after metaphase. Clp1 facilitates proper contractile ring dynamics and timely cytokinesis by antagonizing Cdk1 phosphorylations that negatively regulate the septation initiation network (SIN) and antagonize the formation of the contractile ring (Guertin, Chang et al. 2000; Trautmann, Wolfe et al. 2001; Clifford, Wolfe et al. 2008; Dischinger, Krapp et al. 2008; Roberts-Galbraith, Ohi et al.). Our data show that abrogation of the Clp1-Cdc25 feedback reduces the abruptness

of cytokinesis. Therefore, unlike *S. cerevisiae* Cdc14, which facilitates the mitotic exit switch at the metaphase-anaphase transition, *S. pombe* Clp1 controls the abruptness of the mitotic exit switch primarily by promoting proper SIN and contractile ring activity.

CHAPTER V

CONCLUSIONS AND FUTURE DIRECTIONS

In this work, I present an analysis of the phosphoregulation of Cdc25 by Cdk1, the role of the Cdk1-Cdc25 feedback loop in the G2/M transition for undisrupted cells and the contribution of the feedback loop between Clp1 and Cdc25 to mitotic exit.

Chapter Highlights

In Chapter II, I explained the biochemical, genetic, and mathematical modeling techniques used in this thesis. Most unique and pertinent for this study are methods for measuring Cdc25 activation, for measuring cell lengths at septation and time to cytokinesis to assess disturbance to the mitotic entry and mitotic exit switches, and for the mathematical modeling of mitotic entry. Although assaying immunoprecipitated Cdc25 activity by testing its ability to activate Cdk1 *in vivo*, and then measuring Cdk1's ability to phosphorylate histone H1, is more indirect than directly testing Cdc25's activity against an artificial substrate, Cdc25 is up to 3000 times more sensitive towards Cdk1 than towards commonly used artificial substrates like mFP or pNPP (Rudolph, Epstein et al. 2001). Thus, the *in vivo* Cdc25 activity assay is used, in all organisms, to test immunoprecipitated Cdc25 activity due to the assay's high sensitivity.

While cell length at septation is a common measure for mitotic entry time, to our knowledge, this is the only study that measures variance in cell lengths as a test for disturbance in the mitotic switch. Our study shows that measuring variance in length and

time to easily observable mitotic events such as cytokinesis, are sensitive and effective ways to test disturbances in feedback loops that contribute to switch-like cell cycle events.

Finally, collaboration with the Novak lab to mathematically model mitotic entry allowed us to simplify a number of *in vivo* variables to focus on the contribution of the Wee1-Cdk1-Cdc25 feedback loops to mitotic entry. We show that even within a simplified cell cycle model, we can predict variations in cell lengths due to changes in the Cdk1-Cdc25 feedback loop, validating that our experimentally predicted mechanism – of progressive, distributive, and ultrasensitive phosphorylation and activation of Cdc25 by Cdk1. While mechanisms of interaction for Cdk1, Wee1, and Cdc25 with other proteins need to be added to the model for a more complete picture of mitotic entry, we believe that the model presented is a step towards a more detailed mechanistic understanding of mitotic entry.

In Chapter III, we clarified the role of Cdk1 phosphorylation on Cdc25. Previous to this thesis, it was known that Cdc25 localized to the nucleus and is most active and stable when it is hyperphosphorylated by Cdk1 at mitotic entry. Dephosphorylation by Clp1 at mitotic exit was associated with Cdc25 degradation (Wolfe and Gould 2004). In addition, the specific sites of Cdk1 phosphorylation on Cdc25 were not known. Our data convincingly show that Cdk1 phosphorylation directly activates Cdc25 and does not play a role in Cdc25 accumulation and nuclear localization at mitotic entry nor affects Cdc25 ubiquitylation and degradation at mitotic exit. This is also the first study where Cdk1 phosphorylation was comprehensively identified on Cdc25 by tryptic peptide mapping and tandem affinity purification followed by mass spectrometric (MS) identification.

In Chapter IV, we show that Cdk1 ultrasensitively phosphorylates Cdc25 in a cooperative and distributive mechanism and importantly contributes to the positive feedback between Cdk1-Cdc25 that rapidly switches the system into mitosis. We verified our proposed mechanism of Cdc25 phosphoregulation by validating our predictions against a mathematical model. Finally, we identified a potentially important feedback loop involving Clp1 dephosphorylation of Cdk1 sites on Cdc25 in mitotic exit. Prior to this work, all mathematical modeling of the feedback loops contributing to the mitotic entry switch were based on experimental data from *ex vivo Xenopus* egg lysates. Our work is the first and only model of the mitotic entrance loop based on the behavior of undisturbed cells that are able to properly enter mitosis, control mitotic events, exit mitosis, and normally progress through other phases of the cell cycle. By observing *S. pombe* cells, we are able to observe how an undisrupted system responds to interference to an important feedback arm of the mitotic switch. Without the Cdk1-Cdc25 feedback loop, cells cannot specifically control when they enter mitosis, having substantially varied times to mitosis between generations. This disruption in mitotic timing may be universal in cells that have interrupted Cdk1-Cdc25 feedback loops. It will be interesting to investigate the importance of mitotic coordination in organisms where timing to mitosis is important for organ development and pathogenesis. Finally, mitotic exit has always been thought of as a dampening of Cdk1 stimulated events, and specific mechanisms controlling exit timing events have not been comprehensively studied. Our study shows that Clp1 dephosphorylation of Cdc25 on Cdk1 sites is a control mechanism that allows for the rapid switch from late mitotic events to cytokinesis. Our study

highlights Clp1 as an important regulator of cytokinesis, and points to, for the first time a role for Cdc25 activity during mitotic exit.

Figure 5-1 is a comprehensive model of our findings, showing that Cdk1 distributively and non-selectively phosphorylates Cdc25, allowing for the ultrasensitive activation of Cdc25 and Cdk1 and for switch-like entrance into mitosis. The Clp1-Cdc25 negative feedback loop, in turn, rapidly turns off Cdc25 and Cdk1 at mitotic exit, facilitating the switch like exit from mitosis, during cytokinesis.

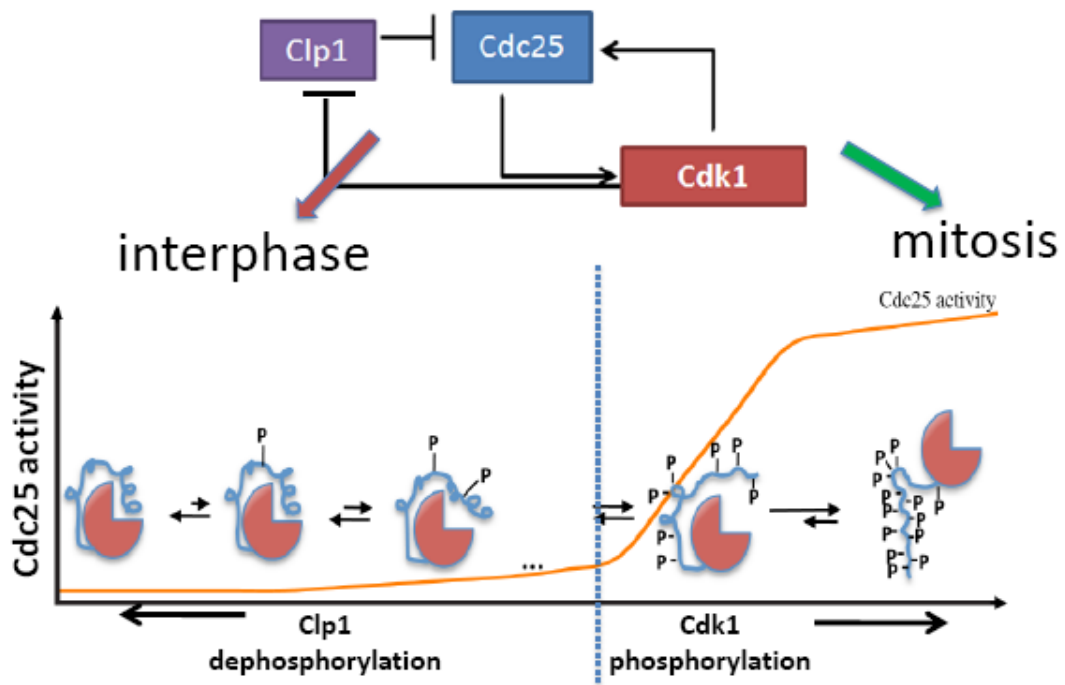


Figure 5-1. Cdc25 is involved in two feedback loops that significantly contribute to mitotic bistability.

Cdc25 is phosphorylated by Cdk1 in an ultrasensitive and distributive manner. This ultrasensitive phosphorylation cooperatively drives the positive feedback between Cdk1 and Cdc25 to rapidly switch the cells into mitosis. Cdk1 phosphorylation inhibits Clp1 activity until mitotic exit. When Cdk1 activity decreases during late mitosis, Clp1 dephosphorylates and activates itself. Clp1 also dephosphorylates Cdc25 in a double negative feedback loop, in which Cdc25 activation of Cdk1 inactivates Clp1 and Clp1 further inactivates Cdc25. This dephosphorylation loop not only controls proper timing to cytokinesis but also is important in the switch-like exit from mitosis to interphase.

Future Directions

Wee1-Cdk1 Negative Feedback in the Mitotic Entrance Switch

Both the Wee1-Cdk1 negative feedback and Cdc25-Cdk1 positive feedback loops are important in driving mitotic entry in *Xenopus* cell extracts (as detailed in Chapter I) (Trunnell et al. 2011; Kim and Ferrell, 2004). The existence of the Wee1-Cdk1 feedback loop in *S. pombe* and other undisrupted cells and how this feedback may affect mitosis have not yet been explored. To understand if and how the Wee1-Cdk1 double negative feedback loop contributes to the *S. pombe* cell cycle, we first performed an *in vitro* Cdk1 kinase assay with MBP-Wee1 using recombinantly expressed *S. pombe* proteins, and showed that with increasing Cdk1 levels, Wee1 becomes phosphorylated in an ultrasensitive manner. In addition, by MS analysis following *in vitro* Cdk1 kinase assay, we have found at least 17 S/T-P sites on recombinant Wee1. We plan to further examine the roles of these phosphorylation sites *in vivo* by examining the effects of mutating these sites to nonphosphorylatable alanines and phosphomimetic glutamate. In addition, we will explore the *in vitro* (by recombinant protein expression) and *in vivo* (by kinase assays using immunopurified proteins) activation levels and stability of these phosphomutants. Finally, we plan to assess how disrupting this negative feedback loop *in vivo* will alter the mitotic entrance and potentially mitotic exit switches by examining time to and in mitosis and mitotic events.

Other Kinases that Affect Mitosis Through Cdc25

Activation of Cdc25 is necessary for mitotic entry, as *cdc25-22* cells blocked at the restrictive temperature cannot enter mitosis. *cdc25-13A* cells take longer to reach mitosis, reflecting a decrease in Cdc25 total activation; however, the fact that cells still

septate and go through mitotic events suggest Cdc25-13A can still effectively activate Cdk1. Cdc25-13A has residual phosphorylation at prometaphase, indicating kinases other than Cdk1 also phosphorylate the protein. Thus, Cdc25 activation may be controlled by Cdk1 and other kinases at mitotic entrance.

Along with Cdk1 phosphorylation on Cdc25, we also identified by MS analysis, a number of other phosphorylated sites on Cdc25 at mitotic entrance. The non-S/TP sites identified by our MS analysis include previously identified RXXS sites (Graves, Lovly et al. 2001) phosphorylated by Chk1/Spc1 kinases (six of the nine consensus sites were phosphorylated), at least two potential Polo-like kinase sites, and several other unknown phosphorylation sites. Polo-like kinases phosphorylate Cdc25 to control Cdc25 activity and localization at mitotic entry in human and *Xenopus* cells but their role in controlling Cdc25 in *S. pombe* not yet been explored. We verified that both *in vivo* immunoprecipitated and baculoviral expressed *S. pombe* Plo1 phosphorylate Cdc25. Plo1 phosphorylates multiple other sites on Cdc25 in addition to those found by MS analysis. Mutating the Plo1 related phosphosites on Cdc25 to nonphosphorylatable alanines and potentially phosphomimetic glutamates seem to affect the cell cycle during both mitotic entrance and later mitotic events. Future directions include finding all the Plo1 directed sites on Cdc25, examining the specific roles and mechanisms of Plo1 phosphorylation on Cdc25 and understanding how these phosphorylations contribute to mitotic events.

Thus, along with Cdc25 dephosphorylation by Clp1 playing a role in regulating mitotic exit timing, our recent work in Plo1-Cdc25 interaction suggests that while Cdc25 has always been thought to be important in mitotic entry, it also plays previously unexplored roles in late mitosis that deserve further examination.

Functional Characterization of the Cdc25 N-terminus

Cdk1 phosphorylates the N-terminal unstructured regulatory domain of Cdc25 to activate Cdc25. How the N-terminus, or parts of the N-terminus, specifically modulates the activation of Cdc25 is not known. A section of the N-terminus could directly structurally obstruct the catalytic domain of Cdc25 (in cis or trans manner), an obstruction that could be alleviated by Cdk1 phosphorylation. The N-terminus could dimerize in the presence or absence of Cdk1 phosphorylation to modulate Cdc25 activity. Phosphorylation of the N-terminus may directly alter the structure and thus activation level of the catalytic domain. Finally, the N-terminus could associate with the Cdk1-Cyclin B complex directly, allowing for spatial proximity for Cdk1 and Cdc25 to activate one another. To differentiate between these possibilities, and to explore other possibilities, we have expressed several truncated forms of Cdc25 recombinants with various sections of the N-terminus removed, to explore which segment of the N-terminus is most important for Cdc25 activation. In addition, we have generated, and are in the process of designing more Cdc25 N-terminal truncated peptides of various sizes, with and without the catalytic domain, for two-hybrid interaction assays to understand N-terminus binding properties to itself, Cdk1, CyclinB and the Cdc25 catalytic domain. Finally, these Cdc25 truncation and deletion constructs will be integrated into cells to explore the *in vivo* effects of disrupting N-terminal function in Cdc25 activation, mitotic entry, and other potential protein interactions.

Multisite Phosphorylation and Dephosphorylation in the Cell Cycle and Beyond

Previous *ex vivo* methods only speculated on the positive feedback nature of Cdk1-Cdc25, we definitely verified the existence of the ultrasensitive feedback loop *in vivo* while showing that this loop can indeed allow for the rapid switch-like change into and out of mitosis. Given the importance of rapidly turning off interphase events, such as DNA replication, while turning on DNA and nuclear separation in mitosis, this positive feedback loop likely exists *in vivo* in all organisms. We also showed a mechanism by which Cdk1 distributively phosphorylates Cdc25 and directly activates Cdc25 in a cooperative phosphorylatory manner. This simple method of direct Cdc25 activation is likely a mechanism that adds significantly to the bistable nature of mitotic entrance in all eukaryotes; however, in other organisms, such as metazoans with more Cdc25 isoforms, and increased need to control mitotic entrance timing (due to multi-cell coordination), multisite phosphorylation may also control Cdc25 stability, by directly altering Cdc25 structure or by preventing Cdc25 association with ubiquitin and proteasome components, and control Cdc25 localization- it has been seen that co-localization of Cdk1 effector proteins (such as CyclinB) with Cdk1 in important mitotic “hot spots” contributes to the switch-like entrance into mitosis (Santos, Wollman et al. 2012). Finally, while we have found that Cdk1 phosphorylation of Cdc25 is distributive or semi-processive *in vitro* and that Cdk1 phosphorylation sites do not seem to be specific *in vivo* in the progressive activation of Cdc25, these mechanisms may not be conserved in all Cdk1-substrate interactions. In *S. cerevisiae*, for example, Sic1 phosphorylation by Cdk1 involves Cdk1 priming specific sites on Sic1, followed by semi-processive phosphorylation of clusters of sites near these primed sites (Koivomagi, Valk et al. 2011). Indeed, in addition to other

Cdk1-substrate interactions, even the specific mechanism of phosphorylation on Cdc25 by Cdk1, in *S. pombe* and other organisms deserve further, and more detailed, exploration.

Protein phosphorylations by kinases have been investigated as important post-translational modification events for almost a century. It has often been assumed that dephosphorylation counters kinase-specified events, but interest in specific phosphatase interactions, especially in cell cycle studies, is a new field that has come into prominence only in the past few decades. Phosphatases, such as Protein phosphatase 1 (PP1) and Protein phosphatase 2A (PP2A) counter Aurora kinase phosphorylations during chromosome congression, kinetochore capture, and chromosome segregation. Cdc14 and PP2A counter Cdk1 phosphorylations by directly interacting with Cdk1 substrates, one of the most investigated of which being Cdc25 (reviewed in (Wurzenberger and Gerlich 2011)). Dephosphorylation of Cdc25 through control of mitotic timing have been found to be conserved in *S. pombe*, *S. cerevisiae* and human cells ((Esteban, Blanco et al. 2004; Wolfe and Gould 2004; Lu, Domingo-Sananes et al. 2012; Forester, Maddox et al. 2007; Pal, Paraz et al. 2008)). Studies have also shown that in *S. pombe* and *S. cerevisiae*, specific Cdc14/Clp1 dephosphorylation and association with other substrates are involved in the metaphase-anaphase switch and cytokinetic timing (Wolfe, McDonald et al. 2006; Clifford, Wolfe et al. 2008; Roberts-Galbraith, Chen et al. 2009; Koivomagi, Valk et al. 2011; Lu, Domingo-Sananes et al. 2012). In addition, in *S. pombe*, Clp1 associates with Mid1, a cytokinetic ring regulator, and controls cytokinetic ring stability, in a Cdk1 phosphorylation independent manner, suggesting that phosphatases may be involved in mechanisms of mitotic regulation that are independent from mitotic kinase

driven activity (Clifford, Wolfe et al. 2008). Thus, the contributions of phosphatases in mitosis are many and varied; however, the specific mechanism and kinetics of dephosphorylation, as well as how phosphatase contributes to the effectiveness of mitotic events, including the Clp1-Cdc25 control of cytokinetic timing, need to be further explored.

Finally, this work adds to the growing understanding of how phosphoregulation mechanisms affect protein activity and interaction to allow for a system to fine tune its response to cellular and environmental changes. Multisite phosphorylation has recently been hypothesized, using *in silico* modeling, to be an important component for the switch-like activation of a protein or transitions in a system. While multisite phosphorylation is seen in many proteins in various cellular protein cascades, the EGF receptor and p53, of the growth factor and mitogen-activated protein kinase (MAPK) pathways respectively, just to name a few (reviewed in (Cohen 2000)), Cdc25 is part of only three proteins found by *in vivo* and *ex vivo* experimental data, to display switch-like and ultrasensitive characteristics after multisite phosphoregulation. The two other proteins found to add ultrasensitivity to their systems are both Cdk1 targets, and are Wee1 (in *X. laevis*), which contributes to mitotic entry, and Sic1 (in *S. cerevisiae*), which contributes to the metaphase-anaphase transition (Pomerening, Sontag et al. 2003; Kim and Ferrell 2007; Koivomagi, Valk et al. 2011). The contributions of substrate multisite phosphorylation by Cdk1 and other mitotic kinases, such as Plks and Aurora kinases, as well as proteins from other cellular systems that display switch-like behavior (such as the MAPK pathway), have not been studied and deserve further exploration.

Conclusions

In summary, using *S. pombe*, I was able to explore the mechanisms of Cdc25 phosphorylation, and show for the first time that the Cdk1-Cdc25 positive feedback loop and the Cdc25-Clp1 negative feedback loop exist *in vivo* and have significant effects in mitotic entry and mitotic exit. This work contributes importantly to the growing understanding of protein phosphoregulation and its contributions to the bistability of cellular systems.

BIBLIOGRAPHY

- Archambault, V. and D. M. Glover (2009). "Polo-like kinases: conservation and divergence in their functions and regulation." *Nat Rev Mol Cell Biol* **10**(4): 265-275.
- Aszmann, O. C. (2000). "The life and work of Theodore Schwann." *Journal of reconstructive microsurgery* **16** (4): 291-295.
- Bahassi el, M., R. F. Hennigan, et al. (2004). "Cdc25C phosphorylation on serine 191 by Plk3 promotes its nuclear translocation." *Oncogene* **23**(15): 2658-2663.
- Bähler, J., J. Q. Wu, et al. (1998). "Heterologous modules for efficient and versatile PCR-based gene targeting in *Schizosaccharomyces pombe*." *Yeast* **14**(10): 943-951.
- Baldin, V., K. Pelpel, et al. (2002). "Nuclear localization of CDC25B1 and serine 146 integrity are required for induction of mitosis." *J Biol Chem* **277**(38): 35176-35182.
- Blomberg, I. and I. Hoffmann (1999). "Ectopic expression of Cdc25A accelerates the G(1)/S transition and leads to premature activation of cyclin E- and cyclin A-dependent kinases." *Mol Cell Biol* **19**(9): 6183-6194.
- Boutros, R. and B. Ducommun (2008). "Asymmetric localization of the CDC25B phosphatase to the mother centrosome during interphase." *Cell Cycle* **7**(3): 401-406.
- Boyle, W. J., P. van der Geer, et al. (1991). "Phosphopeptide mapping and phosphoamino acid analysis by two-dimensional separation on thin-layer cellulose plates." *Methods Enzymol* **201**: 110-149.
- Bueno, A. and P. Russell (1993). "Two fission yeast B-type cyclins, cig2 and Cdc13, have different functions in mitosis." *Mol Cell Biol* **13**(4): 2286-2297.
- Busino, L., M. Chiesa, et al. (2004). "Cdc25A phosphatase: combinatorial phosphorylation, ubiquitylation and proteolysis." *Oncogene* **23**(11): 2050-2056.
- Busino, L., M. Donzelli, et al. (2003). "Degradation of Cdc25A by beta-TrCP during S phase and in response to DNA damage." *Nature* **426**(6962): 87-91.
- Cazales, M., E. Schmitt, et al. (2005). "CDC25B phosphorylation by Aurora-A occurs at the G2/M transition and is inhibited by DNA damage." *Cell Cycle* **4**(9): 1233-1238.
- Chua, G., C. Lingner, et al. (2002). "The sal3+ Gene Encodes an Importin- β Implicated in the Nuclear Import of Cdc25 in *Schizosaccharomyces pombe*. ." *Genetics* **162**(2): 689-703.
- Clifford, D. M., B. A. Wolfe, et al. (2008). "The Clp1/Cdc14 phosphatase contributes to the robustness of cytokinesis by association with anillin-related Mid1." *J Cell Biol* **181**(1): 79-88.
- Cohen, P. (2000). "The regulation of protein function by multisite phosphorylation--a 25 year update." *Trends Biochem Sci* **25**(12): 596-601.
- Cueille, N., E. Salimova, et al. (2001). "Flp1, a fission yeast orthologue of the *S. cerevisiae* CDC14 gene, is not required for cyclin degradation or rum1p stabilisation at the end of mitosis." *J Cell Sci* **114**(Pt 14): 2649-2664.

- Deibler, R. W. and M. W. Kirschner (2010). "Quantitative reconstitution of mitotic CDK1 activation in somatic cell extracts." *Mol Cell* **37**(6): 753-767.
- Dischinger, S., A. Krapp, et al. (2008). "Chemical genetic analysis of the regulatory role of Cdc2p in the *S. pombe* septation initiation network." *J Cell Sci* **121**(Pt 6): 843-853.
- Domingo-Sananes, M. R. and B. Novak (2010). "Different effects of redundant feedback loops on a bistable switch." *Chaos* **20**(4): 045120.
- Donzelli, M., M. Squatrito, et al. (2002). "Dual mode of degradation of Cdc25 A phosphatase." *EMBO* **21**(18): 4875-4884.
- Esteban, V., M. Blanco, et al. (2004). "A role for the Cdc14-family phosphatase Flp1p at the end of the cell cycle in controlling the rapid degradation of the mitotic inducer Cdc25p in fission yeast." *Journal of Cell Science* **117**: 2461-2468.
- Esteban, V., M. Sacristan, et al. (2008). "The Flp1/Clp1 phosphatase cooperates with HECT-type Pub1/2 protein-ubiquitin ligases in *Schizosaccharomyces pombe*." *Cell Cycle* **7**(9): 1269-1276.
- Esteban, V., M. Sacristán, et al. (2008). "The Flp1/Clp1 phosphatase cooperates with HECT-type Pub1/2 protein-ubiquitin ligases in *Schizosaccharomyces pombe*." *Cell Cycle*(7): 1269-1276.
- Falck, J., N. Mailand, et al. (2001). "The ATM-Chk2-Cdc25A checkpoint pathway guards against radioresistant DNA synthesis." *Nature* **410**(6830): 842-847.
- Fantes, P. A. (1977). "Control of cell size and cycle time in *Schizosaccharomyces pombe*." *J Cell Sci* **24**: 51-67.
- Ferrell, J. E., Jr. (2008). "Feedback regulation of opposing enzymes generates robust, all-or-none bistable responses." *Curr Biol* **18**(6): R244-245.
- Ferrell, J. E., Jr. (2009). "Q&A: Cooperativity." *J Biol* **8**(6): 53.
- Ferrell, J. E. and W. Xiong (2001). "Bistability in cell signaling: How to make continuous processes discontinuous, and reversible processes irreversible." *Chaos* **11**(1): 227-236.
- Forester, C. M., J. Maddox, et al. (2007). "Control of mitotic exit by PP2A regulation of Cdc25C and Cdk1." *Proc Natl Acad Sci U S A* **104**(50): 19867-19872.
- Fraser, R. S. and P. Nurse (1978). "Novel cell cycle control of RNA synthesis in yeast." *Nature* **271**(5647): 726-730.
- Furnari, B., A. Blasina, et al. (1999). "Cdc25 inhibited in vivo and in vitro by checkpoint kinases Cds1 and Chk1." *Mol Biol Cell* **10**(4): 833-845.
- Georgi, A. B., P. T. Stukenberg, et al. (2002). "Timing of events in mitosis." *Curr Biol* **12**(2): 105-114.
- Gopinathan, L., C. K. Ratnacaram, et al. (2011). "Established and novel Cdk/cyclin complexes regulating the cell cycle and development." *Results Probl Cell Differ* **53**: 365-389.
- Gould, K. L., S. Moreno, et al. (1991). "Phosphorylation at Thr167 is required for *Schizosaccharomyces pombe* p34cdc2 function." *EMBO* **10**(11): 3297-3309.
- Gould, K. L. and P. Nurse (1989). "Tyrosine phosphorylation of the fission yeast cdc2+ protein kinase regulates entry into mitosis. ." *Nature* **342**(6245): 39-45.
- Graves, P. R., C. M. Lovly, et al. (2001). "Localization of human Cdc25C is regulated both by nuclear export and 14-3-3 protein binding." *Oncogene* **20**(15): 1839-1851.

- Guertin, D. A., L. Chang, et al. (2000). "The role of the sid1p kinase and cdc14p in regulating the onset of cytokinesis in fission yeast." *EMBO J* **19**(8): 1803-1815.
- He, E., O. Kapuy, et al. (2011). "System-level feedbacks make the anaphase switch irreversible." *Proc Natl Acad Sci U S A* **108**(24): 10016-10021.
- Hoffmann, I., P. R. Clarke, et al. (1993). "Phosphorylation and activation of human cdc25-C by cdc2--cyclin B and its involvement in the self-amplification of MPF at mitosis." *EMBO J* **12**(1): 53-63.
- Hoffmann, I., G. Draetta, et al. (1994). "Activation of the phosphatase activity of human cdc25A by a cdk2-cyclin E dependent phosphorylation at the G1/S transition." *EMBO J* **13**(18): 4302-4310.
- Holt, L. J., A. N. Krutchinsky, et al. (2008). "Positive feedback sharpens the anaphase switch." *Nature* **454**(7202): 353-357.
- Isoda, M., K. Sako, et al. (2011). "Dynamic regulation of Emi2 by Emi2-bound Cdk1/Plk1/CK1 and PP2A-B56 in meiotic arrest of *Xenopus* eggs." *Dev Cell* **21**(3): 506-519.
- Jackson, C. W. (1990). "Megakaryocyte endomitosis: a review." *Int J Cell Cloning* **8**(4): 224-226.
- Jinno, S., K. Suto, et al. (1994). "Cdc25A is a novel phosphatase functioning early in the cell cycle." *EMBO J* **13**(7): 1549-1556.
- Johnson, A. E. and K. L. Gould (2011). "Dma1 ubiquitinates the SIN scaffold, Sid4, to impede the mitotic localization of Plo1 kinase." *EMBO J* **30**(2): 341-354.
- Kapuy, O., D. Barik, et al. (2009). "Bistability by multiple phosphorylation of regulatory proteins." *Progress in Biophysics and Molecular Biology* **100**: 47-56.
- Karlsson-Rosenthal, C. and J. B. Millar (2006). "Cdc25: mechanisms of checkpoint inhibition and recovery." *Trends in cell biology* **16** (6).
- Keeney, J. B. and J. D. Boeke (1994). "Efficient targeted integration at leu1-32 and ura4-294 in *Schizosaccharomyces pombe*." *Genetics* **136**(3): 849-856.
- Khaled, A. R., D. V. Bulavin, et al. (2005). "Cytokine-driven cell cycling is mediated through Cdc25A." *J Cell Biol* **169**(5): 755-763.
- Kieffer, I., C. Lorenzo, et al. (2007). "Differential mitotic degradation of the CDC25B phosphatase variants." *Oncogene* **26**(57): 7847-7858.
- Kim, S. Y. and J. E. J. Ferrell (2007). "Substrate competition as a source of ultrasensitivity in the inactivation of Wee1." *Cell* **128**(6): 1133-1145.
- Koivomagi, M., E. Valk, et al. (2011). "Cascades of multisite phosphorylation control Sic1 destruction at the onset of S phase." *Nature* **480**(7375): 128-131.
- Kovelman, R. and P. Russell (1996). "Stockpiling of Cdc25 during a DNA replication checkpoint arrest in *Schizosaccharomyces pombe*." *Molecular Cell Biology* **16**(1): 86-93.
- Kumagai, A. and W. G. Dunphy (1996). "Purification and molecular cloning of Plx1, a Cdc25-regulatory kinase from *Xenopus* egg extracts." *Science* **273**(5280): 1377-1380.
- Langerak, P. and P. Russell (2011). "Regulatory networks integrating cell cycle control with DNA damage checkpoints and double-strand break repair." *Philos Trans R Soc Lond B Biol Sci* **366**(1584): 3562-3571.
- Lincoln, A. J., D. Wickramasinghe, et al. (2002). "Cdc25b phosphatase is required for resumption of meiosis during oocyte maturation." *Nat Genet* **30**(4): 446-449.

- Lindner, P. (1893). "Schizosaccharomyces pombe." ein neuer Gahrungserreger **10:1298-1300**.
- Lindqvist, A., H. Kallstrom, et al. (2005). "Cdc25B cooperates with Cdc25A to induce mitosis but has a unique role in activating cyclin B1-Cdk1 at the centrosome." Journal of Cell Biology **171(2)**: 35-45.
- Lindqvist, A., V. Rodriguez-Bravo, et al. (2009). "The decision to enter mitosis: feedback and redundancy in the mitotic entry network." J Cell Biol **185(2)**: 193-202.
- Lobjois, V., D. Jullien, et al. (2009). "The polo-like kinase 1 regulates CDC25B-dependent mitosis entry." Biochim Biophys Acta **1793(3)**: 462-468.
- Lopez-Aviles, S., M. Grande, et al. (2005). "Inactivation of the Cdc25 phosphatase by the stress-activated Srk1 kinase in fission yeast." Mol Cell **17(1)**: 49-59.
- Lopez-Aviles, S., O. Kapuy, et al. (2009). "Irreversibility of mitotic exit is the consequence of systems-level feedback." Nature **459(7246)**: 592-595.
- Lopez-Girona, A., B. Furnari, et al. (1999). "Nuclear localization of Cdc25 is regulated by DNA damage and a 14-3-3 protein." Nature **397(6715)**: 172-175.
- Lu, L. X., M. R. Domingo-Sananes, et al. (2012). "Multisite phosphoregulation of Cdc25 activity refines the mitotic entrance and exit switches." Proc Natl Acad Sci U S A **109(25)**: 9899-9904.
- Lukas, J., C. Lukas, et al. (2004). "Mammalian cell cycle checkpoints: signalling pathways and their organization in space and time." DNA Repair (Amst) **3(8-9)**: 997-1007.
- Lundgren, K., N. Walworth, et al. (1991). "mik1 and wee1 cooperate in the inhibitory tyrosine phosphorylation of cdc2." Cell **64(6)**: 1111-1122.
- Ma, Z. Q., S. Dasari, et al. (2009). "IDPicker 2.0: Improved protein assembly with high discrimination peptide identification filtering." J Proteome Res **8(8)**: 3872-3881.
- Mailand, N., J. Falck, et al. (2000). "Rapid destruction of human Cdc25A in response to DNA damage." Science **288(5470)**: 1425-1429.
- Mailand, N., A. V. Podtelejnikov, et al. (2002). "Regulation of G(2)/M events by Cdc25A through phosphorylation-dependent modulation of its stability." EMBO J **21(21)**: 5911-5920.
- Manke, I. A., A. Nguyen, et al. (2005). "MAPKAP kinase-2 is a cell cycle checkpoint kinase that regulates the G2/M transition and S phase progression in response to UV irradiation." Mol Cell **17(1)**: 37-48.
- Mazumdar, A. and M. Mazumdar (2002). "How one becomes many: blastoderm cellularization in Drosophila melanogaster." Bioessays **24(11)**: 1012-1022.
- McDonald, W. H. and J. R. Yates, 3rd (2002). "Shotgun proteomics and biomarker discovery." Dis Markers **18(2)**: 99-105.
- McGowan, C. H. and P. Russell (1993). "Human Wee1 kinase inhibits cell division by phosphorylating p34cdc2 exclusively on Tyr15." EMBO J **12(1)**: 75-85.
- McLean, J. R., D. Chaix, et al. (2011). "State of the APC/C: organization, function, and structure." Crit Rev Biochem Mol Biol **46(2)**: 118-136.
- Michael, W. M. and J. Newport (1998). "Coupling of mitosis to the completion of S phase through Cdc34-mediated degradation of Wee1." Science **282(5395)**: 1886-1889.
- Moreno, S., P. Nurse, et al. (1990). "Regulation of mitosis by cyclic accumulation of p80cdc25 mitotic inducer in fission yeast." Nature **344(6266)**: 549-552.

- Morgan, D. O. (1997). "Cyclin-dependent kinases: engines, clocks, and microprocessors." *Annu Rev Cell Dev Biol* **13**: 261-291.
- Morgan, D. O. (2007). "The Cell Cycle: Principles of Control."
- Mueller, P. R., T. R. Coleman, et al. (1995). "Myt1: a membrane-associated inhibitory kinase that phosphorylates Cdc2 on both threonine-14 and tyrosine-15." *Science* **270**(5233): 86-90.
- Murray, A. W. and T. Hunt (1993). "The Cell Cycle: an introduction."
- Nabeshima, K., T. Nakagawa, et al. (1998). "Dynamics of centromeres during metaphase-anaphase transition in fission yeast: Dis1 is implicated in force balance in metaphase bipolar spindle." *Mol Biol Cell* **9**(11): 3211-3225.
- Nakajima, H., F. Toyoshima-Morimoto, et al. (2003). "Identification of a consensus motif for Plk (Polo-like kinase) phosphorylation reveals Myt1 as a Plk1 substrate." *J Biol Chem* **278**(28): 25277-25280.
- Nefsky, B. and D. Beach (1996). "Pub1 acts as an E6-AP-like protein ubiquitin ligase in the degradation of cdc25." *EMBO* **15**(6): 1301-1312.
- Novak, B., O. Kapuy, et al. (2010). "Regulated protein kinases and phosphatases in cell cycle decisions." *Curr Opin Cell Biol* **22**(6): 801-808.
- Novak, B. and J. J. Tyson (1993). "Modeling the cell division cycle: M-phase trigger, oscillations, and size control." *J. Theor. Biol.* **165**: 101-134.
- Novak, B. and J. J. Tyson (1993). "Numerical analysis of a comprehensive model of M-phase control in *Xenopus* oocyte extracts and intact embryos." *J Cell Sci* **106** (Pt 4): 1153-1168.
- Nurse, P. (2004). "Wee beasties." *Nature* **432**(7017): 557.
- Pal, G., M. T. Paraz, et al. (2008). "Regulation of Mih1/Cdc25 by protein phosphatase 2A and casein kinase 1." *J Cell Biol* **180**(5): 931-945.
- Pomerening, J. R. (2009). "Positive-feedback loops in cell cycle progression." *FEBS Lett* **583**(21): 3388-3396.
- Pomerening, J. R., S. Y. Kim, et al. (2005). "Systems-level dissection of the cell-cycle oscillator: bypassing positive feedback produces damped oscillations." *Cell* **122**(4): 565-578.
- Pomerening, J. R., E. D. Sontag, et al. (2003). "Building a cell cycle oscillator: hysteresis and bistability in the activation of Cdc2." *Nat Cell Biol* **5**(4): 346-351.
- Qian, Y. W., E. Erikson, et al. (2001). "The polo-like kinase Plx1 is required for activation of the phosphatase Cdc25C and cyclin B-Cdc2 in *Xenopus* oocytes." *Mol Biol Cell* **12**(6): 1791-1799.
- Rape, M., S. K. Reddy, et al. (2006). "The processivity of multiubiquitination by the APC determines the order of substrate degradation." *Cell* **124**(1): 89-103.
- Ray, D., Y. Terao, et al. (2007). "Hemizygous disruption of Cdc25A inhibits cellular transformation and mammary tumorigenesis in mice." *Cancer Res* **67**(14): 6605-6611.
- Roberts-Galbraith, R. H., J. S. Chen, et al. (2009). "The SH3 domains of two PCH family members cooperate in assembly of the *Schizosaccharomyces pombe* contractile ring." *J Cell Biol* **184**(1): 113-127.
- Roberts-Galbraith, R. H., M. D. Ohi, et al. (2010). "Dephosphorylation of F-BAR protein Cdc15 modulates its conformation and stimulates its scaffolding activity at the cell division site." *Mol Cell* **39**(1): 86-99.

- Rudolph, J., D. M. Epstein, et al. (2001). "Specificity of natural and artificial substrates for human Cdc25A." *Analytical Biochemistry* **289**(1): 43-51.
- Russell, P. and P. Nurse (1986). "cdc25+ functions as an inducer in the mitotic control of fission yeast." *Cell* **45**(1): 145-153.
- Russell, P. and P. Nurse (1987). "Negative regulation of mitosis by wee1+, a gene encoding a protein kinase homolog." *Cell* **49**(4): 559-567.
- Santos, S. D., R. Wollman, et al. (2012). "Spatial positive feedback at the onset of mitosis." *Cell* **149**(7): 1500-1513.
- Satyanarayana, A. and P. Kaldis (2009). "Mammalian cell-cycle regulation: several Cdks, numerous cyclins and diverse compensatory mechanisms." *Oncogene* **28**(33): 2925-2939.
- Sexl, V., J. A. Diehl, et al. (1999). "A rate limiting function of cdc25A for S phase entry inversely correlates with tyrosine dephosphorylation of Cdk2." *Oncogene* **18**(3): 573-582.
- Smith, A., S. Simanski, et al. (2007). "Redundant ubiquitin ligase activities regulate wee1 degradation and mitotic entry." *Cell Cycle*.
- Stegmeier, F. and A. Amon (2004). "Closing mitosis: the functions of the Cdc14 phosphatase and its regulation." *Annu Rev Genet* **38**: 203-232.
- Sveiczer, A., B. Novak, et al. (1996). "The size control of fission yeast revisited." *J Cell Sci* **109** (Pt 12): 2947-2957.
- Thron, C. D. (1996). "A model for a bistable biochemical trigger of mitosis." *Biophys Chem* **57**(2-3): 239-251.
- Timofeev, O., O. Cizmecioglu, et al. (2010). "Cdc25 phosphatases are required for timely assembly of CDK1-cyclin B at the G2/M transition." *J Biol Chem* **285**(22): 16978-16990.
- Toyoshima-Morimoto, F., E. Taniguchi, et al. (2002). "Plk1 promotes nuclear translocation of human Cdc25C during prophase." *EMBO Rep* **3**(4): 341-348.
- Toyoshima-Morimoto, F., E. Taniguchi, et al. (2001). "Polo-like kinase 1 phosphorylates cyclin B1 and targets it to the nucleus during prophase." *Nature* **410**(6825): 215-220.
- Trautmann, S., B. A. Wolfe, et al. (2001). "Fission yeast Clp1p phosphatase regulates G2/M transition and coordination of cytokinesis with cell cycle progression." *Current Biology* **11**(12): 931-940.
- Trinkle-Mulcahy, L. and A. L. Lamond (2006). "Mitotic phosphatases: no longer silent partners." *Current Opinion in Cell Biology* **18**(6): 623-631.
- Trunnell, N. B., A. C. Poon, et al. (2011). "Ultrasensitivity in the Regulation of Cdc25C by Cdk1." *Mol Cell* **41**(3): 263-274.
- Tumurbaatar, I., O. Cizmecioglu, et al. (2011). "Human Cdc14B promotes progression through mitosis by dephosphorylating Cdc25 and regulating Cdk1/cyclin B activity." *PLoS One* **6**(2): e14711.
- Tyson, J. J. (1991). "Modeling the cell division cycle: cdc2 and cyclin interactions." *Proc Natl Acad Sci U S A* **88**(16): 7328-7332.
- Uchida, S., N. Watanabe, et al. (2011). "SCFbeta(TrCP) mediates stress-activated MAPK-induced Cdc25B degradation." *J Cell Sci* **124**(Pt 16): 2816-2825.

- Uchida, S., K. Yoshioka, et al. (2009). "Stress-activated mitogen-activated protein kinases c-Jun NH2-terminal kinase and p38 target Cdc25B for degradation." Cancer Res **69**(16): 6438-6444.
- Watanabe, N., H. Arai, et al. (2004). "M-phase kinases induce phospho-dependent ubiquitination of somatic Wee1 by SCFbeta-TrCP." PNAS **101**(13): 4419-4424.
- Wolfe, B. A. and K. L. Gould (2004). "Fission yeast Clp1p phosphatase affects G2/M transition and mitotic exit through Cdc25p inactivation." EMBO(23): 919-929.
- Wolfe, B. A., W. H. McDonald, et al. (2006). "Phospho-regulation of the Cdc14/Clp1 phosphatase delays late mitotic events in *S. pombe*." Dev Cell **11**(3): 423-430.
- Wurzenberger, C. and D. W. Gerlich (2011). "Phosphatases: providing safe passage through mitotic exit." Nat Rev Mol Cell Biol **12**(8): 469-482.
- Yang, L., W. R. MacLellan, et al. (2004). "Multisite phosphorylation and network dynamics of cyclin-dependent kinase signaling in the eukaryotic cell cycle." Biophys J **86**(6): 3432-3443.